UNIVERSIDAD NACIONAL AUTÓNOMA DE MÉXICO

PROGRAMA DE POSGRADO EN CIENCIAS DE LA TIERRA

INSTITUTO DE GEOLOGÍA, ERNO

Influencia de la mineralogía y tamaño de partícula en la bioaccesibilidad de plomo en polvo urbano en Hermosillo, Sonora

T E S I S

QUE PARA OPTAR POR EL GRADO DE

DOCTOR EN CIENCIAS DE LA TIERRA

PRESENTA

BELEM GONZÁLEZ GRIJALVA.

TUTOR
Dra. Diana Meza Figueroa, UNISON

COMITÉ TUTOR
Dr. Francisco Martín Romero, UNAM
Dr. Rafael Del Río Salas, ERNO, UNAM

Hermosillo, Sonora.   Septiembre, 2021

Financiamiento

BIBLIOTECA CENTRAL

Dedicada especialmente a mi familia por su inmenso amor, apoyo y comprensión

Mi esposo Deneb Antonio

Mis queridos hijos David A. y Uziel F.

Mis padres Marco A y Rosalina

Mi abuelita María Dolores †

Mis hermanos Marco D, Israel y Daniela

Agradecimientos

ÍNDICE GENERAL

Resumen

El pigmento mineral crocoíta (PbCrO$_4$) utilizado en pintura amarilla de tráfico, representa una fuente importante de plomo (Pb) en el medio ambiente que no ha sido estudiada a detalle en países en desarrollo. La identificación del destino ambiental de este pigmento es particularmente importante en zonas áridas y semi-áridas en donde las temperaturas extremas, baja humedad y constante actividad antropogénica promueven la erosión y degradación de la pintura. Esto favorece la integración de los pigmentos sólidos al polvo de calle, a los suelos y a la atmósfera. En las zonas urbanas, los suelos son los principales reservorios de contaminantes y a su vez son emisores de polvo hacia el ambiente. Los elementos potencialmente tóxicos que se encuentran en las fases minerales pueden ser liberados en fluidos biológicos, dependiendo de su solubilidad. Es así como de la concentración total de un metal o metaloide, una fracción puede ser bioaccesible. Esto dependerá de varios factores como el tamaño de la partícula mineral, y el grupo mineral en el que se encuentre el elemento de interés. Por ejemplo, si el plomo ocurre como un carbonato en un suelo, y el carbonato es la especie dominante, su liberación en el fluido biológico o bioaccesibilidad puede ser desde una fracción hasta el 100%. De esta fracción liberada, el total o una parte podrá estar biodisponible (pasar a torrente sanguíneo). Por lo anterior, la evaluación de riesgos a la salud, especialmente en niños expuestos a Pb a través de la ingestión de suelo debe incluir la fracción bioaccesible y no la concentración total, para evitar una sobreestimación del riesgo. En el tema de bioaccesibilidad oral, el papel de la mineralogía del suelo no ha sido ampliamente estudiado. En el presente estudio, se evalúa la bioaccesibilidad oral del plomo a partir de pigmentos, considerando la influencia de la mineralogía de suelos locales, para ello, se identificó y caracterizó una fuente de área (pinturas amarillas de tráfico con crocoíta) con aporte continuo de Pb en el área de estudio (Artículo 1, Science of the Total Environment (2018), 630, 1596–1607). Se determinó la concentración de metales potencialmente tóxicos en particulado suspendido a nivel peatonal y techo, durante un año, en una zona de la ciudad con alto tráfico y en donde ocurre acumulación de sedimentos finos, posteriormente a la temporada de lluvia (Artículo 2, Atmospheric Environment (2016), 138, 4-14). En este artículo se muestra que las concentraciones de Pb y Cr son mayores a nivel peatonal y que se asocian a fuentes de tráfico. Para comprender el riesgo por exposición a plomo derivado de estos pigmentos se realizó un experimento fortificando suelos naturales periurbanos en su fracción más fina (20 µm) con mineral de crocoíta encontrado en pinturas amarillas (Articulo 3, Science of the Total Environment (2019), 657, 1468-1479). Los resultados muestran (i) una alta concentración de Pb y Cr, debido a los micro y nano-cristales de crocoíta que se encuentran en la pintura amarilla; (ii) la presencia de crocoita en el polvo atmosférico y en el colectado en calles; (iii) una mayor concentración de Pb en el polvo suspendido a nivel peatonal; (iv) la mineralogía de los suelos influye en la bioaccesibilidad oral del

Pb asociado a la crocoita, en particular, los minerales neutralizadores y la caolinita favoreciendo su bioaccesibilidad; (v) este estudio propone la siguiente ecuación de predicción del nivel de bioaccesibilidad de Pb ($y = 0.5286x - 6.948$) siendo "y" la bioaccesibilidad estimada mediante una concentración de Pb total conocida "X" para la estimación de Pb que llegará a ser disponible para su absorción en el sistema gástrico e intestinal, lo que podría representar el riesgo a la salud dependiendo del tipo de suelo.

Abstract

The mineral pigment crocoite ($PbCrO_4$) is commonly used in yellow traffic paint. It represents an important source of lead (Pb) in the environment that has not been studied in detail in developing countries. The identification of the environmental fate of this pigment is particularly important in arid and semi-arid areas where extreme temperatures, low humidity and constant anthropogenic activity promote the erosion and degradation of paint. This causes the integration of solid pigments into road dust, soils, and the atmosphere. In urban areas, soils are the main reservoirs of pollutants, and in turn are the main emission sources of particulate matter into the environment. Potentially toxic elements found in mineral phases can be released into biological fluids, depending on their solubility. Thus, of the total concentration of a metal or metalloid, a fraction can be bioaccessible. This will depend on several factors such as the size of the mineral particle and the mineral group in which the element of interest is located. For example, if lead occurs as carbonate in soil, and carbonate is the dominant species, its release into the biological fluid or bioaccessibility can be from a fraction to 100%. Of this fraction released, all or a part may be bioavailable (pass into the bloodstream). Therefore, health risk assessment, especially in children exposed to Pb through soil ingestion should include the bioaccessible fraction and not the total concentration to avoid an overestimation of risk. Despite its importance, the role of soil mineralogy in oral bioaccessibility of Pb has not been widely studied. In this study, the mineral pigment crocoite is characterized and identified as a source of Pb in the urban environment in the study area (Article 1, Science of the Total Environment (2018), vol 639: 1596-1607). Pedestrian exposure to resuspended dust enriched in Pb, Cr and other potentially toxic elements is studied in a high-traffic area of the city where accumulation of fine sediments occurs, following the rainy season (Article 2, Atmospheric Environment, (2016), 138: 4-14). This article shows that the concentration of Pb and Cr is higher at the pedestrian level than roof level, because of turbulence induced by traffic. To understand the real risk from lead exposure from these pigments, an experiment was conducted. Samples representing fine-grained fraction of periurban superficial soils (<20μm) were fortified with yellow traffic paint (crocoite pigment). Gastric and intestinal Pb-bioaccessibility was estimated (Article 3, Science of the Total Environment, (2019), 657:1468-1479). The results show: (i) a high concentration of Pb and Cr, due to the micro- and nanocrystals of crocoite from yellow paint; (ii) the presence of crocoite in atmospheric dust and road dust; (iii) a higher concentration of Pb and Cr in the dust suspended at pedestrian level by traffic-induced turbulence; (iv) soil mineralogy influences the oral bioaccessibility of Pb associated to crocoite, in particular total neutralizing minerals and kaolinite stimulating their bioaccessibility; (v) this study proposes the following prediction equation for the level of bioaccessibility of Pb ($y = 0.5286x - 6.948$) for the estimation of Pb that will become available for absorption in the gastric and intestinal system, which could represent the risk of health according to the soil type.

I. INTRODUCCIÓN

A pesar de que los metales o elementos tóxicos están presentes en la corteza terrestre a niveles traza, las actividades antropogénicas diseminan y aportan estos metales al medio ambiente, siendo los suelos los principales reservorios en donde pueden acumularse (Thakur et al., 2004). Las emisiones excesivas de metales frecuentemente aparecen en formas de partículas o emisiones no exhaustivas (Duzgoren-Aydin et al., 2006) y pueden ser depositadas directamente al suelo o formar parte del material particulado atmosférico y posteriormente depositarse en forma de polvo. Las fuentes antropogénicas tales como la emisiones por el tráfico vehicular, fundidoras de metal, refinerías, plantas cementeras, incineradores municipales, etc., incrementan los niveles de contaminación por metales potencialmente tóxicos en ambientes urbanos (Al-Khashman, 2004, 2007; Banerjee, 2003).

Los metales y los elementos potencialmente tóxicos en el polvo pueden ser acumulados en los tejidos grasos y órganos internos del cuerpo humano vía inhalación, ingestión y contacto dérmico (Lu et al., 2009; Zheng et al., 2010), causando efectos y deterioros en la salud humana (Faiz et al., 2009), que pueden afectar al sistema nervioso central, y actuar como cofactores, iniciadores o promotores de otras enfermedades (Faiz et al., 2009; Han et al.,2006) especialmente en niños, siendo más sensibles que los adultos (Kong et al., 2011; Maas et al., 2010; Meza-Figueroa et al., 2007; Shi et al., 2008).

Los productos en base a pigmentos se consideran como un vector importante de contaminación por metales, ya que se compone de una fracción inorgánica que posee una variedad de metales en pigmentos y adhesivos dispuesto en una matriz orgánica de solventes y polímeros (White et al., 2014). Las pinturas representan una fuente importante de contaminación por plomo a través de los cromatos de plomo ($PbCrO_4$) (Lanphear et al., 1998; Pirkle et al., 1998; Romieu et al., 1994). Se encuentran formando parte de la composición de la pintura amarilla de calle, y actualmente está prohibido su uso en Estados Unidos debido a que el $PbCrO_4$ es reconocido como un agente cancerígeno (Newman, 1890; Davies 1984; Frentzel-Beyme, 1983; Hayes 1988; Leonard et al., 2002, 2004). Debido a vacíos legales en la regulación de pinturas con plomo para señalizaciones en vías públicas, este tipo de pintura continúa utilizándose en nuestro país y la mayoría de países de Latinoamérica. A la fecha, no existen en México estudios enfocados a entender el destino ambiental de pigmentos minerales con plomo derivados de pintura, así como su bioaccesibilidad oral una vez integrados a los suelos y al polvo urbano. En este trabajo de investigación se pretende (i) caracterizar los pigmentos de Pb-Cr (crocoita) en pintura amarilla; (ii) identificar el destino ambiental de estos pigmentos en la zona urbanizada de Hermosillo; (iii) evaluar la bioaccesibilidad oral de plomo derivado de estas pinturas, una vez integrado a los suelos de Hermosillo.

II. ANTECEDENTES

Las partículas suspendidas o material particulado representan a una diversidad de sustancias suspendidas en la atmósfera que existen en forma de material sólido finamente particulado con un amplio intervalo de tamaño (0.005 a 100 µm). Estas son generadas por fuentes antropogénicas tales como el tráfico, actividad industrial, minería, cerámica, emisiones de polvos fugitivos por la actividad de construcción, sector energético, etc, así como por fuentes naturales conformadas por partículas primarias provenientes principalmente de la geología, suelos y aerosoles marinos de océanos y mares (US-EPA, 2009). El tiempo de permanencia en el aire, dependerá de su diámetro aerodinámico, composición química y sus propiedades termodinámicas (Karanasiou et al., 2011; Creamean et al., 2013).

La emisión y transporte de estas partículas puede ocurrir (i) a partir del suelo, por rodamiento, saltación y saltación modificada. Una vez incorporadas a la atmósfera, las partículas pueden ser removidas por (ii) depositación atmosférica húmeda (lluvia) y/o seca. A partir de estos procesos, el material de una fuente es transportado por viento (airborne dust), removido a partir de la captación superficial del material atmosférico (Nicholson, 2009) y/o depositado lentamente en forma de polvo por acción de la gravedad (IUPAC, 1990) (véase figura II.1.a). Siendo este último un medio efectivo de trasporte y redistribución de contaminantes (Fergusson y Kim, 1991; Tong y Lam, 2000; Rasmussen et al., 2001; Hooker y Nathanail, 2006; Meza-Figueroa et al., 2007; García-Rico et al., 2016), afectando la calidad del medio ambiente y la salud humana (Khairy et al., 2011; Lu et al., 2009 a, b).

El tamaño de las partículas es uno de los factores que determinan el tiempo de residencia de estas en la atmósfera. Las partículas <20 µm pueden permanecer suspendidas en la atmósfera durante horas, mientras que las partículas entre 2 y 3 µm pueden permanecer de 2 a 4 días. Las que se encuentran en un rango de tamaño de 0.1 a 1 µm muestran mayor tiempo de residencia en la atmósfera y son removidas principalmente por precipitación pluvial (Wilson y Suh, 1997).

Los suelos representan no solo un reservorio natural para captación de metales ya sea de la atmósfera (por sedimentación de material particulado emitido por industria, tráfico, minas, etc.), riego (a partir de aguas impactadas), emisiones urbanas (quema de combustible fósil), etc., sino la interfase geológica más importante en la captación de metales por la cadena trófica. Siendo estos de particular preocupación debido a su largo tiempo de residencia en los suelos y su potencial toxico en los humanos (Chen et al., 2010; Kabata-Pendias, 2011; Khan et al., 2011; Carrero et al., 2013; Szolnoki et al., 2013).

Los metales pueden ser ingeridos inadvertidamente, e ingresados al organismo por medio de la vía de exposición del tracto gastrointestinal (TGI). Cuando algún tóxico ingresa por esta vía, una fracción del mismo, puede ser bioaccesible, es decir, es liberada de su matriz (suelo, sedimento,

etc) solubilizada a nivel TGI para ser potencialmente absorbido por el torrente sanguíneo (Ruby et al., 1999). La mayor dilución ocurre en el estómago, y la mayor absorción en el tracto intestinal (Sipes y Badger, 2001; Peña et.al, 2003).

La mayoría de los estudios de riesgo a salud consideran principalmente datos epidemiológicos, así como la toxicometría basada en publicaciones internacionales, por lo que las rutas de exposición no son estudiadas a detalle; es decir solo se observa un esquema causa-efecto o fuente-receptor. En otros casos, cuando se considera la ruta de exposición referente a la ingestión de material particulado, ya sea a partir de suelos o de material resuspendido, generalmente se utiliza la concentración total del metal en la muestra, sin hacer mayor caracterización de la mineralogía (Hu et al., 2012).

Se ha documentado que la solubilidad de un mineral depende no solo de su tamaño de partícula sino de su estructura cristalina (Ruby et al., 1999; Plumlee, 1999; Plumlee et al., 2003; Nordstrom and Alpers, 1999). Los resultados de varios estudios in vitro indican que algunos aspectos del destino de los metales lixiviados de materiales geológicos que ingresan al sistema gastrointestinal pueden entenderse con base en la información mineralógica y a como estos compuestos responden a las condiciones redox, de pH y composición de fluidos en el estómago e intestino (Ruby et al., 1993, 1996, 1999; Davis et al., 1992, 1993, 1996; Borch et al., 1994; Dieter et al., 1993).

En las zonas áridas, el material particulado emitido por resuspensión de suelos representa un vehículo de transporte importante para los metales y ha sido ampliamente estudiado (Ferreira-Baptista y De Miguel, 2005; Guney et al., 2010; Zheng et al., 2010; Meza-Montenegro et al., 2012; Meza-Figueroa et al., 2007), sin embargo, la mayoría de estos estudios consideran solamente los valores totales de metales sin caracterizar la mineralogía o el tamaño de partícula al que se asocia el metal.

Dos elementos de particular interés son plomo y cromo hexavalente por su alta toxicidad. La exposición a plomo es bien reconocida por sus efectos tóxicos en huesos, tracto gastrointestinal, riñones, cardiacos, reproductivos y sistema nervioso (Alatise y Schrauzer, 2010; Anttila et al., 1995; Tiffany-Castiglioni, 1993). Se reconoce al plomo como perjudicial en el desarrollo neurológico en niños, causando trastornos en comportamiento y aprendizaje (Tong et al., 2000). El cromo tiene efectos tóxicos en riñones, hígado y sangre, estudios previos han demostrado que este elemento induce citocidad, estrés oxidativo, daños en ADN, apoptosis, y alteración en la expresión de la información genética (Pan et al., 2009). Por su parte el cromo hexavalente (VI) es reconocido como tóxico y cancerígeno en humanos a través de la ruta de inhalación, la ruta de ingestión aún no ha sido bien caracterizada (ATSDR, 2012; IARC, 2012; OSHA, 2006). Este último, se presenta en minerales poco comunes como la crocoita ($PbCrO_4$) (Hurlbut, 1971; Papp y Lipin, 2001), siendo un cromato de plomo utilizado extensivamente en las pinturas amarillas de

señalamientos de tráfico (Jeffs y Jones, 1999, Cornelis et al., 2005). Los compuestos con cromo VI provienen principalmente de fuentes antropogénicas (Alimonti et al., 2000; Barceloux, 1999; Johnson et al., 2006; Shanker et al., 2005). La principal fuente de plomo en las zonas urbanas es la pintura (Filippelli et al., 2018)

La pintura amarilla de tráfico está compuesta de pigmentos minerales finamente molidos (crocoita) mezclados en una matriz de polímeros (Walraven et al., 2015). La crocoita es un mineral que ocurre como fase secundaria en zonas oxidadas en sistemas hidrotermales, así como producto de fluidos enriquecidos en Cr en rocas ultramáficas (Frost, 2004). Los depósitos minerales con crocoita más importantes se localizan en Tasmania y Australia (Crane et al., 2001). En algunos países desarrollados se ha prohibido el uso de estos pigmentos en la fabricación de pinturas, sin embargo, su uso continúa en algunos países en los que no hay regulación para este tipo de pintura (Gottesfeld et al., 2014). Sin embargo, es posible que este tipo de pigmento aparezca como un pasivo ambiental en suelos. Recientemente, se documentó que la pintura amarilla es una fuente importante de Cr y Pb en particulado atmosférico en ambientes urbanos en Asia, Estados Unidos y Reino Unido (Lee et al., 2016; Turner et al., 2016; White et al., 2014); sin embargo, no existen reportes del uso de estos pigmentos en pinturas y su destino ambiental, en países de Latinoamérica.

Las pinturas amarillas con cromatos de plomo tienen en promedio cerca de 20 000 mg/kg de plomo y casi 5000 mg/kg de cromo hexavalente. Estos cristales pueden incorporarse al polvo debido a la erosión de la pintura y la cubierta del pavimento (véase figura II.1 b-d). La degradación de la pintura puede estar relacionada con condiciones climáticas ya que la oxidación de los constituyentes orgánicos de la misma se incrementa a mayor temperatura (Monico et al., 2016). Estudios recientes muestran que la fotodegradación de cromatos de plomo es mayor que en pigmentos asociados a sulfatos (Amat et al., 2016). Una vez liberados al medio ambiente, los pigmentos pueden incorporarse al polvo atmosférico y a los suelos.

En este trabajo, se considera como una fuente de área al plomo asociado con el pigmento mineral crocoita en la pintura de tráfico. Una vez liberado el pigmento, puede incorporarse directamente al suelo o por procesos secundarios a partir de las partículas suspendidas en aire, las cuales pueden depositar en suelos por vía seca o húmeda. Una vez en el suelo, y dependiendo del tipo de suelo, es posible que la bioaccesibilidad del plomo varíe, y por lo tanto la estimación del riesgo por exposición a plomo, puede también variar. En este trabajo se busca entender (i) si el Pb se asocia a una fuente de área como la pintura de tráfico; (ii) si los procesos de resuspensión en la zona urbana, como el tráfico, integran el pigmento a la atmósfera; (iii) si el tipo de suelo tiene una influencia en la bioaccesibilidad del plomo.
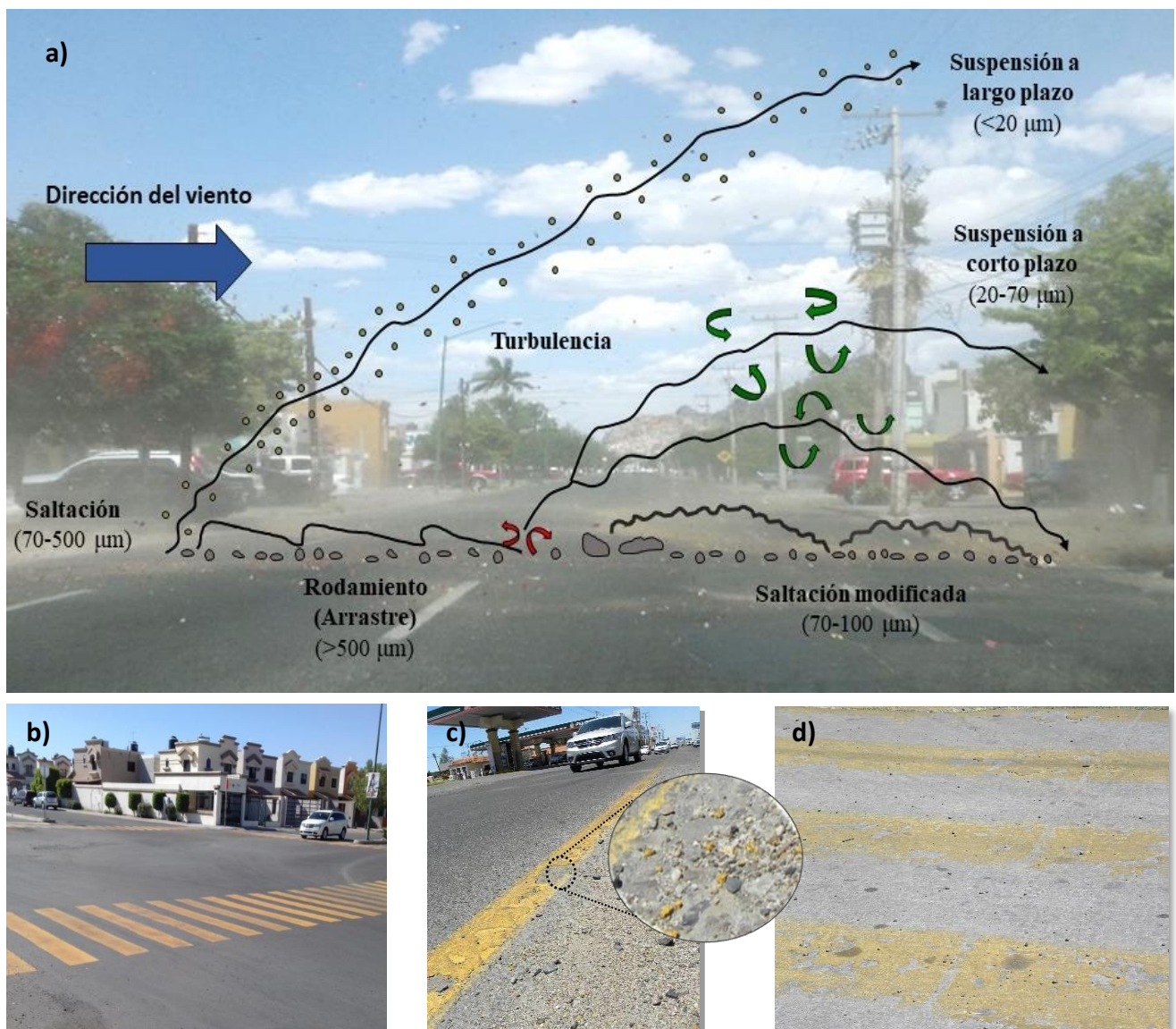
Figura II.1. a) Transporte por viento de sedimentos y particulado, imagen modificada de Nickling y McKenna Neuman (2009), sobre fotografía panorámica ubicada en el área de estudio. b) Calle con pintura amarilla de tráfico recién aplicada. c) y d) Pintura amarilla degradada sobre calles principales de la ciudad.

III. OBJETIVOS

III.1. General.

Evaluar el papel de la mineralogía en la bioaccesibilidad oral de plomo en polvo urbano.

III.2 Específicos

- Identificar y caracterizar el pigmento crocoita como una fuente de plomo.
- Evaluar el contenido de metales en polvo resuspendido por tráfico vehicular.
- Evaluar el papel de la mineralogía del suelo en la bioaccesibilidad oral de Pb y sus implicaciones en la estimación del riesgo y el uso de suelo.

IV. METODOLOGÍA

IV.1 Área de estudio

Hermosillo, Sonora, México, se localiza en el paralelo 29° 05 de latitud Norte y el meridiano 110° 57 de longitud Oeste de Greenwich, a una altura de 282 metros sobre el nivel del mar. Se encuentra a 270 kilómetros de la frontera con los Estados Unidos. De acuerdo a INEGI (Censo del 2010), la ciudad cuenta con 715, 061 habitantes. La ciudad de Hermosillo está rodeada por actividades de tipo industrial y de agricultura, y el área de estudio se caracteriza por un rápido índice de crecimiento. El clima en Hermosillo es en su mayoría cálido-seco, con temperaturas de 38°- 42°C, durante el verano, y con inviernos fríos llegando alcanzar 7° C (Meza-Figueroa et al., 2007; Del Río-Salas et al., 2012). La geología de Hermosillo puede simplificarse en cuatro dominios: 1. Calizas del Mesozoico, 2. Intrusiones graníticas del Laramídico, 3. Flujos volcánicos del Mioceno, y 4. Cubierta del Cuaternario (Del Río-Salas et al., 2012). Los suelos en Hermosillo están compuestos principalmente por limo y material calcáreo residual producto de la cobertura, con un pH de 7 a 8, estos suelos son clasificados como arcilla arenosa basados en el análisis textural (arena: 52.2%; arcilla: 31.2 %; limo: 16.36 %). Los principales suelos localizados dentro del casco urbano son de tipo calcisol, cambisol, phaeozem y regosol. El suelo vertisol y leptosol se encuentran cerca de los límites de la ciudad (INEGI, 2007).
De acuerdo con las estadísticas de INEGI 2017, Hermosillo cuenta con un parque vehicular de 382,665 vehículos de motor registrados en circulación. Presentando una tasa de incremento del 45.18% con respecto al año 2007.

IV.2 Muestreo

En esta sección se indica de forma general las metodologías utilizadas en la presente investigación. Detalles del muestreo, preparación de muestra, técnicas analíticas e interpretación

de datos se indican en los artículos publicados que conforman el cuerpo de esta tesis en la sección Resultados.

IV.2.1. Muestreo de pintura amarilla

Se colectó pintura amarilla de calles en zonas de alto y bajo tráfico, utilizando una espátula de acero inoxidable y resguardándola en bolsa de polietileno (n=80). Detalles sobre las técnicas se proporcionan en la sección de Resultados, artículo 1, "Source apportionment and environmental fate of lead chromates in atmospheric dust in arid environments", apartado 3.1. Sampling and sample preparation.

IV.2.2. Muestreo de polvo

Se colectaron muestras de polvo de calle (n=146) de acuerdo con lo descrito por la USEPA AP-42C.1 (USEPA 2003), polvo sedimentado en techos (n= 21) y patios de escuela de escuelas primarias (n=35) siguiendo el procedimiento de Meza-Figueroa et al. (2007). Utilizando escobas y bolsas de polietileno. Detalles sobre las técnicas se proporcionan en la sección de Resultados, artículo 1, "Source apportionment and environmental fate of lead chromates in atmospheric dust in arid environments", apartado 3.1. Sampling and sample preparation.

IV.2.3. Monitoreo de concentración de Partículas Suspendidas Totales (PST).

Se monitorearon las Partículas suspendidas Totales a nivel suelo (peatonal) y nivel techo, mediante equipos manuales de alto volumen TISCH modelo TE-500 con flujos de aire entre 1.1–1.7 m^3/min, durante 24 horas, cada seis días, durante un año. El sitio de muestreo se ubicó en el centro de la ciudad en las instalaciones de la Estación Regional del Noroeste-UNAM. Se utilizaron filtros de fibra de cuarzo (Whatman 41) previamente estabilizados (T=20 ± 1 °C, 50% humedad), cada filtro se pesó al inicio y final con una balanza micro analítica modelo A200S-DB. Los muestreos y la obtención de concentración de partículas se realizaron con los parámetros y método gravimétrico de la USEPA- 40 CFR part 50 (USEPA,1997). Durante este periodo, nos integramos y colaboramos en el Programa de Evaluación y Mejoramiento de Calidad de Aire (PEMCA), dirigido por el ayuntamiento de Hermosillo. Obteniendo muestras de PST de cuatro sitios de muestreos ubicados estratégicamente en la ciudad (estación norte, noroeste y sur). Detalles sobre las técnicas se proporcionan en la sección de Resultados, artículo 2, "Traffic signatures in suspended dust at pedestrian levels in semiarid zones: Implications for human exposure", apartado 2.2. Sampling.

IV.2.4. Aforo vehicular

Se contabilizó el tráfico vehicular en el sitio de estudio, utilizando contadores manuales en un lapso de catorce horas continuas. Se clasificaron los vehículos en dos categorías: 1. vehículos pesados (camiones, remolques, autobuses) y 2. vehículos ligeros (camionetas, automóviles semicompactos y motocicletas) El aforo vehicular se realizó en dos ocasiones durante el periodo de monitoreo de PST. Detalles sobre las técnicas se proporcionan en la sección de Resultados, artículo 2, "Traffic signatures in suspended dust at pedestrian levels in semiarid zones: Implications for human exposure", apartado 2.2. Sampling.

IV.2.5. Muestreo de suelos periurbanos y urbanos

Se llevó acabo un muestreo de suelos periurbanos (n=5) y urbanos (n=10) en base a la norma NMX-AA-132-SCFI-2006. Utilizando la técnica de muestreo superficial de tresbolillo para la formación de una muestra compuesta. Se colectó una muestra por cada tipo de suelo presente fuera del área urbanizada de Hermosillo, Sonora, obteniéndose una muestra representativa del suelo tipo phaeozem, vertisol, calcisol, cambisol y regosol. Detalles sobre las técnicas se proporcionan en la sección de Resultados, artículo 3, "The role of soil mineralogy on oral bioaccessibility of lead: Implications for land use and risk assessment", apartado 2.1. Sampling and sample preparation.

IV.3 Procesamiento de muestras.

En esta sección se indica de forma general el procesamiento y tratamiento de las muestras utilizadas en la presente investigación. Se desglosan detalles en los artículos publicados que conforman el cuerpo de esta tesis en la sección Resultados.

Los filtros de fibra de cuarzo se cortaron y resguardaron siguiendo los estándares de calidad que dicta el procedimiento de la USEPA. Las muestras de polvos y suelos se secaron en horno a una temperatura de 36°C durante 24 horas, posteriormente se tamizaron para obtener la fracción más fina utilizando las mallas No. 18 (1000 µm), No. 35 (500 µm), No. 60 (250 µm), No. 120 (125 µm), No. 230 (63 µm), No. 325 (44 µm), No. 635 (20 µm) y No. < 635 (< 20 µm).

IV.4. Experimento de suelos y pigmentos amarillos.

Se tomó una muestra de pintura amarilla de calle y se pulverizó hasta llegar a la fracción más fina (<20m), se añadió 0.2 g de pintura a 3 g de cada tipo de suelo y se homogenizó la muestra. Posteriormente estas muestras se sometieron a un proceso in vitro para obtener la

bioaccesibilidad oral de acuerdo con Ruby et al (1993). Detalles sobre las técnicas se proporcionan en la sección de Resultados, artículo 3, "The role of soil mineralogy on oral bioaccessibility of lead: Implications for land use and risk assesment", apartado 2.1. Sampling and sample preparation.

IV.5 Técnicas analíticas

En esta sección se indica de forma general las técnicas analíticas utilizadas en la presente investigación. Se desglosan detalles en los artículos publicados que conforman el cuerpo de esta tesis en la sección Resultados.

IV.5.1. Técnica de bioaccesibilidad

Para obtener la bioaccesibilidad del plomo se realizó la prueba de extracción basada en fluidos fisiológicos PBET y su posterior análisis por ICP-OES (Ruby et al., 1993, 1996) en el Laboratorio de Geoquímica Ambiental del Laboratorio Nacional de Geoquímica y Mineralogía, en el Instituto de Geología de la Universidad Nacional Autónoma de México (UNAM). La prueba se realizó en (i) muestras de suelos fortificados con pintura amarilla con cromatos de plomo (crocoita) y (ii) suelos superficiales colectados en patios de juegos de escuelas primarias de Hermosillo, Sonora. La prueba PBET es un sistema de pruebas in vitro, en el que se simulan las condiciones fisicoquímicas del tracto gastrointestinal, incluyendo estómago e intestino delgado. La preparación de los fluidos y condiciones analíticas se detallan en la sección de Resultados, dentro del apartado 2.3. Pb bioaccessibility, del artículo 3 "The role of soil mineralogy on oral bioaccessibility of lead: Implications for land use and risk assesment".

IV.5.2. Técnica de fluorescencia de rayos X

Para obtener la concentración total de los elementos compuestos en la muestra de suelos y pintura, se llevó a cabo el análisis con un equipo portátil de fluorescencia de rayos X, mediante el método 6200 US EPA, y utilizando el equipo Equipo Thermo Scientific Nitton XLt3. Para el análisis se utilizó el método TestAll. Detalles sobre las condiciones de operación del equipo se detallan en la sección de Materiales y métodos, apartado 2.2. Mineralogy and total Pb concentration, del artículo 3 "The role of soil mineralogy on oral bioaccessibility of lead: Implications for land use and risk assesment".

IV.5.3. Técnica de microscopía electrónica de barrido y raman

Se analizaron las muestras de pintura, por la técnica de microscopia electrónica de barrido con equipo Hitachi Modelo TM3030 y Phenom ProX de Thermo Scientific, utilizando electrones secundarios (SE), electrones retrodispersados (BSE) y análisis composicional (EDS) para determinar la morfología y composición de cada muestra. Adicionalmente se llevó a cabo un análisis Raman utilizando el equipo X'plora modelo BX41TF OLYMPUS HORIBA Jovin IVON. Detalles sobre las condiciones de operación del equipo se incluyen en la sección de Materiales y métodos, apartado 3.2. Analytical techniques, del artículo 1 "Source apportionment and environmental fate of lead chromates in atmospheric dust in arid environments".

IV.5.4. Técnica de difracción de rayos X

Las muestras de suelo colectadas se analizaron con el Difractómetro PANalytical modelo Empyrean, emplazado en el Laboratorio de Difracción de Rayos X en el Instituto de Geología de la Universidad Nacional Autónoma de México. Así mismo se utilizó el equipo Difractometro Bruker modelo D8 Advance, localizado en el Laboratorio de Geoquímica y Cristalografía del Departamento de Geología de la Universidad de Sonora. Para la interpretación de difractogramas se utilizó el software Diffrac-plus EVA. Detalles sobre las condiciones de operación de los equipos se proporcionan en la sección de Resultados, dentro del apartado 2.2. Mineralogy and total Pb concentration del artículo 3 "The role of soil mineralogy on oral bioaccessibility of lead: Implications for land use and risk assesment".

V. RESULTADOS

V.1. **Distribución de la fuente y destino ambiental de los cromatos de plomo en polvo atmosférico en ambientes áridos.** Artículo: Meza-Figueroa, D., González-Grijalva, B., Romero, F., Ruiz, J., Pedroza-Montero, M., Rivero, C. I.-D., . . . Navarro-Espinoza, S. (2018). Source apportionment and environmental fate of lead chromates in atmospheric dust in arid environments. Science of The Total Environment, 630, 1596-1607. doi: https://doi.org/10.1016/j.scitotenv.2018.02.285

Source apportionment and environmental fate of lead chromates in atmospheric dust in arid environments

Diana Meza-Figueroa [a,f,*], Belem González-Grijalva [b], Francisco Romero [c,f], Joaquin Ruiz [d], Martín Pedroza-Montero [e], Carlos Ibañez-Del Rivero [f], Mónica Acosta-Elías [e], Lucas Ochoa-Landin [a,g], Sofía Navarro-Espinoza [f]

[a] Department of Geology. University of Sonora, Rosales y Encinas, Hermosillo, Sonora 83000, Mexico
[b] Earth Sciences Graduate Program. Institute of Geology, National University of Mexico. Colosio y Madrid, Hermosillo, Sonora 83240, Mexico
[c] Institute of Geology. National University of Mexico, Ciudad Universitaria, Delegación Coyoacán, Ciudad de México 04510, Mexico
[d] Department of Geosciences, The University of Arizona, 1040 E. 4thSt, Gould-Simpson Building 77, Tucson, AZ 85721, United States
[e] Department of Physics Research, University of Sonora, Rosales y Encinas, Hermosillo, Sonora 83000, Mexico
[f] Department of Geology. Graduate Program, Rosales y Encinas, Hermosillo, Sonora 83000, Mexico
[g] Laboratorio Nacional de Geoquímica y Mineralogía-LANGEM, Mexico

HIGHLIGHTS

- Isotopic data assess the presence of lead chromates on atmospheric dust
- Photodegradation of traffic yellow paint promotes crocoite crystals emission
- Crocoite crystals size range from <0.1 to 1 um representing inhalable fractions
- Pb—Cr common origin is reported for road dust, atmospheric dust, and settled dust on roofs

GRAPHICAL ABSTRACT
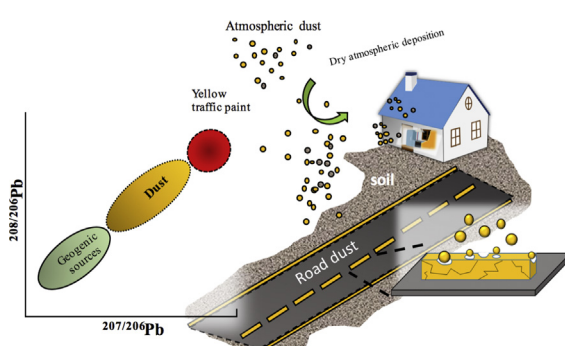
ARTICLE INFO

ABSTRACT

The environmental fate of lead derived from traffic paint has been poorly studied in developing countries, mainly in arid zones. For this purpose, a developing city located in the Sonoran desert (Hermosillo, Mexico), was chosen to conduct a study. In this paper the lead chromate (crocoite) sources in atmospheric dust were addressed using a combination of Raman microspectroscopy, X-ray diffraction, scanning electron microscopy (SEM), and Pb isotope measurements. A high concentration of Pb and Cr as micro- and nanostructured pigments of crocoite is reported in yellow traffic paint ($n = 80$), road dust ($n = 146$), settled dust in roofs ($n = 21$), and atmospheric dust ($n = 20$) from a developing city located in the Sonoran Desert. 10 samples of peri-urban soils were collected for local geochemical background. The paint photodegradation and erosion of the asphaltic cover are enhanced by the climate, and the presence of the mineral crocoite ($PbCrO_4$) in road dust with an aerodynamic diameter ranging from 100 nm to 2 μm suggests its integration into the atmosphere by wind resuspension processes. A positive Pb—Cr correlation ($R^2 = 0.977$) was found for all studied samples, suggesting a common source. The Pb-isotope data show signatures in atmospheric dust as a product of the mixing of two end members: i) local soils and ii) crocoite crystals as pigments in paint. The presence of lead chromates in atmospheric dust has not been previously

* Corresponding author at: Department of Geology. University of Sonora, Rosales y Encinas, Hermosillo, Sonora 83000, Mexico.
E-mail address: dmeza@ciencias.uson.mx (D. Meza-Figueroa).

documented in Latin America, and it represents an unknown health risk to the exposed population because the identified size of crystals can reach the deepest part of lungs.

1. Introduction

Arid conditions in urban environments are of special interest in environmental studies because extreme temperatures, low humidity, and the daily anthropogenic activity within a city may enhance the resuspension, transportation, and redeposition of dust in more sensitive environments (Sorooshian et al., 2012; Csavina et al., 2014; Laidlaw and Taylor, 2011). The dust in arid zones is an effective media of transport for traffic-derived contaminants (Karanasiou et al., 2011; Meza-Figueroa et al., 2016; Patra et al., 2008; Thorpe and Harrison, 2008); such pollutants include tire and brake abrasion products, combustion exhaust, traffic paint and pavement wear that are incorporated into the soil components, producing changes in the geochemical signatures of the mineral dust (Meza-Figueroa et al., 2016; Amato et al., 2011; Del Rio-Salas et al., 2012; Kreider et al., 2010). Road traffic emissions contribute to particulate matter pollution by: (i) exhaust emissions from motor vehicles; and (ii) non-exhaust emissions from vehicles, road surface abrasion, and re-suspension of road dust due to traffic-induced turbulence (Thorpe and Harrison, 2008; Meza-Figueroa et al., 2016). Implemented emission regulations in most countries, as well as the use of cleaner fuels, have reduced the primary exhaust emissions. However, Rexeis and Hausberger (2009) documented that 80 to 90% of total traffic emissions relate to non-exhaust sources. In such environmental context, non-exhaust emission to air pollution is particularly important for arid zones in developing countries where there are scarce regulations for this type of sources.

Traffic paint is a thin layer of blended materials, mainly composed of finely ground mineral pigments of crocoite ($PbCrO_4$) that are mixed into an organic matrix of polymers or a binder system for the characteristic yellow colour (Jeffs and Jones, 1999; Walraven et al., 2015). Crocoite naturally occurs as a secondary phase in the oxidizing domains of hydrothermal systems as a consequence of the release of Cr-rich fluids from ultramafic rocks (Frost, 2004), and the most important ore settings are located in Tasmania and Australia (Crane et al., 2001). In some developed countries, the crocoite-based pigments have been replaced with lead-free and chromium-free yellow substitute pigments. However, few countries have enacted regulations to phase-out all lead paints, and companies continue to market where there are no regulatory constraints (Gottesfeld et al., 2014). Recently, yellow paint has been considered to be an important source for Cr and Pb in urban environments in Asia, the United States and the United Kingdom (Lee et al., 2016; Turner et al., 2016; White et al., 2014). Nevertheless, in developing countries, there is a lack of information regarding the lead chromate presence in traffic paints in such a way that there is no knowledge about its potential risk to human health. Lead chromate from the yellow striping materials may contain nearly 20,000 mg·kg^{-1} of lead and nearly 5000 mg·kg^{-1} of hexavalent chromium, and they can be incorporated into the dust after road erosion. The alteration of organic and inorganic compounds in the paint could be related to climate conditions. The oxidation of the organic constituents is higher with increasing temperature and humidity, whereas changes in the oxidation states of the inorganic pigments are activated by light exposure (Monico et al., 2016). In arid climates, where the erosion processes are enhanced by higher temperatures and radiation induced by climate change, the degradation of the asphaltic cover led to the emission of particulate matter composed of geogenic (mineral) material and traffic-related pollutants, including the yellow paint particles; therefore, the hexavalent chromium, and lead from the released crocoite pigments could be inhaled.

Hexavalent chromium (CrVI) has been classified as an important toxic contaminant because there is no threshold with respect to chromium carcinogenesis (Alexeeff et al., 1989; Collins et al., 2010; Haney et al., 2014). In particular, Cr(VI) affects humans because mammalian cells are very sensitive to this pollutant, since they lack an efficient chromate detoxifying strategy (Liu et al., 2015). The presence of lead chromates in air is relevant because the water-insoluble micro- and nanosized particles of crocoite are more potent lung carcinogens, with a prolonged extracellular dissolution of hexavalent chromium (ATSDR, 2012; De Flora, 2000; Nickens et al., 2010). Recent studies documenting the photodegradation of chrome yellows show that $PbCrO_4$ is more prone to light-induced reduction than sulfate-based pigments (Amat et al., 2016); thus, crocoite pigment degradation may represent a particular risk in arid environments where extremely high temperatures are common. Previous work (Potgieter-Vermaak et al., 2012) documented that up to 19.3% of Cr and 46.5% of Pb derived from crocoite are readily mobilized in artificial lysosomal liquid. To the best of our knowledge, there are no previous reports from Mexico or Latin America regarding the presence of lead chromates associated with traffic paint in road dust and atmospheric dust collected by air filters. The aim of this work is (i) to examine whether yellow traffic paint (fresh and degraded) contained hexavalent chromium related to crocoite pigment, (ii) to investigate the distribution of Cr and Pb in the road and atmospheric-dust, and (iii) to evaluate whether the lead chromates affected atmospheric dust using lead isotopic fingerprinting.

2. Study area

Hermosillo City is located in northwestern Mexico, within the Sonoran Desert province (Fig. 1). The weather conditions are characterized by a high temperature range from 35 to 49 °C during summer, and a low temperature ranging from 8 to 5 °C during winter. The climate is dry for most of the year, and the region is affected by short duration but intense rainfall during the summertime monsoon. The erosive potential of the North American Monsoon in Hermosillo enhances dust emissions within the urban area, mainly because of strong surface runoff, the erosion of paved and unpaved roads, and the subsequent suspension processes due to traffic (Meza-Figueroa et al., 2016; Moreno-Rodríguez et al., 2015). In the last two decades, the city has experienced rapid growth from 406,417 inhabitants in 1990 to 715,061 in 2010 (Del Rio-Salas et al., 2012), with a population increase rate of ~3%, greater than the increase rate of state population (1.4%). This suggests the migration of the state population into Hermosillo City and a rise in the vehicular traffic volume. Due to the strong erosion of street surfaces during the rainy season, traffic signals on the paved surface must be constantly painted during the year.

3. Materials and methods

3.1. Sampling and sample preparation

Samples of yellow traffic paint samples ($n = 80$) were obtained by scratching the road with a stainless spatula. Road dust ($n = 146$), dust settled in roofs ($n = 21$), and atmospheric dust or total suspended particulate matter in air filters ($n = 20$), samples were collected from high and low traffic areas. The geochemical background was obtained from 10 soil samples that were not impacted by anthropogenic activities. Soil sampling sites are located outside the urbanized area (Fig. 1). Soil samples were collected to a depth of 10 cm after surface was scraped
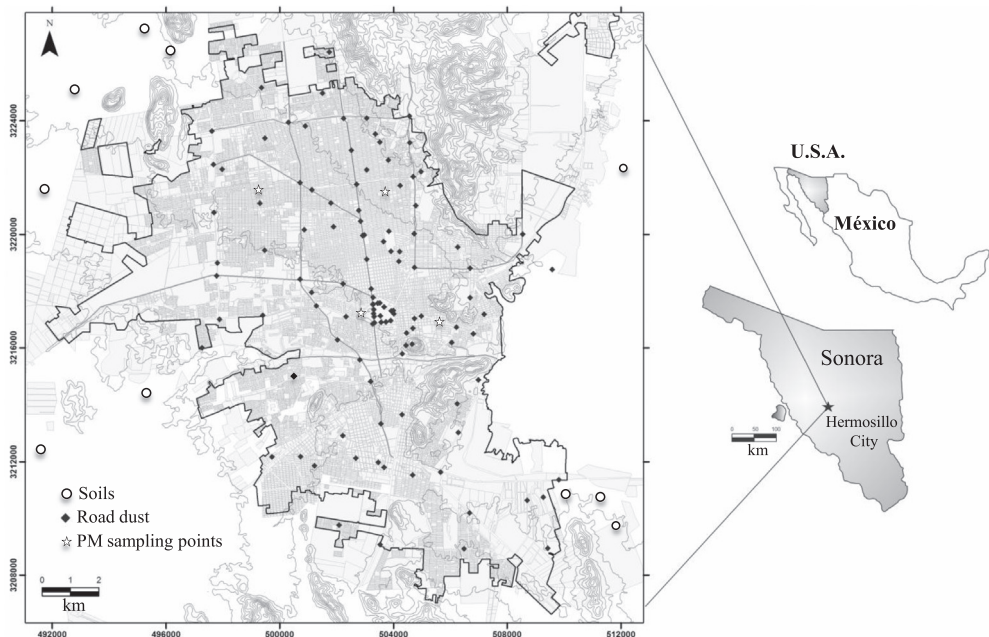
Fig. 1. Location map of the sampling points. Dark lines are high traffic roads. PM sampling points: atmospheric dust. Soils were collected outside the urbanized area (peri-urban soils).

to remove smeared soil, a stainless steel spoon was used and collected samples were placed in plastic bags, labeled and dried overnight at 40 °C. Dried bulk soil samples were powdered with an agate mortar for further analysis.

The road surface dust samples were collected within an area of two square meters using a polyethylene brush, tray, and bags according to procedures described by the U.S. EPA in AP-42C.1 documents (USEPA, 2003). Settled dust samples from elementary school roofs were collected following procedures described in Meza-Figueroa et al. (2007). Road dust, roof dust, and soil samples were sieved, and a final fraction passing through the mesh #325 was obtained. This fraction corresponds to a particle size smaller than 44 μm in aerodynamic diameter, representing a fraction that is most likely to be suspended in arid environments, or it could remain within the upper part of respiratory tract (Ruby and Lowney, 2012; Newman, 2001).

Atmospheric dust samples were collected using a high-volume TISCH air sampler model TE-5000, with a flow rate of 1.1 m^3 min^{-1}, at four sampling sites. Samples were collected on Whatman 41 quartz microfiber filters. The air filters were equilibrated in a desiccator for 48 h and then weighed before aerosol sampling. The gravimetric determination of the mass filters was performed in a humidity and temperature controlled room (50%, and 20 ± 1 °C, respectively), and a Sartorius analytical microbalance, Model A200S-D1B, was used. The quartz fiber field blanks and sample filters were transferred into clean high-density polyethylene vials and sent for sample digestion and analysis.

3.2. Analytical techniques

The hexavalent chromium in the collected traffic paint was analyzed by the ALS Environmental, Group, Jacksonville, FL, USA, according to EPA Method 3060A based on alkaline digestion (0.28 M Na_2CO_3/0.5 M NaOH) to solubilize both water-insoluble and water-soluble Cr(VI) compounds in solid samples. The quantification of Cr(VI) was conducted using Method 7196 (colorimetric detection by UV-VIS spectrophotometry), based on the reaction of Cr(VI) with diphenylcarbazide. Reported detection limit for hexavalent chromium is 0.040 mg·kg^{-1}.

A portable XRF analyzer, a Niton XL3t instrument from Thermo Scientific, was used to obtain the Cr and Pb concentrations in the road dust, settled dust in roofs, and paint samples following Method 6200 of the

US EPA. The detection limits of Cr and Pb were 25 mg·kg^{-1} and 10 mg·kg^{-1}, respectively. With the purpose of validating the quality of the data obtained, a set of samples were analyzed at ALS CHEMEX Laboratory in Toronto, Canada, and at the Arizona Laboratory of Emerging Contaminants (ALEC-University of Arizona, Tucson), and the obtained results were compared with those retrieved using the portable XRF analyzer. The data agree within a 95% confidence level. Filters with atmospheric dust samples were analyzed at the ALEC-University of Arizona (Tucson), according to Method IO-3.1 (USEPA, 1999).

Road dust samples and yellow traffic paint samples were analyzed by means of micro-Raman spectroscopy without previous treatment using X'plora equipment, model BX41TF Olympus Horiba Jobin YVON, with a class 3B argon laser (20–25 mW and 532 nm) at the University of Sonora. The operating conditions were as follows: spectral field resolution of 2400 g/mm in a wave vector range of 50–2000 cm^{-1} with the dispersion of a 50 μm slot at 6.5 cm^{-1}/mm. The acquisition time for the spectra collection in extended mode, using a continuous grating mode, was 10 s with 15 cycles for most of the samples. The fitting of the spectrum was performed using Lab Spec software and SigmaPlot 11.0 (pseudo-Voigt function).

Traffic paint and road dust samples were also analyzed by X-ray powder diffraction (XRD) using a Bruker Advance D8 diffractometer. The urban dust and paint samples were homogenized and compacted. The operating conditions were 40 kV/35 mA with a Cu-radiation source $\lambda(K\alpha1) = 1.5406$ Å. The collection of the XRD patterns was based on a 2θ range of 4–55 and a step size of 0.005°.

The morphology and semi-quantitative analyses of the crocoite crystals in paint were performed at the National Laboratory of Geochemistry and Mineralogy using a Hitachi tabletop scanning electron microscope TM3030plus, coupled with a Bruker Quantax 70 energy dispersive X-ray spectroscopy (EDX) analysis system operating at 15 kV. The morphology and particle size images with a detection range of 100 nm to 100 μm (magnification range of 80–130,000× and resolution of ≤14 nm) were obtained using a Phenom ProX desktop SEM/EDS analysis system with the assistance of PetroServicios Company in Mexico. A crocoite solid standard (ASTIMEX MINM25-53 Serial 1Al) was used to check instrument performance.

Twice distilled acids were used for sample preparation and treatment in the measurements of the lead isotope ratios in the dust and

Table 1
Chromium (Cr) and lead (Pb) concentrations in the studied samples. All concentrations are in mg·kg^{-1}, unless otherwise stated. SD: Standard Deviation.

	Traffic paint			Local soils		Road dust		Atmospheric dust (filters)		Settled dust in roofs	
	n = 3	n = 80		n = 10		n = 146		n = 20		n = 21	
	Cr^{IV}	Cr	Pb	Cr	Pb	Cr	Pb	Cr	Pb	Cr	Pb
Maximum	4460	11758.1	88662.1	120	38	257.5	778.1	10.4	24.5	240.3	261.6
Minimum	3580	1294.2	5909.8	40	15	112.7	21.7	3.6	6.7	128.8	29.3
Average	3981	5839.5	42872.8	66.7	25	168.5	147.4	6	14.7	156	70.3
SD	363.5	3667.6	29472.1	23.1	6.4	28.9	149.9	2	5.8	31.3	56.8

source materials (crocoite crystals from Dundas, Tasmania; yellow traffic paint, rocks, and soils). Approximately 1 g of the finer fraction (<200 mm) was digested using Savillex Teflon containers in 16 M HNO$_3$ and left overnight. After digestion, the samples were evaporated to total dryness. For the lead separation, 8 M HNO$_3$ was added to the samples prior to the chromatographic separation using Sr-Spec resin. The lead isotope analyses were conducted on a GV Instruments multi-collector inductively coupled plasma mass spectrometer (MC-ICP-MS) at the Department of Geosciences, University of Arizona. The analysis of the NBS-981 standard produced the following results: $^{206}Pb/^{204}Pb$ 1/4 16.9405 (0.0029 2s), $^{207}Pb/^{204}Pb$ 1/4 15.4963 (0.0034 2s), and $^{208}Pb/^{204}Pb$ 1/4 36.7219 (0.0099 2s).

3.3. Quality control/quality assurance

For soil, road dust, settled dust in roofs, and traffic paint sampling, sterile plastic sample containers were used to avoid cross contamination. Location of each sample was obtained by a GPS (Global Positioning System device GARMIN).

The analytical performance of the portable X-ray fluorescence equipment, was evaluated by following the procedures described in the 6200 method of the United States Environmental Protection Agency (USEPA). A certified analytical blank of silicon dioxide (quartz) was used. The precision (%RSD) and the accuracy (%) were evaluated on the basis of the analysis of seven replicates of each of the NIST standard

reference materials 2709, 2710, and 2711. An acceptable %RSD obtained range is 92 to 114 for all analyzed elements. Detection limits are expressed in mg·kg^{-1} (based on a 99.7% confidence level for a 120 s test) as follows: Zr (6), Sr (5), Rb (6), Pb (14), As (7), Zn (20), Cu (43), Fe (100), Mn (28), Cr (25), Ti (150), Ca (20), and K (15).

3.4. Statistics

Statistical analysis was carried out with the GraphPad Prism 7 software. The behavior of the data was evaluated by Sharpiro-Wilk normality non-parametric test. This was done by a determination of variance using Kruskal-Wallis test and multiple comparison of medium-sized by Dunn's test, using a confidence interval of 95%.

4. Results and discussion

Table 1 shows a summary of the Cr and Pb concentrations in road dust, traffic paint, atmospheric dust and local soils (geochemical background). The hexavalent Cr average content in the yellow traffic paint was 3981 mg·kg^{-1}. The local soils show low average concentrations of Cr (40 mg·kg^{-1}) and Pb (15 mg·kg^{-1}). The minimum Cr and Pb content in the road dust were 112.7 mg·kg^{-1} and 21.7 mg·kg^{-1}, respectively, which are higher than the average Cr value in the local soils from the study area, thus indicating an anthropogenic component. Atmospheric
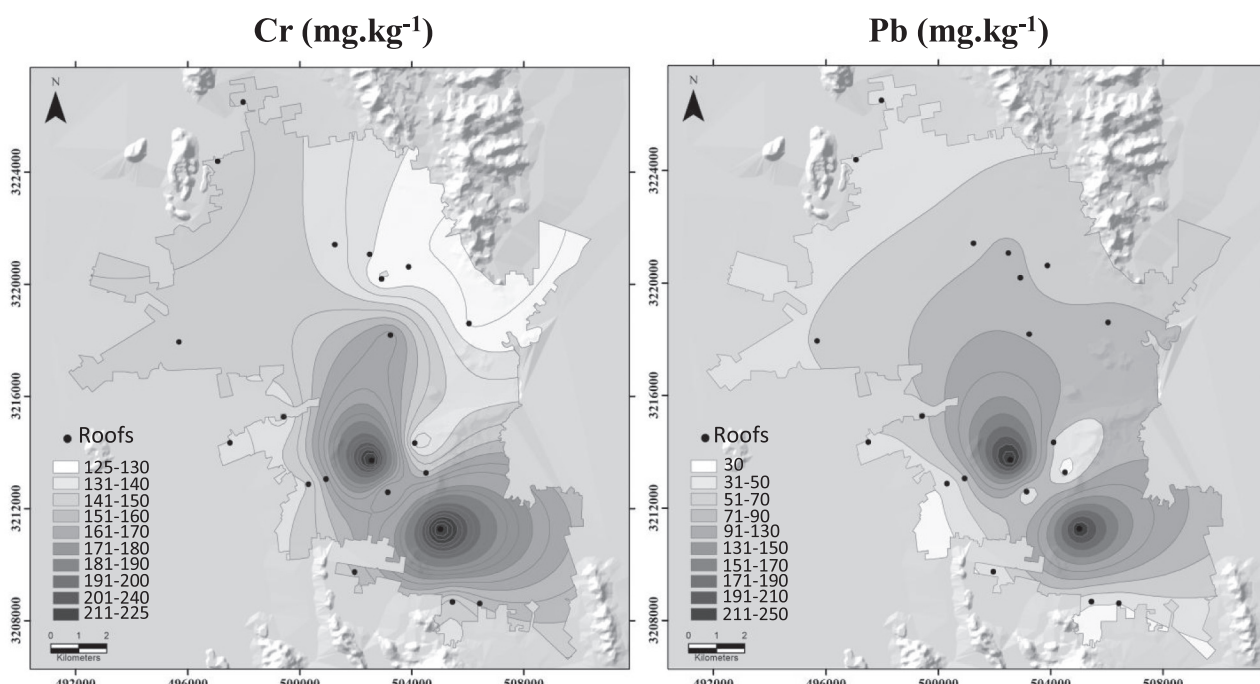
Fig. 2. Spatial Pb and Cr distribution in settled dust collected at roofs. Black solid line shows the urbanized area. Gray lines are main roads. Concentrations are in mg·kg^{-1}.

Cr (mg.kg⁻¹)　　　　　　　　　　Pb (mg.kg⁻¹)
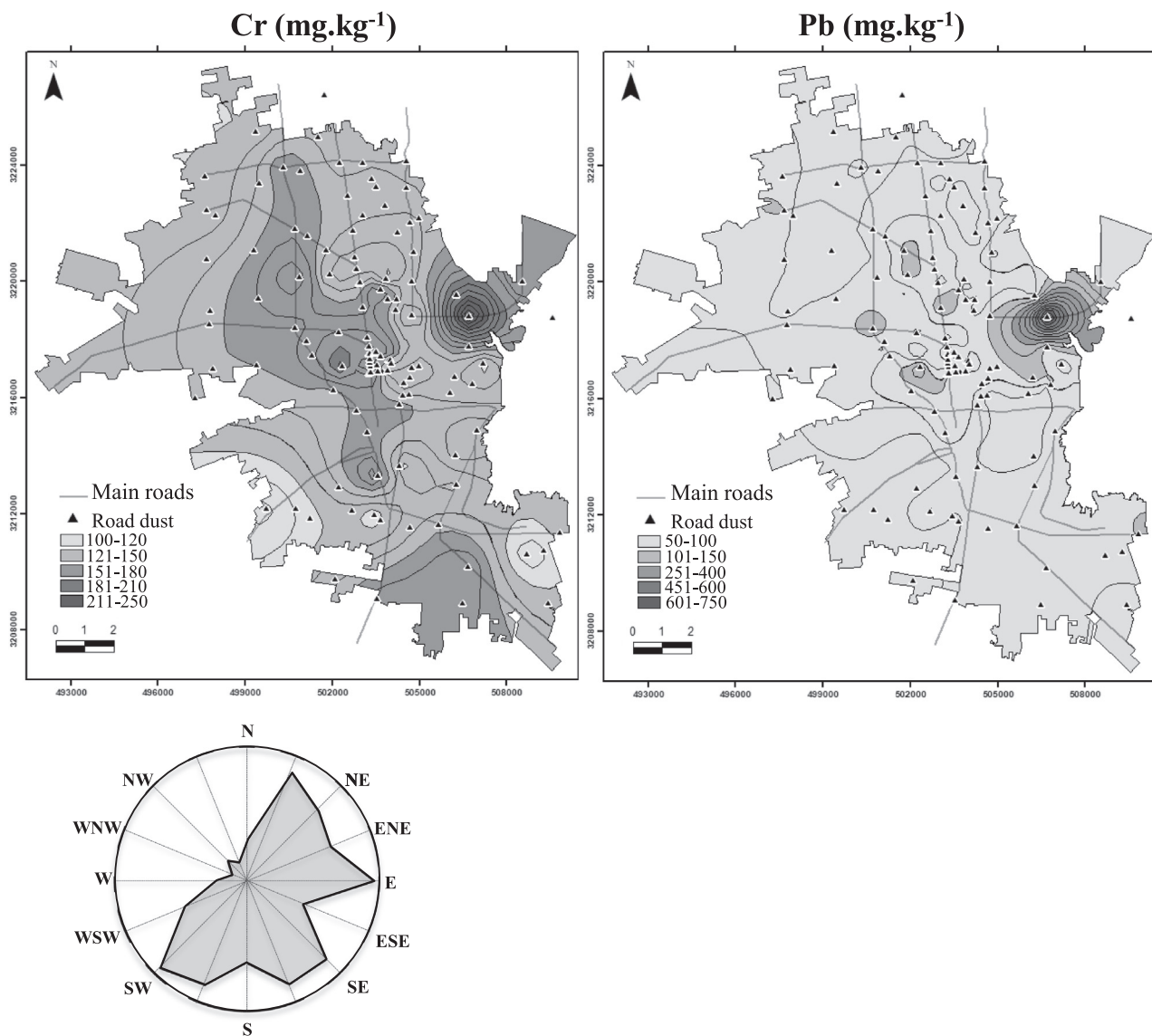
Fig. 3. Spatial Pb, and Cr distribution in road dust. Wind rose is shown for reference. (For interpretation of the references to colour in this figure legend, the reader is referred to the web version of this article.)

dust collected in filters showed Cr and Pb contents lower than settled dust in roofs.

Surface-deposited dust in roofs is a simple medium for assessing seasonally metal loading to atmosphere through eolian processes. The settled dust in roof material represents airborne dust sinking by atmospheric dry deposition. The total Cr, and Pb concentrations in the roof-deposited dust collected in 21 elementary schools are displayed in Fig. 2. The highest Cr and Pb content of 257.5 and 778.1 mg·kg^{-1}

respectively, occurs mainly within the oldest urbanized area around the city, following a pattern previously described as a Pb bulls-eye by Filippelli et al. (2005). This characteristic pattern of urban enrichment trending towards the local geochemical background is documented in surface soils (Laidlaw and Filippelli, 2008) but it is scarcely documented in dust deposited in roofs. This spatial distribution is commonly related to resuspension of road dust and roadside soil with a decreasing concentration proportional to the historical traffic volume (Meza-Figueroa et

Table 2
Cr mean contents in road dust from cities worldwide. nr: not reported. Concentrations are in mg·kg^{-1}.

City	Cr	Pb	Reference
	Median (range)	Median (range)	
Hermosillo, Mexico	142 (50-257.5)	216.5 (47-778.1)	This study
Punjab, Pakistan	6 (5-49)	108 (97-306)	Mohmand et al (2015)
Shiraz, Iran	67.2 (31.6-106)	115.7 (36.8-234.3)	Keshavarzi et al (2015)
Manchester, England	171 (n.r.)	238 (n.r.)	Potgieter-Vermaak et al (2012)
Toronto, Canada	197.9	182.8	Nazzal et al (2013)
Thessaloniki, Greece	187.3	191	Bourliva et al (2017)
Beijing, China	427	596	Zhao et al (2010)
Anand City, Gujarat, India	(118-151.5)	nr	Bhattacharya et al (2013)

Table 3
Geochemical analyses of traffic yellow paint collected from streets at the study site; n is number of samples.

Element	n	Maximum (mg·kg^{-1})	Minimum (mg·kg^{-1})	Mean (mg·kg^{-1})
Zr	80	169.81	32.02	79.66
Sr	80	34,252.68	82.81	10,459.17
Rb	80	26.30	3.57	14.17
Pb	80	88,662.06	5909.84	42,872.75
As	80	4337.11	77.12	1924.25
Zn	80	567	19.34	152.58
Cu	80	48.65	14.49	26.69
Fe	80	5843.27	1192.82	3762.76
Mn	80	383.31	78.23	201.75
Cr	80	11,758	1294	5839
Ti	80	7964	321	2498
Ca	80	297,550	35,241	130,112
K	80	6060	1601	3244
Cr^{VI}	3	4460	3580	3903

al., 2016; Filippelli et al., 2005). Two main areas with high Cr—Pb concentrations can be identified within the city. Each area is related to both main traffic roads and local urban basins, representing both the dust/sediment accumulation areas and emission sources. Rio-Salas et al. (2012) documented a Pb-isotopic signature of leaded gasoline in settled dust collected in roofs at Hermosillo city. Such signature is indicative of a Pb-legacy in soil, as well as evidence of re-suspension processes controlled by traffic, weather, and a NW-SE oriented granitic belt (hills) which acts as a topographic barrier that prevents dust dispersion by wind with a 23°–68° SW-NE direction (50% in wind rose). Fig. 3 shows the spatial distribution of Cr and Pb in road dust. Higher concentrations of both metals are related to main roads in the city, with clusters in the central-eastern side, as well as a N—S pattern (Cr). Central-eastern area of the city corresponds to the oldest urbanization, adjacent to central part of the granitic hills. Yearly wind direction (Fig. 3) shows a pattern that seems to favor the dust dispersion from the main roads and later settled in the roofs. Similar spatial distribution for Cr and Pb in roofs point to a common source.

Table 2 is included for comparison with the Cr contents in road dust from cities worldwide. The maximum Cr value found in this work is higher than the reported values for most cities worldwide and is only lower than the Cr and Pb values reported for Beijing, China (Zhao et al., 2010). The average Cr and Pb values reported in this work are similar to those documented for cities worldwide, thus, depending on the local
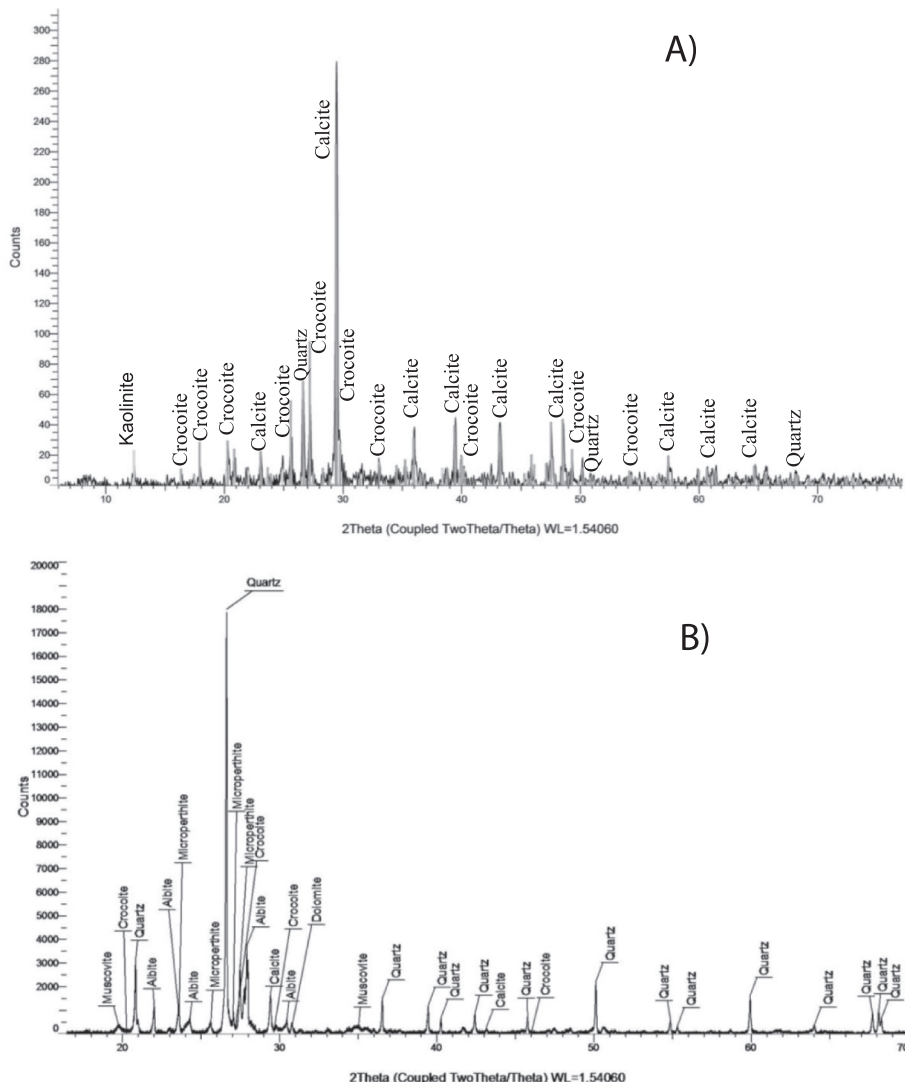

Fig. 4. **(A)** X-ray diffractogram of traffic yellow paint collected in the study area; **(B)** XRD analysis of road dust, showing the presence of quartz, plagioclases, and crocoite (lead chromate). (For interpretation of the references to colour in this figure legend, the reader is referred to the web version of this article.)

geochemical background for these cities, there is the possibility that the source for Pb and Cr could be related with lead chromates.

The yellow traffic paint composition is summarized in Table 3. Zr, Sr, Pb, As, Mn, Ti, Ca, K, S, Sb, Sn and Cr show high values. In this work, XRD analyses of traffic paint (Fig. 4A) show that calcite, quartz, and kaolinite are the major minerals in addition to crocoite. Collected road dust from areas with Cr and Pb enrichment (Fig. 4B) shows the presence of crocoite ($PbCrO_4$) and geogenic components such as quartz, muscovite, albite, and microperthite. Previous work (White et al., 2014; Wang et al., 2010) reported that the presence of calcite in yellow paint may increase the physical degradation of the paint, thus releasing crocoite nano- and micro-pigments over time.

Fig. 5 shows SEM images and representative EDS spectra for A) crocoite standard; B) degraded yellow paint with typical glass spherules (circles show crocoite crystals) within a binder system, and C) fresh yellow paint. Fresh paint was obtained from non-eroded surface in main roads, as well as from a can provided by municipal workers after painting. Degraded paint corresponds to eroded surface after rainy season (summer). In Fig. 5B and C, the crocoite minerals are shown in white colour as subhedral crystals mostly smaller than 1 μm, but Fig. 6 shows crocoite crystals in degraded paint that can be smaller than 0.1 μm (100 nm); particles less than 1 μm reach the deepest portions of the lungs (alveoli), where the active exchange of carbon dioxide and oxygen occurs (Plumlee and Ziegler, 2005). Thus, the physical degradation of yellow paint and the further release of lead chromates represents a particular environmental concern in arid zones (see Supplementary material). White et al. (2014) reported lead chromates in traffic paint collected in the city of Hamilton, Ohio, U.S., authors proposed that there is a legacy of lead chromates pollution in street sediment, air, and in stormwater, however the environmental matrices were not studied to determine the presence of $PbCrO_4$. Potgieter-Vermaak et al. (2012) reported Cr-rich particles with Pb in road dust samples by using micro-Raman spectroscopy. Computer-controlled electron probe X-ray micro-analysis showed a > 50% association of Cr-rich particles with Pb, as well as the presence of PbO, in the study, metals and minerals were not quantified (Potgieter-Vermaak et al., 2012). Lee et al.
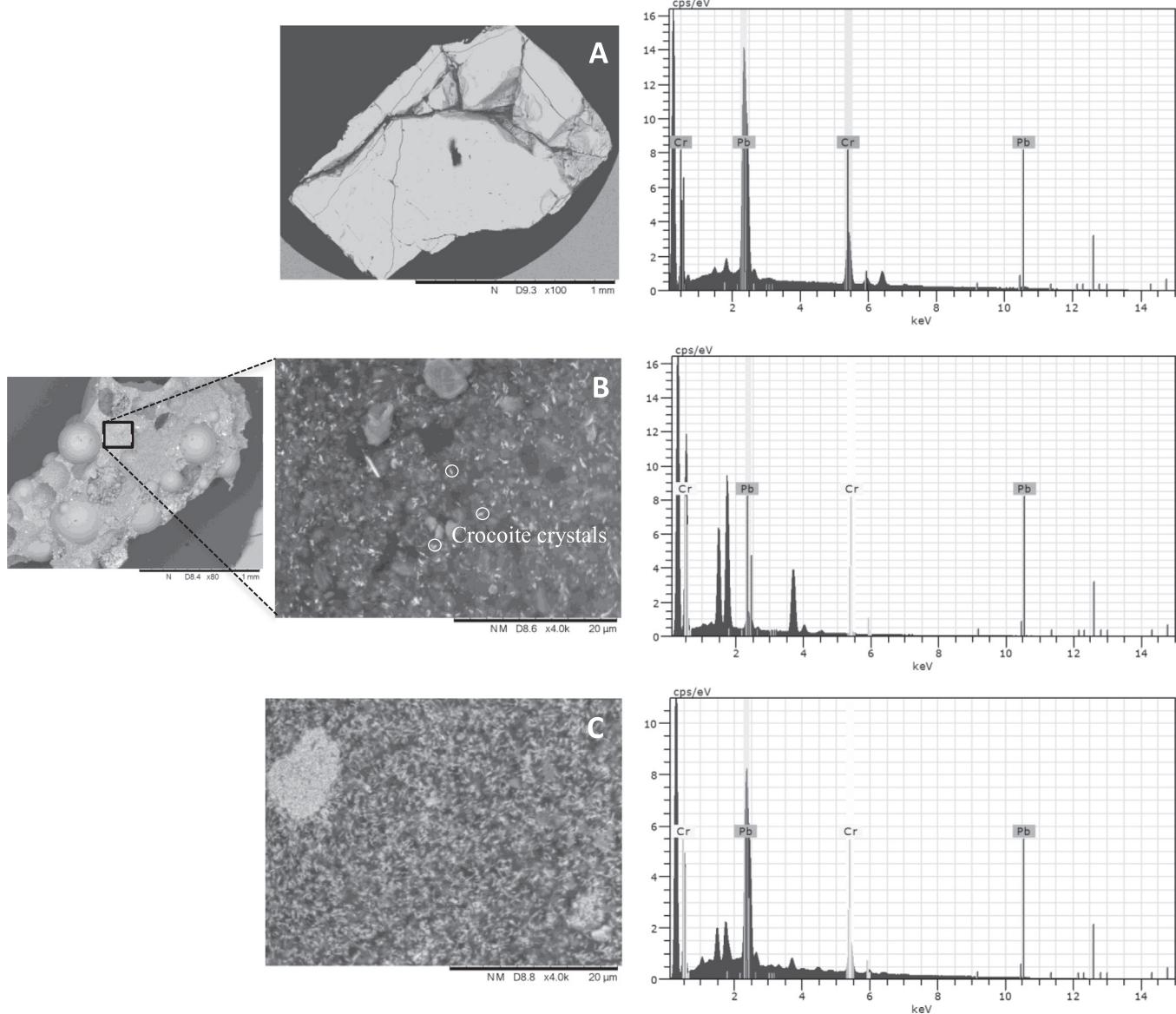
**Fig. 5.** Scanning electron micrographs of particles. A) crocoite standard with characteristic peaks for Pb and Cr. (B) Photodegraded yellow traffic paint showing crocoite crystals smaller than 0.1 um; B) fresh yellow traffic paint showing a greater abundance of lead chromate crystals. (For interpretation of the references to colour in this figure legend, the reader is referred to the web version of this article.)

(2016) identified nanosized lead chromate particles in atmospheric particulate matter, most possibly originated from traffic paint used in roads. For mixed matrices such as dust, the XRD detection limit is approximately 2% of the sample. The identification of lead chromates in road dust in this work is evidence of its presence in amounts above 2%. Previous works (White et al., 2014; Potgieter-Vermaak et al., 2012; Yang et al., 2015) did not report crocoite in urban dust by the XRD technique because of its detection limit. Because there are not previously documented studies of this nature in an arid area, the higher crocoite release rates could remain unidentified in areas with similar climate conditions.

The micro-Raman spectra of road dust from a high-traffic road and yellow paint are shown in Fig. 7. The continuous lines correspond to the pseudo-Voigt function being used in order to obtain better accuracy in the normal modes of vibration of Raman spectroscopy. A spectral comparison was performed using the Rruff Raman Database, and these vibrations can be associated with the presence of undifferentiated iron or lead oxides.

Fig. 7 shows the micro-Raman spectra of fresh yellow paint, depicting typical Raman scattering spectra at 135, 325, 358, 338, 378, 400, and 849 cm^{-1} (similar to those reported by Frost, 2004). There are three distinctive vibrations at ~338 cm^{-1}, ~358 cm^{-1}, and ~840 cm^{-1} wavenumbers, associated with the mineral crocoite contained in the yellow paint.

The fresh yellow traffic paint contains higher Pb and Cr concentrations than those measured for the degraded traffic paint (Fig. 8). This suggests that the photo degradation of the paint releases micro- and nanosized lead chromate pigments as well as lead oxides (scrutinyite) into the environment. These results suggest that more research should be focused on the mineralogical characterization of road dust impacted by traffic paint, since lead oxides are highly bioaccessible. It has been widely documented that the monthly average lead content in children's blood from urbanized environments tends to increase during the hottest months of the year (Haley and Talbot, 2004; Johnson and Bretsch, 2002; Laidlaw and Filippelli, 2008; Yiin et al., 2000). The reported findings suggest that children seem to be more exposed to Pb from indoor
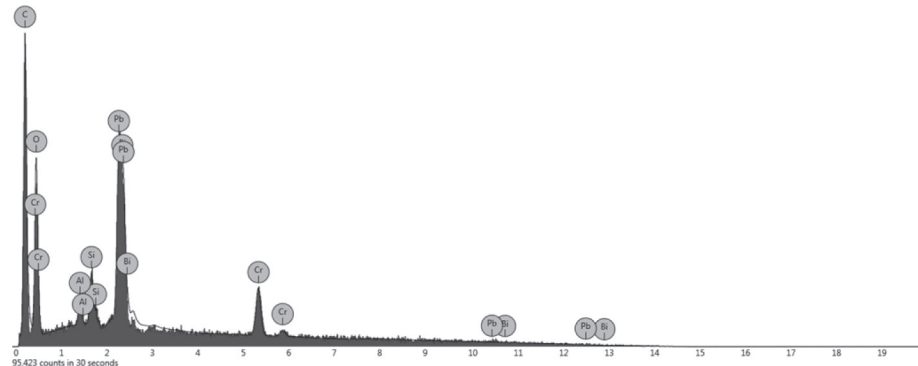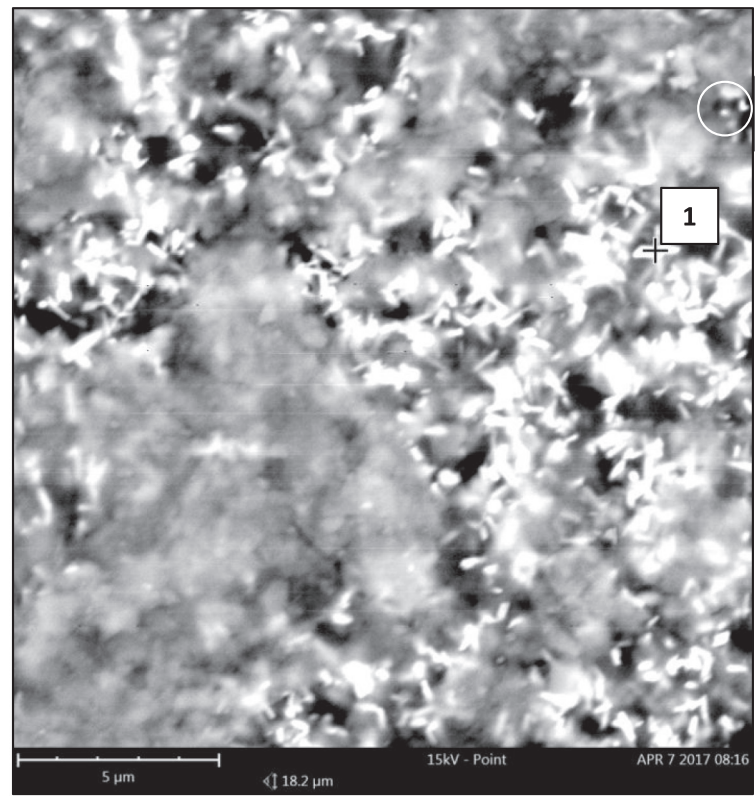

Fig. 6. SEM image of yellow traffic paint and EDS spectra of crocoite crystals smaller than 0.1 μm or 100 nm. 1: EDS spectrum. (For interpretation of the references to colour in this figure legend, the reader is referred to the web version of this article.)
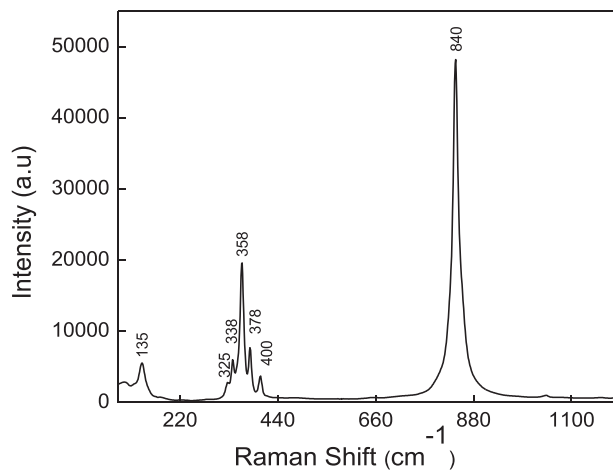
Fig. 7. Representative micro-Raman spectra for crocoite in studied fresh paint.

and outdoor dust during the summer because weather and low soil moisture promote dust suspension and exposure. However, the specific lead sources remain under discussion (Laidlaw et al., 2005). The results from this work suggest that the lead oxides, and lead chromates input into atmospheric dust could be a seasonal source of Pb in urban environments, as well as an important exposure path to lead by ingestion and inhalation.

Despite their toxicity, the presence of lead chromates in urban dust has been scarcely documented (White et al., 2014; Laidlaw and Filippelli, 2008). Laidlaw and Filippelli (2008) proposed that resuspension of roadside soils during dry weather may contribute to the seasonal Pb loading rates in urban areas. Settled dust in the roof surface accumulates from atmospheric dry deposition, thus representing an indicator of seasonal air pollution (Meza-Figueroa et al., 2007; Lye, 2009). A linear regression of Pb and Cr contents in atmospheric dust, road dust, settled dust in roofs, and traffic paint gave a R^2 of 0.977 and a slope of 0.13, indicating a possible common source in all studied matrices most likely

related to traffic paint in addition to leaded gasoline (Fig. 8). The Pb and Cr content decreased as follows: fresh paint > degraded paint > road dust > settled dust > atmospheric dust. This suggests that a traffic-related resuspension process incorporates a distinct anthropogenic geochemical signature into dust. Dunn's test is a non-parametric analog of the Anova test that is used to do comparisons between groups of data to find out which one is significant. It is used after rejection of a Kruskal-Wallis test. According to Dunn's multiple comparison test (95% confidence), road dust and atmospheric dust, as well as road dust and settled dust in roof do not show statistical differences in Pb and Cr. Atmospheric dust and settled dust in roof show significant difference for Cr but not for Pb (Fig. 9).

The results of the lead isotopic ratios are provided as supplementary data file. Lead isotopic ratios suggest the integration of Pb from crocoite into dust (Fig. 10). When the Pb from two endpoints or sources is mixed, the isotopic ratio will remain on a nearly straight line between the end members; in this case, a geogenic source corresponds to soils and rocks, and the "anthropogenic" source is related to sources including leaded gasoline, and the crocoite crystals used to manufacture yellow traffic paint. Lead isotopic signature of leaded gasoline falls within the same field as traffic paint, as well as road dust and settled dust in roofs. In a previous work, Rio-Salas et al. (2012) used lead isotopes in urban dust to discuss an unknown possible end-member for airborne dust in Hermosillo, that seems to be related to Australian and Canadian type lead ores. Whether the anthropogenic end-member corresponds to paint or lead-based motor vehicle wheel weights or contribution from other sources such as Asian dust, it remained under discussion. In this work, the data suggest that the traffic paint contribution to lead is not negligible, and that in arid zones, it could be an important source after leaded gasoline legacy. The positive Pb—Cr correlation among atmospheric dust, settled dust in roofs and road dust seems to support that Pb and Cr has a common origin, and the lead isotopic signatures provide additional evidence that another important source could be the traffic paint. Lead derived from gasoline still the most relevant source in urban environments, but lead chromates contained in traffic paint is linked to hexavalent chromium in the form of crocoite crystals. The importance of the obtained data is that such crystals are occurring in aerodynamic sizes ranging from nanometer to 10 μm. Such size allows these particles to reach deepest areas of lungs were dissolution occur with
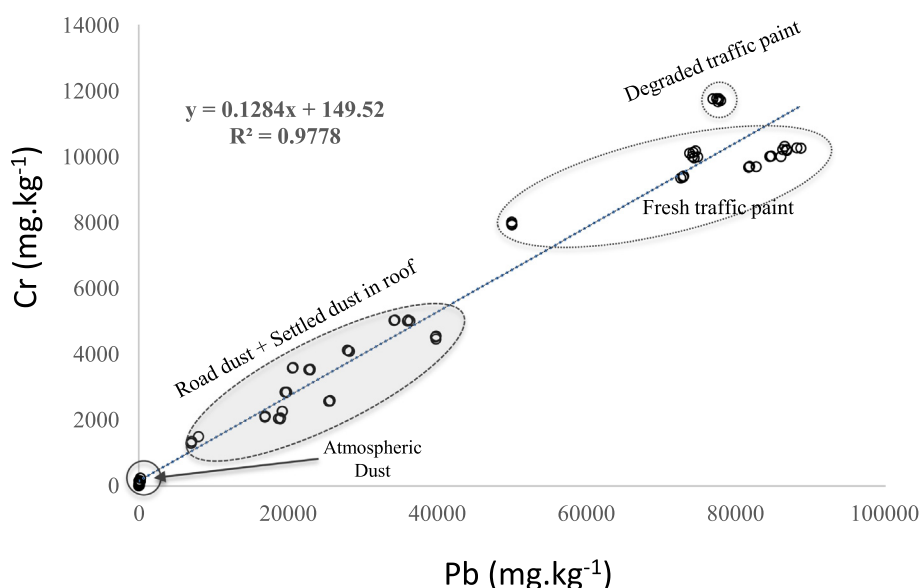
Fig. 8. Linear regression of Pb, and Cr concentrations in the atmospheric dust, settled dust in roofs, road dust, and traffic yellow paint. (For interpretation of the references to colour in this figure legend, the reader is referred to the web version of this article.)
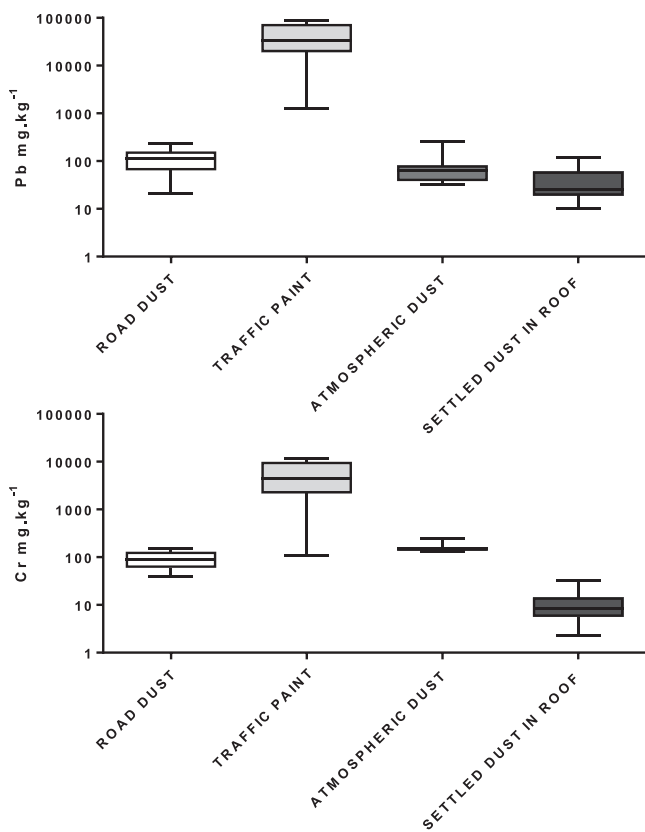
Fig. 9. Mean total Pb and Cr contents (mg·kg^{-1}) and standard errors in the different studied samples.

traffic paint, and the road-dust collected from the streets in Hermosillo. This pattern implies that atmospheric dust (both suspended and settled) is the result of a clear mixing of (i) the dust derived from soil resuspension or geogenic sources, and (ii) polluted dust with different lead sources including leaded gasoline, and crocoite crystals contained in traffic paint.

5. Conclusions

Natural processes such as weathering, erosion, wind transport and deposition of mineral dust in arid zones, enhance mobility of pollutants such as lead chromates (crocoite) related to pigments in traffic yellow paint. Mineral dust in urban environments could act as sink and source for traffic pollutants, and humans can be exposed via ingestion or inhalation. This work provides additional evidence of the presence of nano- to micro-sized crocoite minerals in the atmosphere. Because of the aerodynamic size of identified crystals, these could reach the deepest part of lungs where dissolution and further release of hexavalent chromium and lead could occur. The environmental fate of the crocoite pigments from yellow traffic paint used in Latin America has not been previously addressed, and it represents an unknown health risk to the exposed population, mainly in arid climates where paint photodegradation most likely occurs. This work highlights the strong need for strategies to reduce non-exhaust traffic emissions and suspension of mineral dust.

Supplementary data to this article can be found online at https://doi.org/10.1016/j.scitotenv.2018.02.285.

time, and in such conditions, chromium is not transformed to chromium III but it remains as a hexavalent form which is well documented as carcinogenic.

Fig. 10 shows that atmospheric dust collected from air filters located half way along the line and with the isotopic fingerprint of the yellow

Fig. 10. Lead isotopic compositions (^{208}Pb/^{206}Pb vs ^{207}Pb/^{206}Pb) in dust collected on air filters (atmospheric dust), road dust (dashed line), crocoite crystals, yellow traffic paint, and non-impacted local soils. Shaded-gray area represents settled dust in roofs. The isotopic Pb ratios of the surrounding rocks and settled dust in roofs are taken from Del Rio-Salas et al. (2012). Solid rectangle corresponds to data for Mexican gasoline from Sañudo-Wilhelmy and Flegal (1994). (For interpretation of the references to colour in this figure legend, the reader is referred to the web version of this article.)

Funding

References

Alexeeff, G.V., Satin, K., Painter, P., Zeise, L., Popejoy, C., Murchison, G., 1989. Chromium carcinogenicity: California strategies. Sci. Total Environ. 86:159–168. https://doi.org/10.1016/0048-9697(89)90202-7.

Amat, A., Miliani, C., Fantacci, S., 2016. Structural and electronic properties of the PbCrO₄ chrome yellow pigment and of its light sensitive sulfate-substituted compounds. RSC Adv. 6:36336–36344. https://doi.org/10.1039/c6ra01444e.

Amato, F., Pandolfi, M., Moreno, T., Furger, M., Pey, J., Alastuey, A., Bukowiecki, N., Prevot, A.S.H., Baltensperger, U., Querol, X., 2011. Sources and variability of inhalable road dust particles in three European cities. Atmos. Environ. 45:6777–6787. https://doi.org/10.1016/j.atmosenv.2011.06.003.

ATSDR, Toxicological profile for chromium, 2012. U.S. Department of Health and Human Services, Public Health Service, Agency for Toxic Substances and Disease Registry, Internal Report. p. 592.

Bhattacharya, T., Chakraborty, S., Tuteja, D., Patel, M., 2013. Zinc and chromium load in road dust, suspended particulate matter and foliar dust deposits of Anand City, Gujarat. O. J. Metal. 3:42. https://doi.org/10.4236/ojmetal.2013.32A1006.

Bourliva, A., Christophoridis, C., Papadopoulou, L., Giouri, K., Papadopoulos, A., Mitsika, E., Fytianos, K., 2017. Characterization, heavy metal content and health risk assessment of urban road dusts from the historic center of the city of Thessaloniki, Greece. Environ. Geochem. Health 39:611–634. https://doi.org/10.1007/s10653-016-9836-y.

Collins, B.J., Stout, M.D., Levine, K.E., Kissling, G.E., Melnick, R.L., Fennell, T.R., Walden, R., Abdo, K., Pritchard, J.B., Fernando, R.A., Burka, L.T., Hooth, M.J., 2010. Exposure to hexavalent chromium resulted in significantly higher tissue chromium burden compared with trivalent chromium following similar oral doses to male F344/N rats and female B6C3F1 mice. Toxicol. Sci. 118:368–379. https://doi.org/10.1093/toxsci/kfq263.

Crane, M.J., Leverett, P., Shaddick, L.R., Williams, P.A., Kloprogge, J.T., Frost, R.L., 2001. The PbCrO₄-PbSO₄ system and its mineralogical significance. Neues Jb. Mineral. Monat. 11, 505–519.

Csavina, J., Field, J., Félix, O., Corral-Avitia, A.Y., Sáez, A.E., Betterton, E.A., 2014. Effect of wind speed and relative humidity on atmospheric dust concentrations in semi-arid climates. Sci. Total Environ. 48:82–90. https://doi.org/10.1016/j.scitotenv.2014.03.138.

De Flora, S., 2000. Threshold mechanisms and site specificity in chromium (VI) carcinogenesis. Carcinogenesis 21:533–541. https://doi.org/10.1093/carcin/21.4.533.

Filippelli, G.M., Laidlaw, M.A., Latimer, J.C., Raftis, R., 2005. Urban lead poisoning and medical geology: an unfinished story. GSA Today 15:4–11. https://doi.org/10.1130/1052-5173(2005)0152.0.CO;2.

Frost, R.L., 2004. Raman microscopy of selected chromate minerals. J. Raman Spectrosc. 35:153–158. https://doi.org/10.1002/jrs.1121.

Gottesfeld, P., Pokhrel, D., Pokhrel, A.K., 2014. Lead in new paints in Nepal. Environ. Res. 132:70–75. https://doi.org/10.1016/j.envres.2014.03.036.

Haley, V.B., Talbot, T.O., 2004. Seasonality and trend in blood lead levels of New York State children. BMC Pediatr. 4:8. https://doi.org/10.1186/1471-2431-4-8.

Haney, J.T., Erraguntla, N., Sielken, R.L., Valdez-Flores, C., 2014. Development of an inhalation unit risk factor for hexavalent chromium. Regul. Toxicol. Pharmacol. 68:201–211. https://doi.org/10.1016/j.yrtph.2013.12.005.

Jeffs, R., Jones, W., 1999. Additives for Paint. Paint and Surface Coatings: Theory and Practice. Woodhead Publishing, Cambridge, pp. 185–197.

Johnson, D.L., Bretsch, J.K., 2002. Soil lead and children's blood lead levels in Syracuse, NY, USA. Environ. Geochem. Health 24:375–385. https://doi.org/10.1023/A:1020500504167.

Karanasiou, A., Moreno, T., Amato, F., Lumbreras, J., Narros, A., Borge, R., Reche, C., 2011. Road dust contribution to PM levels–evaluation of the effectiveness of street washing activities by means of positive matrix factorization. Atmos. Environ. 45:2193–2201. https://doi.org/10.1016/j.atmosenv.2011.01.067.

Keshavarzi, B., Tazarvi, Z., Rajabzadeh, M.A., Najmeddin, A., 2015. Chemical speciation, human health risk assessment and pollution level of selected heavy metals in urban street dust of Shiraz, Iran. Atmos. Environ. 119:1–10. https://doi.org/10.1016/j.atmosenv.2015.08.001.

Kreider, M.L., Panko, J.M., McAtee, B.L., Sweet, L.I., Finley, B.L., 2010. Physical and chemical characterization of tire-related particles: comparison of particles generated using different methodologies. Sci. Total Environ. 408:652–659. https://doi.org/10.1016/j.scitotenv.2009.10.016.

Laidlaw, M.A., Filippelli, G.M., 2008. Resuspension of urban soils as a persistent source of lead poisoning in children: a review and new directions. Appl. Geochem. 23:2021–2039. https://doi.org/10.1016/j.apgeochem.2008.05.009.

Laidlaw, M.A., Taylor, M.P., 2011. Potential for childhood lead poisoning in the inner cities of Australia due to exposure to lead in soil dust. Environ. Pollut. 159:1–9. https://doi.org/10.1016/j.envpol.2010.08.020.

Laidlaw, M.A., Mielke, H.W., Filippelli, G.M., Johnson, D.L., Gonzales, C.R., 2005. Seasonality and children's blood lead levels: developing a predictive model using climatic variables and blood lead data from Indianapolis, Indiana, Syracuse, New York, and New Orleans, Louisiana (USA). Environ. Health Persp. 113:793. https://doi.org/10.1289/ehp.7759.

Lee, P.K., Yu, S., Chang, H.J., Cho, H.Y., Kang, M.J., Chae, B.G., 2016. Lead chromate detected as a source of atmospheric Pb and Cr (VI) pollution. Sci. Rep. 6. https://doi.org/10.1038/srep36088.

Liu, X., Wu, G., Zhang, Y., Wu, D., Li, X., Liu, P., 2015. Chromate reductase YieF from Escherichia coli enhances hexavalent chromium resistance of human HepG2 cells. Int. J. Mol. Sci. 16:11892–11902. https://doi.org/10.3390/ijms160611892.

Lye, D.J., 2009. Rooftop runoff as a source of contamination: a review. Sci. Total Environ. 407:5429–5434. https://doi.org/10.1016/j.scitotenv.2009.07.011.

Meza-Figueroa, D., De la O-Villanueva, M., De la Parra, M.L., 2007. Heavy metal distribution in dust from elementary schools in Hermosillo, Sonora, México. Atmos. Environ. 138:4–14. https://doi.org/10.1016/j.atmosenv.2016.05.005.

Meza-Figueroa, D., González-Grijalva, B., Del Río-Salas, R., Coimbra, R., Ochoa-Landin, L., Moreno-Rodríguez, V., 2016. Traffic signatures in suspended dust at pedestrian levels in semiarid zones: implications for human exposure. Atmos. Environ. 138:4–14. https://doi.org/10.1016/j.atmosenv.2016.05.005.

Mohmand, J., Eqani, S.A.M.A.S., Fasola, M., Alamdar, A., Mustafa, I., Ali, N., Liu, L., Peng, S., Shen, H., 2015. Human exposure to toxic metals via contaminated dust: bio-accumulation trends and their potential risk estimation. Chemosphere 132:142–151. https://doi.org/10.1016/j.chemosphere.2015.03.004.

Monico, L., Janssens, K., Cotte, M., Sorace, L., Vanmeert, F., Brunetti, B.G., Miliani, C., 2016. Chromium speciation methods and infrared spectroscopy for studying the chemical reactivity of lead chromate-based pigments in oil medium. Microchem. J. 124:272–282. https://doi.org/10.1016/j.microc.2015.08.028.

Moreno-Rodríguez, V., Del Rio-Salas, R., Adams, D.K., Ochoa-Landin, L., Zepeda, J., Gómez-Alvarez, A., Palafox-Reyes, J., Meza-Figueroa, D., 2015. Historical trends and sources of TSP in a Sonoran desert city: can the North America monsoon enhance dust emissions? Atmos. Environ. 110:111–121. https://doi.org/10.1016/j.atmosenv.2015.03.049.

Nazzal, Y., Rosen, M.A., Al-Rawabdeh, A.M., 2013. Assessment of metal pollution in urban road dusts from selected highways of the greater Toronto area in Canada. Environ. Monit. Assess. 185:1847–1858. https://doi.org/10.1007/s10661-012-2672-3.

Newman, L.S., 2001. Health effects of occupational exposure to respirable crystalline silica. NIOSH Hazard Review, DHHS (NIOSH) Publication 2002-129. National Institutes of Occupational Safety and Health (126pp).

Nickens, K.P., Patierno, S.R., Ceryak, S., 2010. Chromium genotoxicity: a double-edged sword. Chem. Int. 188:276–288. https://doi.org/10.1016/j.cbi.2010.04.018.

Patra, A., Colvile, R., Arnold, S., Bowen, E., Shallcross, D., Martin, D., Price, C., Tate, J., ApSimon, H., Robins, A., 2008. On street observations of particulate matter movement and dispersion due to traffic on an urban road. Atmos. Environ. 42:3911–3926. https://doi.org/10.1016/j.atmosenv.2006.10.070.

Plumlee, G., Ziegler, T., 2005. Soils, and other earth materials. Environ. Geochem. 9, 263.

Potgieter-Vermaak, S., Rotondo, G., Novakovic, V., Rollins, S., Van Grieken, R., 2012. Component-specific toxic concerns of the inhalable fraction of urban road dust. Environ. Geochem. Health 34:689–696. https://doi.org/10.1007/s10653-012-9488-5.

Rexeis, M., Hausberger, S., 2009. Trend of vehicle emission levels until 2020-prognosis based on current vehicle measurements and future emission legislation. Atmos. Environ. 43 (31):4689–4698. https://doi.org/10.1016/j.atmosenv.2008.09.034.

Del Rio-Salas, R., Ruiz, J., De la O-Villanueva, M., Valencia-Moreno, M., Moreno-Rodríguez, V., Gómez-Alvarez, A., Grijalva, T., Mendivil, H., Paz-Moreno, F., Meza-Figueroa, D., 2012. Tracing geogenic and anthropogenic sources in urban dusts: insights from lead isotopes. Atmos. Environ. 60:202–210. https://doi.org/10.1016/j.atmosenv.2012.06.061.

Ruby, M.V., Lowney, Y.W., 2012. Selective soil particle adherence to hands: implications for understanding oral exposure to soil contaminants. Environ. Sci. Technol. 46:12759–12771. https://doi.org/10.1021/es302473q.

Sañudo-Wilhelmy, S.A., Flegal, A.R., 1994. Temporal variations in lead concentrations and isotopic composition in the Southern California Bight. Geochim. Cosmochim. Acta 58 (15), 3315–3320.

Sorooshian, A., Csavina, J., Shingler, T., Dey, S., Brechtel, F.J., Sáez, A.E., Betterton, E.A., 2012. Hygroscopic and chemical properties of aerosols collected near a copper smelter: implications for public and environmental health. Environ. Sci. Technol. 46:9473–9480. https://doi.org/10.1021/es302275k.

Thorpe, A., Harrison, R.M., 2008. Sources and properties of non-exhaust particulate matter from road traffic: a review. Sci. Total Environ. 400:270–282. https://doi.org/10.1016/j.scitotenv.2008.06.007.

Turner, A., Kearl, E.R., Solman, K.R., 2016. Lead and other toxic metals in playground paints from South West England. Sci. Total Environ. 544:460–466. https://doi.org/10.1016/j.scitotenv.2015.11.078.

USEPA, 1999. Preparation and extraction of filter material. Compendium of Methods for the Determination of Inorganic Compounds in Ambient Air, Center for Environmental Research Information.

USEPA, 2003. Procedures for Sampling Surface/Bulk Dust Loading. Fifth Edition. US Environmental Protection Agency, Washington, DC Appendix C.1.

Walraven, N., Bakker, M., Van Os, B.J.H., Klaver, G.T., Middelburg, J.J., Davies, G.R., 2015. Factors controlling the oral bioaccessibility of anthropogenic Pb in polluted soils. Sci. Total Environ. 506:149–163. https://doi.org/10.1016/j.scitotenv.2014.10.118.

Wang, Y., Xie, Y., Li, W., Wang, Z., Giammar, D.E., 2010. Formation of lead (IV) oxides from lead (II) compounds. Environ. Sci. Technol. 44:8950–8956. https://doi.org/10.1021/es102318z.

White, K., Detherage, T., Verellen, M., Tully, J., Krekeler, M.P., 2014. An investigation of lead chromate (crocoite-PbCrO₄) and other inorganic pigments in aged traffic paint samples from Hamilton, Ohio: implications for lead in the environment. Environ. Earth Sci. 71:3517–3528. https://doi.org/10.1007/s12665-013-2741-0.

Yang, J., Zhang, C., Tang, Y., 2015. Metal distribution in soils of an in-service urban parking lot. Environ. Monit. Assess. 187:1–11. https://doi.org/10.1007/s10661-015-4699-8.

Yiin, L.M., Rhoads, G.G., Lioy, P.J., 2000. Seasonal influences on childhood lead exposure. Environ. Health Perspect. 108:177–182. https://doi.org/10.230/3454518.

Zhao, H., Li, X., Wang, X., Tian, D., 2010. Grain size distribution of road-deposited sediment and its contribution to heavy metal pollution in urban runoff in Beijing, China. J. Hazard. Mater. 183:203–210. https://doi.org/10.1016/j.jhazmat.2010.07.012.

V.2. **Firmas de tráfico en polvo suspendido a nivel peatonal en zonas semi áridas: Implicaciones en exposición humana.** Artículo: Meza-Figueroa, D., González-Grijalva, B., Del Río-Salas, R., Coimbra, R., Ochoa-Landin, L., Y Moreno-Rodríguez, V. (2016). Traffic signatures in suspended dust at pedestrian levels in semiarid zones: Implications for human exposure. Atmospheric Environment, 138, 4-14. doi: https://doi.org/10.1016/j.atmosenv.2016.05.005
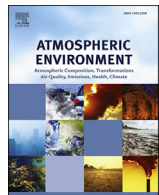
Traffic signatures in suspended dust at pedestrian levels in semiarid zones: Implications for human exposure

Diana Meza-Figueroa [a, e, *], Belem González-Grijalva [b], Rafael Del Río-Salas [c, e], Rute Coimbra [d, f], Lucas Ochoa-Landin [a, e], Verónica Moreno-Rodríguez [b]

[a] *Departamento de Geología, División de Ciencias Exactas y Naturales, Universidad de Sonora, Rosales y Encinas s/n, 83000 Hermosillo, Sonora, Mexico*
[b] *Posgrado en Ciencias de la Tierra, Instituto de Geología, Estación Regional del Noroeste, Universidad Nacional Autónoma de México, Mexico*
[c] *Instituto de Geología, Estación Regional del Noroeste, Universidad Nacional Autónoma de México, Colosio y Madrid s/n, 83240 Hermosillo, Sonora, Mexico*
[d] *Departamento de Geociências, Universidade de Aveiro, Campus de Santiago, 3810-193 Aveiro, Portugal*
[e] *Laboratorio Nacional de Geoquímica y Mineralogía-LANGEM, Mexico*
[f] *GeoBioTec, Departamento de Geociências, Universidade de Aveiro, Campus de Santiago, 3810-193 Aveiro, Portugal*

HIGHLIGHTS

- Dust suspension of coarse particles affecting pedestrian.
- Pixel counting showing metal-enriched agglomerates.
- Coarse particles act as main carriers for emergent pollutants.
- Traffic geochemical signatures dominate dust at pedestrian level.
- Underestimation of human health impact by dust suspension.

ARTICLE INFO

ABSTRACT

Deeper knowledge on dust suspension processes along semiarid zones is critical for understanding potential impacts on human health. Hermosillo city, located in the heart of the Sonoran Desert was chosen to evaluate such impacts. A one-year survey of Total Suspended Particulate Matter (TSPM) was conducted at two different heights (pedestrian and rooftop level). The minimum values of TSPM were reported during monsoon season and winter. Maximum values showed a bimodal distribution, with major peaks associated with increase and decrease of temperature, as well as decreasing humidity. Concentrations of TSPM were significantly exceeded at pedestrian level (~44% of analyzed days) when compared to roof level (~18% of analyzed days). Metal concentrations of As, Pb, Cu, Sb, Be, Mg, Ni, and Co were higher at pedestrian level than at roof level. Pixel counting and interpretations based on scanning electron microscopy of dust filters showed a higher percentage of fine particulate fractions at pedestrian level. These fractions occur mainly as metal-enriched agglomerates resembling coarser particles. According to worldwide guidelines, particulate matter sampling should be conducted by monitoring particle sizes equal and inferior to PM_{10}. However, this work suggests that such procedures may compromise risk assessment in semiarid environments, where coarse particles act as main carriers for emergent contaminants related to traffic. This effect is especially concerning at pedestrian level, leading to an underestimation of potential impacts of human exposure. This study brings forward novel aspects that are of relevance for those concerned with dust suspension processes across semiarid regions and related impact on human health.

1. Introduction

Human exposure to metals in dust-rich atmospheric systems remains poorly understood. In recent years, studies related to impact of fine particles (aerodynamic diameter size smaller than

* Corresponding author. Departamento de Geología, División de Ciencias Exactas y Naturales, Universidad de Sonora, Rosales y Encinas s/n, 83000 Hermosillo, Sonora, Mexico.
E-mail address: dmeza@ciencias.uson.mx (D. Meza-Figueroa).
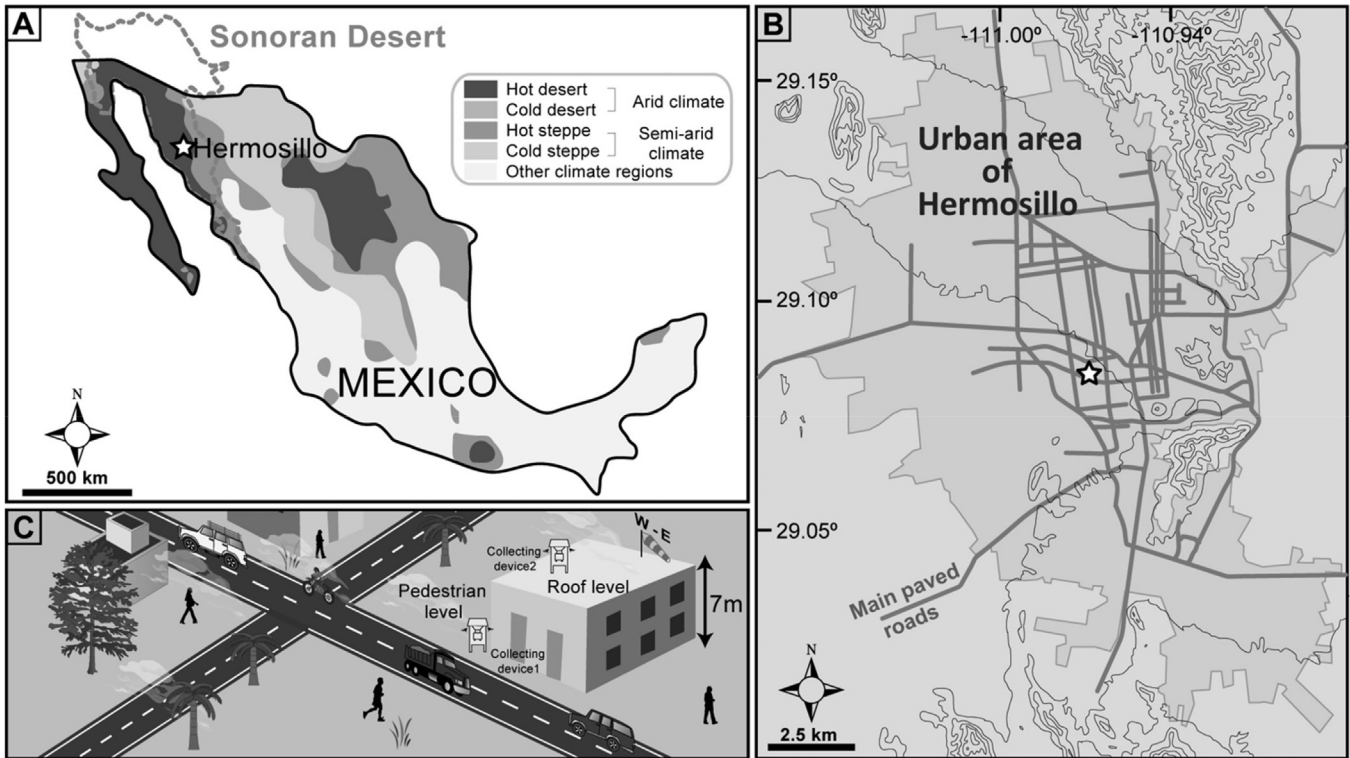
Fig. 1. Geographic location of the study area and sampling strategy. A) Distribution of arid and semi-arid regions across Mexico (after the Köppen-Geiger climate classification, adapted from Peel et al., 2007) and delimitation of the Sonoran Desert, where the studied area is located, at the city of Hermosillo (indicated by star); B) Simplified morphologic and road map within the urban area of Hermosillo. C) Schematic representation of the selected sampling sites, with two dust collecting devices positioned at pedestrian and roof level.

2.5 μm) have increased and received more attention than those related to coarse particles (aerodynamic diameter size larger than 2.5 μm). This is because fine particles are potentially more harmfull, as only these may reach the alveoli of the lungs (Lippmann and Chen, 2009).

Coarse particulate matter is less commonly taken into account, since their emission and transport is related to mechanical processes including wind erosion and wind-blown soil. Health impact is thereby presumably lower due to the short residence time in atmosphere because of gravitational settling (Zheng et al., 2010; Pasha and Alharbi, 2015). However, areas with continuous vehicular movement are highly prone to dust suspension processes by means of traffic-related atmospheric contamination (Fujiwara et al., 2011). This local source represents a potentially dangerous chronic pedestrian exposure.

Rapidly growing cities in semiarid zones face a particular environmental dynamics mainly driven by dust transport processes linked to climate and traffic sources (Fenger, 1999; Moreno-Rodríguez et al., 2015). Soil suspension, surface runoff, and aeolian erosion are the dominant promoting processes of dust emission in these climates. Such processes are particularly enhanced in developing countries like Mexico, where public transportation service is poorly managed, forcing citizens to an overuse of vehicles for daily transportation. In an effort for reduction of dust emission to atmosphere, concreted paved surface percentage has noticeable increased in cities located in desertic zones along Mexico (Moreno-Rodríguez et al., 2015). But this mitigation solution has only a limited effectiveness.

The environmental impact of traffic emissions in urban areas is strongly related to transport demand, climate conditions, and road physical conditions (Barrios et al., 2012). The interaction between turbulence and suspension of road dust can be particularly complex

during dry periods, because high evapotranspiration could act as a driver for contaminated particulate matter loading in urban

Table 1
Descriptive statistics of trace metals analyzed from filters at pedestrian and roof-levels. Concentrations in mg kg^{-1} for all elements, except when marked * (ng g^{-1}); sd: standard deviation; dl: detection limit.

	dl	Pedestrian level		Roof level	
		Min−max	Mean ± sd	Min−max	Mean ± sd
Be	0.005	0.1−0.3	0.2 ± 0.1	0.06−0.15	0.09 ± 0.04
Mg	0.270	450−1840	985 ± 326	374−1400	799 ± 252
Ca	4.730	4780−22,725	13,561 ± 3065	610−20,615	13,797 ± 3359
Cu	0.012	26−317	73 ± 38	23−143	65.7 ± 24.3
V	0.010	5−160	86 ± 42	5.5−149	87.4 ± 39.09
Cr	0.018	4.4−407	262 ± 107	2−347	264 ± 108
Ti	8.110	24−101	51 ± 18	28−67	38 ± 9.8
Fe	0.160	494−4745	1735 ± 745	561−3310	1768 ± 669
Co	0.001	0.5−64	18 ± 22	0.6−60	24 ± 20
Na	2.710	9005−24,487	16,573 ± 4634	6305−2002	12,026 ± 4882
Al	0.580	1680−5506	3514 ± 1233	1430−4722	2445 ± 1199
K	8.110	3318−20,750	16,567 ± 3710	2700−19,013	16,123 ± 4545
Ba	0.003	2080−17,227	7657 ± 5030	865−12,097	4847 ± 4138
Ce	99*	505.6−4244	1923 ± 1025	622−3023	1651 ± 823
As	0.015	1.7−15.5	4 ± 1.6	1.7−9.7	3.9 ± 1.4
Se	0.003	0.2−15.9	1.5 ± 0.4	0.2−1	0.5 ± 0.2
Mo	0.031	0.5−17	3 ± 4	0.4−2	0.8 ± 0.4
Ag	0.002	0.1−0.5	0.2 ± 0.1	0.1−0.3	0.1 ± 0.1
Cd	0.023	0.1−0.5	0.3 ± 0.1	0.2−0.7	0.3 ± 0.1
Sn	0.017	1.4−4	2.5 ± 1	0.9−4	2.3 ± 1
Sb	0.005	0.5−8	3 ± 2.1	1−6	2.8 ± 1.8
Pb	0.003	2−25	10 ± 6.6	3.3−24	9.8 ± 6.1
Ni	0.052	2−38	18.7 ± 10	2−37	18.8 ± 9
Mn	0.023	34−6681	528 ± 843	33−528	376 ± 137
Zn	0.134	28.15−62,209	12,842 ± 6380	1870−18,411	12,569 ± 4077
Sr	0.100	65−755	138 ± 79	65−209	130 ± 33
La	91*	256−2143	986 ± 539	310−1510	842 ± 447
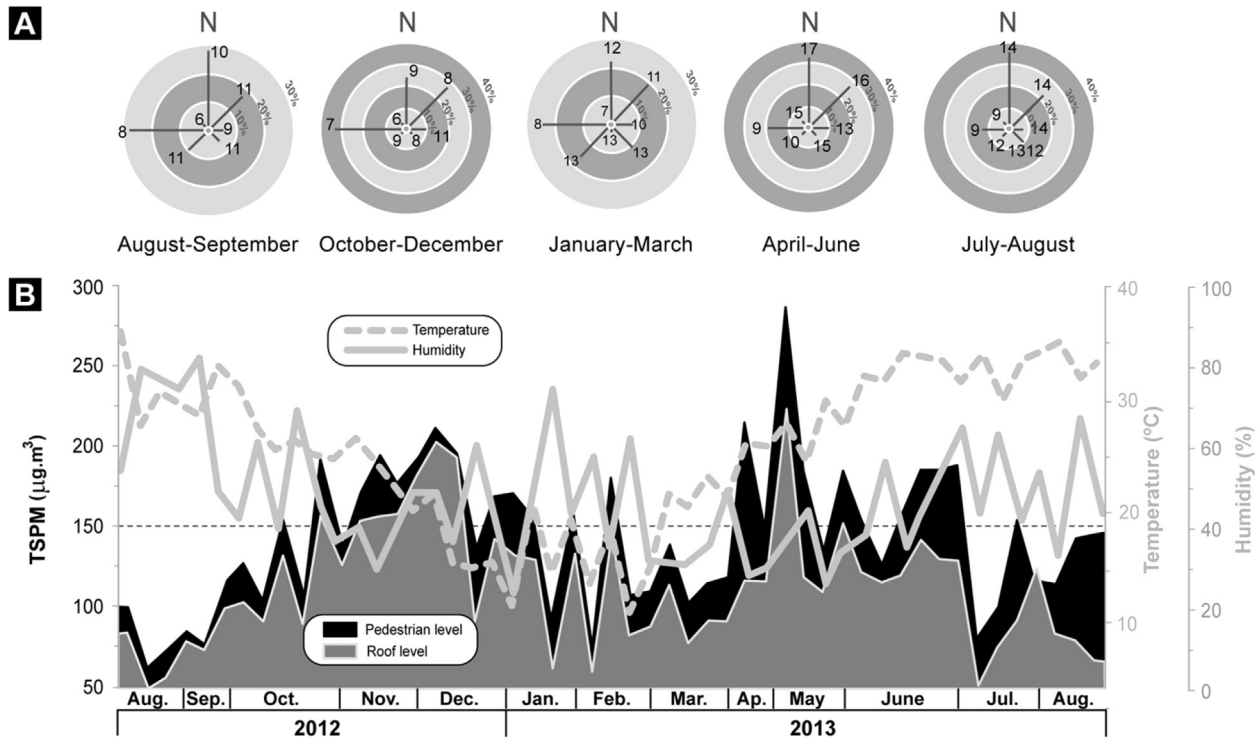
Fig. 2. A) seasonal wind rose: numbers represent wind speed in knots and % represents the frequency; B) TSPM levels at pedestrian (black) and roof (light grey) levels, along with temperature (dotted line) and humidity (solid) values. Horizontal dashed line in B represents TSPM background in Hermosillo, deduced from the TSPM average calculated on the basis of twelve years from four fixed high-volume sampling stations within the urban area.

atmosphere (Moreno-Rodríguez et al., 2015). Turbulence induced-suspension has been suggested as a dominant process of exterior Pb loading in urban environments (Laidlaw and Filippelli, 2008).

Coarse particulate matter is commonly assumed of natural origin (dust, pollen, seaspray, etc.), and less toxic because it is deposited in the upper airways of human body due to its aerodynamic diameter (Fenger, 1999). Additionally, there is still a debate on the adverse health effects due to exposure to coarse particulate matter (Michikawa et al., 2015; Samoli et al., 2013). Notwithstanding, Liu et al. (2015) show that ambient coarse particles may also affect systemic biomarkers and they are associated with increased blood vascular endothelial growth factor. In addition, Meister et al. (2012) alerted to serious health effects of coarse particles, showing an increase in human daily mortality linked to elevated levels of TSPM. Toxicological evidence regarding adverse effects of TSPM includes cytotoxicity and inflammatory effects through increased oxidative stress resulting from exposure to traffic-related particles (Gualtieri et al., 2010; Park et al., 2011; James et al., 2012). However, there is also increasing evidence that coarse particles may activate inflammatory pathways (Schwarze et al., 2007; Jalava et al., 2008), in a similar way as observed for fine particles on an equal mass basis (Schwarze et al., 2007). Additionally, it has been documented that Asian dust events affect the mass of coarse particles, with locally As and Pb contents higher than those of fine particles (Lee et al., 2015). Similarly, in northern Mexico, the Monsoon season has been shown to enhance dust emission in the city of Hermosillo, located at the Sonoran desert (Moreno-Rodríguez et al., 2015). All presented evidence therefore points towards the urgency of research dedicated to a deeper understanding of the adverse effects of TSPM.

Regarding potential sources of TSPM, source apportionment studies have demonstrated that soil- and road-dust can be important sources of particulate (Lee et al., 2015). Wind erosion models generally predict that aerosols are generated as a portion of the suspension component of eroded soil (Mirzamostafa et al., 1998), neglecting a coarser fraction of dust usually distributed below 2 m height of the air column. Road dust is particulate matter generated by frictional processes on road surface, and it is a mixture of geogenic material, road surface wear, combustion contaminants, tires, traffic-paint, and brake wear (Nicholson and Branson, 1990; Berger and Denby, 2011).

Despite the obvious needs for further research, the study of road dust dispersion in urban areas is a complex task. Turbulent wind currents among urban infrastructure promote mixing and diffusion processes (Pascheke et al., 2008), often hard to quantify. The removal of dust from source areas is in fact significant, as evidenced by decreasing concentrations of particles downwind, which rapidly attenuate to the background. However, such decrease can not be attributed solely to deposition (Watson and Chow, 2000). Instead, an important particle fraction remains in suspension and the decrease in concentration can be due primarily to the vertical mixing of particles and is not necessarily due to deposition near the emission source. This re-suspended fraction is therefore hard to ascertain, hence often underestimated in health risk assessment and air-quality evaluation. As a consequence, scarce studies document the vertical distribution of air pollutants in buildings near major roads (Janhäll et al., 2003; Wu et al., 2002). The main concern of air quality regulations is human health; it is therefore important to evaluate population exposure in the most realistic way possible.

The aim of this work is to provide a better understanding of suspended dust by documenting a representative monitoring site located along a semiarid region, near a high traffic road and within a city lacking a rain drainage system. The chosen site is characterized by accumulation of sediments after rainy season, thus representing an area where re-suspension of TSPM by vehicular traffic is dominant. The elemental concentration and relative distribution of
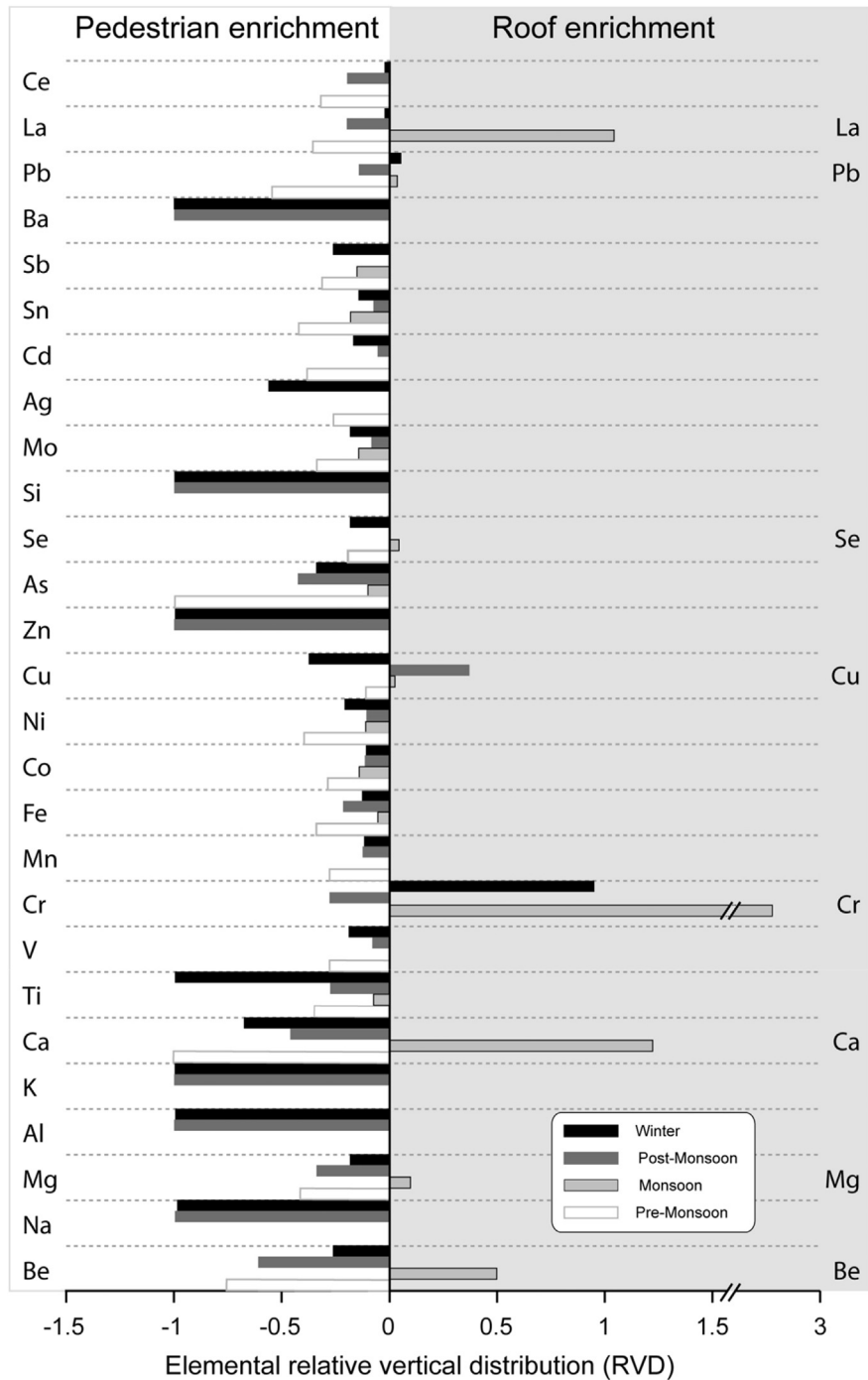
Fig. 3. Relative vertical distribution for each analyzed element at pedestrian and roof levels. Positive RVD values reflect enrichment of studied trace elements on roof. Conversely, negative RVD values correspond to enrichment of elements on pedestrian level. Note significant enrichment of Cr and Cu at roof level.

TSPM at pedestrian and roof levels are interpreted as a combination of geochemical evidence and image analysis of filters. Obtained data are discussed in terms of climate fluctuations, source identification, relative vertical distribution of metals, and implications to potential human exposure.

2. Methods

2.1. Study area

Hermosillo is a city located in the Sonoran desert, 250 km south of the U.S.-Mexico border, in northern Mexico (Fig. 1A and B). It has more tan 700,000 inhabitants, presenting an elevation of 282 m above sea level. The eastern side of the city is limited by hills with NNW-SSE trend. Unpaved roads in Hermosillo represent around 23% of the urban area. An estimate of 274,640 vehicles is registered in Hermosillo city (www.cenapra.salud.gob.mx). Prevailing wind directions are from west to east, however, historical seasonal variations and speed are largely unknown. The movement of local air masses seems to be linked to topography and building distribution. Thermal inversion is commonly observed during winter. Potential local pollutants can be attributed to emissions of vehicular traffic,
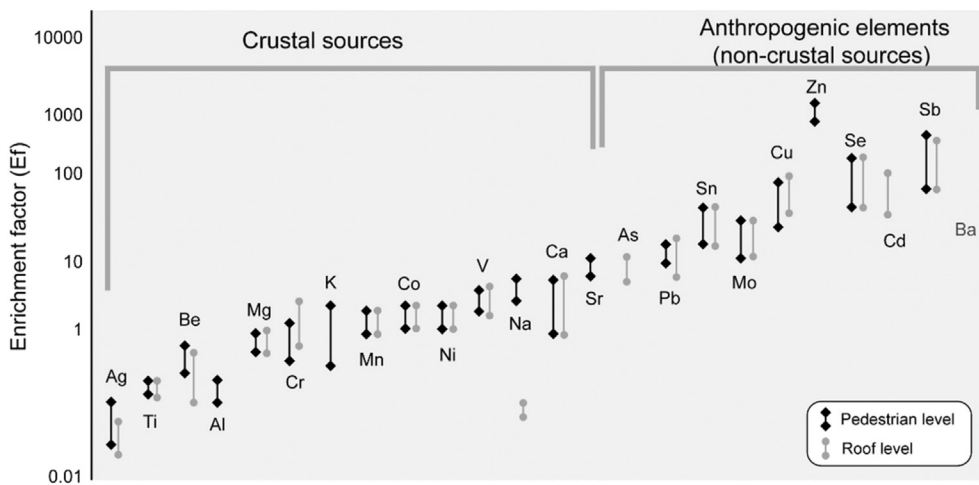
Fig. 4. Enrichment factors for each studied element at pedestrian and roof levels. Dashed line separates elements with Ef higher than 10; dotted line separates crustal and non-crustal sources.

cement industries, and agricultural activities. The chosen sampling site is located at the campus of Regional Research Center of the National Autonomous University of Mexico (Fig. 1B, and C). Traffic was measured on adjacent roads with manual counters during 14 h, considering two vehicle categories: (1) Heavy-duty vehicles (HDV), including trucks with semi-trailers, trucks with trailers, trucks, and buses; and (2) light-duty vehicles (LDV) including cars, vans and motor bikes. Meterological parameters were obtained from a Davis Weather Station Model Vantage Pro2 6152, located at the sampling site.

2.2. Sampling

Samples were collected from a monitoring site at two heights (Fig. 1C): pedestrian (ground level) and roof (7 m above ground). TSPM samples were collected on Whatman 41 quartz microfibre filters (Whatman International Ltd., 20.3 × 25.4 cm^2) using high-volume TISCH air samplers Model TE-5000, with a flow rate of 1.1 m^3 min^{-1}, meeting the USEPA former method for PM sampling (USEPA, 1997; Method 40 CFR part 50). Filters were equilibrated in a desiccator for 24 h and then weighed before sampling. The sampling time was set for 24 h. A total of 14 filters were collected every week from August 2012 to August 2013. Initial and final weighing was carried out in temperature and humidity controlled room (T = 20 ± 1 °C, under 50%, respectively). Gravimetric determination of the mass was carried out by three consecutive measurements using a Sartorius analytical microbalance Model A200S-D1B. Mass concentrations were then calculated using the actual weight of the particulates collected. This was obtained by subtracting the pre-collection weight from post-collection weight. The resulting weight was divided by air volume passed through the filter (μg m^{-3}) during sampling, in order to obtain the mass concentration. After the gravimetric analysis, blanks and sample filters were transferred into a clean high-density polyethilene vial and stored for further chemical analysis.

2.3. Elemental concentrations

In order to determine elemental concentrations, each filter was digested with a mixture of 8% HCl-3% HNO$_3$ in acid cleaned Teflon PFA vessels and heated in microwave system after Method IO-3.1 (USEPA, 1999). Twenty-seven elements (Be, Mg, Ca, Cu, V, Cr, Ti, Fe, Co, Na, Al, K, Ba, Ce, As, Se, Mo, Ag, Cd, Sn, Sb, Pb, Ni, Mn, Zn, Sr,

and La) were measured by inductively coupled plasma mass spectrometry at the Arizona Laboratory for Emerging Contaminants (ALEC-University of Arizona, Tucson). Detection limits and analytical results are summarized in Table 1.

2.4. Mineralogy and particle size distribution

Morphology, mineralogy, and chemical composition of filters were analyzed using a Hitachi tabletop scanning electron microscope TM3030plus, coupled with a Bruker Quantax 70 Energy-Dispersive X-Ray spectroscopy (EDX) operating at 15 kV, at the National Laboratory of Geochemistry and Mineralogy (LANGEM) in Hermosillo, Sonora. EDX device can detect elements from B(5) to Am(95); sensitivity of analysis is influenced by sample porosity, identifiable elemental density and detector type, however accuracy is within 0.1 e 0.5 wt% (Wilkinson et al., 2011).

Particle abundance and size classification was performed by means of pixel counting, following the procedure of Coimbra and Olóriz (2012). Very high quality scanning electron microscope (SEM) images of airborne particles (20 μm and 100 μm) allowed image treatment at optimum magnifications up to 1200%. Particle abundance was estimated using two independent approaches: indirect and direct pixel counting. The indirect method consisted on selecting and counting pixels of elements that did not correspond to particles (background and filaments) and indirectly calculating the abundance of particles in the analyzed image. For the direct method, each particle was outlined, and the pixels contained inside these objects were directly estimated. Once the objects are drawn, size classification can be performed. This last step consisted on assigning a color code to selected intervals of particle size, and calculating the pixels corresponding to each color. The result is a colored map of each SEM image. The percentage of each particle size interval is presented in respect to the total abundance and it is also recalculated to 100%.

2.5. Enrichment factor and vertical variation

Enrichment factor (Ef) of each element in filters was calculated in order to understand the contribution of crustal and non-crustal sources, using aluminum as reference element. Aluminum is commonly used as a reference element assuming that its anthropogenic sources to atmosphere are negligible (Chithra and Nagendra, 2013). The following equation was used in this study:

Table 2

Pearson correlation matrix for pedestrian (white background) and roof (light grey background) levels. Bold lettering refers to statistically significant correlation (>0.8).

	Be	Mg	Ca	Ti	V	Cr	Mn	Fe	Co	Ni	Cu	As	Se	Mo	Ag	Cd	Sn	Sb	Pb
Be	1	0.602	0.424	0.105	0.857	-0.225	-0.026	0.153	-0.545	0.587	0.890	0.245	0.626	0.031	-0.007	-0.043	0.302	-0.078	0.074
Mg	**0.930**	1	-0.199	-0.036	0.698	-0.719	0.742	0.320	0.189	0.017	0.670	-0.540	**0.887**	-0.482	-0.212	-0.738	-0.332	-0.489	-0.362
Ca	0.253	0.051	1	**0.892**	0.492	0.608	-0.440	0.023	-0.228	**0.960**	0.372	0.789	-0.091	0.722	0.587	0.255	0.703	0.558	0.655
Ti	0.606	0.478	0.341	1	-0.085	0.662	0.184	**0.904**	0.096	0.167	-0.264	0.548	-0.428	0.798	**0.918**	0.285	**0.802**	**0.868**	**0.890**
V	0.052	0.392	-0.164	0.086	1	-0.350	0.174	-0.005	-0.147	0.701	**0.962**	0.017	**0.812**	-0.102	-0.044	-0.447	0.041	-0.256	-0.081
Cr	-0.045	-0.255	**0.933**	0.724	-0.252	1	-0.488	0.290	-0.101	0.364	-0.472	**0.862**	-0.827	**0.953**	**0.814**	0.679	**0.842**	**0.946**	**0.905**
Mn	**0.945**	**0.998**	0.101	0.515	0.358	0.280	1	0.547	0.731	-0.357	0.046	-0.684	0.469	-0.354	0.051	-0.814	-0.397	-0.263	-0.216
Fe	**0.888**	**0.832**	0.585	**0.855**	0.207	-0.188	**0.861**	1	0.257	-0.076	-0.170	0.165	-0.137	0.467	0.716	-0.034	0.507	0.577	0.612
Co	**0.894**	**0.962**	0.054	0.497	0.400	0.165	**0.950**	0.771	1	-0.252	-0.337	-0.520	0.045	-0.116	0.217	-0.707	-0.379	-0.059	-0.070
Ni	0.487	0.668	0.328	0.640	0.794	-0.348	0.656	0.677	0.718	1	0.607	0.632	0.182	0.514	0.398	0.076	0.537	0.324	0.452
Cu	-0.503	-0.208	-0.347	-0.402	0.660	**0.994**	-0.226	-0.310	-0.324	0.144	1	-0.033	0.559	-0.018	-0.266	-0.354	-0.060	-0.407	-0.247
As	-0.052	-0.267	**0.945**	0.717	-0.272	-0.768	0.444	0.289	-0.228	0.129	-0.305	1	-0.550	**0.954**	0.654	0.772	**0.933**	**0.822**	**0.838**
Se	0.152	0.492	-0.656	-0.328	**0.804**	**0.933**	-0.369	0.034	0.471	0.468	0.559	-0.785	1	-0.643	-0.494	-0.736	-0.504	-0.726	-0.594
Mo	-0.264	-0.411	**0.863**	0.576	-0.143	0.618	-0.012	0.143	-0.408	0.100	-0.018	**0.954**	-0.694	1	**0.915**	0.573	**0.942**	**0.977**	**0.985**
Ag	-0.040	-0.056	0.730	0.576	0.216	0.328	-0.348	0.405	-0.185	0.335	0.358	0.677	-0.279	0.799	1	0.250	**0.821**	**0.927**	**0.954**
Cd	-0.147	-0.405	0.358	0.029	-0.716	0.679	-0.475	-0.046	-0.573	-0.643	-0.120	0.411	-0.718	0.444	0.416	1	0.656	0.591	0.511
Sn	-0.434	-0.519	0.638	0.293	-0.096	0.869	-0.253	-0.021	-0.617	-0.083	0.324	0.739	-0.549	**0.892**	**0.876**	0.622	1	**0.915**	**0.947**
Sb	-0.165	-0.303	**0.872**	0.607	-0.108	0.867	0.251	0.259	-0.360	0.125	0.059	**0.911**	-0.637	**0.973**	**0.902**	0.535	**0.933**	1	**0.984**
Pb	0.450	0.204	**0.955**	**0.922**	-0.281			0.670	0.235	0.310	-0.593	**0.864**	-0.663	0.700	0.519	0.296	0.402	0.697	1

$$Ef_i = [C_i/C_{Al}]_{Air} / [C_i/C_{Al}]_{UC}$$

where, Ef_i is the enrichment factor of element i; $[C_i/C_{Al}]_{Air}$ is the concentration ratio of element i to Al in air and $[C_i/C_{Al}]_{UC}$ is the concentration ratio of element i to Al in Upper Continental Crust (Rudnick and Gao, 2003). Local geochemical background was not considered because all analyzed natural soils (not shown in this study) were impacted by anthropogenic activities. Since the lithology in Hermosillo area is representative of Upper Continental Crust (UC), average values from Rudnick and Gao (2003) were considered.

Relative vertical distribution (RVD) for each studied metal was estimated according to equation $RVD = (R - P)/P$, modified from Pirintsos et al. (2006), where R is concentration of metal at roof level (7 m), and P is concentration of metal at pedestrian level. Negative and positive RVD values indicate metal enrichment at pedestrian and roof levels, respectively.

3. Results and discussion

3.1. Vertical variation of PM concentration and climate

The one-year sampling period was conveniently divided into four time intervals: winter (January–March); pre-monsoon (late April–June); monsoon season, with the highest precipitation and temperature records (July–September); and post-monsoon (October–December). Fig. 2A and B shows seasonal wind roses and TSPM content during the one-year survey. Eventhough the temporal pattern is similar for both studied height, TSPM pedestrian values are higher than TSPM roof values, more significantly during pre-monsoon and post-monsoon seasons. According to the 150 $\mu g\ m^{-3}$ threshold (Fig. 2B), relatively higher values are considered as "dusty days" and may reflect either a regional input of dust or a local reason for dust re-suspension. Dusty days occur mainly during October–December (post-monsoon) and April–June (pre-monsoon), coinciding with the highest difference among pedestrian and roof level, as well as to the time intervals when a SW-NE wind direction component is missing in the wind roses. Hence, the SW-NE wind direction seems to play an important role in the differences on the TSPM contents at pedestrian and roof levels (Fig. 2). Fig. 2B also shows that the humidity is a main controlling factor for TSPM content, which is in agreement with previous interpretations of humidity as the main driver for dust generation and transport in Arizona (Csavina et al., 2014).

TSPM is classified in three modes based on source and formation: i) ultrafine or nuclei mode, consisting of particles below 0.1 μm forming after vapor condensation during combustion processes; ii) accumulation mode particles, resulting from nuclei mode particles which were subjected to coagulation processes, resulting in accumulation mode particles (0.1–2 μm) that remain in the atmosphere for days to weeks; iii) coarse mode particles, which are associated with mechanical processes including aeolian erosion and airborne transport, construction activities, and soil re-suspension that usually remain in the atmosphere for hours to a few days (Zheng et al., 2010). Even though coarse mode particles are considered to have a short residence time, TSPM contents observed in this work were high at pedestrian levels, especially during the post-monsoon and pre-monsoon seasons, resulting in a dust-enriched environment lasting for at least periods of two months (October–December, and April–June). Such pattern suggests a constant mechanism of suspension possibly related to vehicular traffic or other urban activities; this process has been historically underestimated in risk assessment studies.
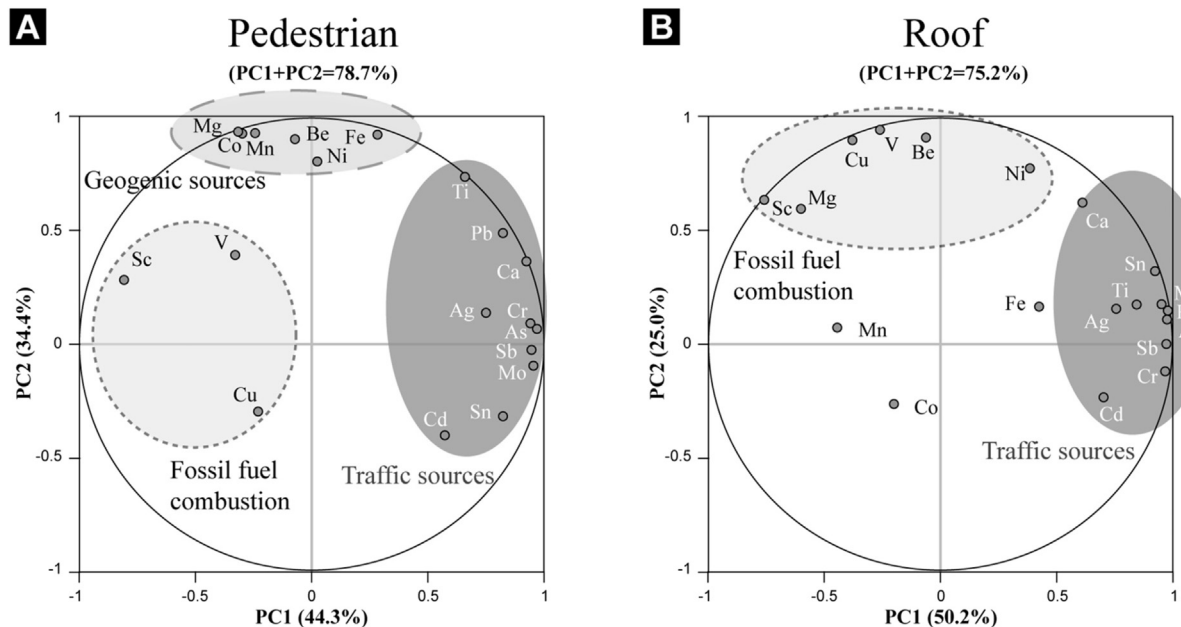
Fig. 5. Scatter plot representation of the first two factorial planes of principal component analysis for TSPM values from pedestrian and roof levels showing interrelationships among the elements. Varimax rotation was applied in order to maximize interpretations.

Table 3
Principal component analysis results for the elemental dataset (n = 190). Bold values indicate factor loadings of the principal components.

Component	Initial eigenvalues			Element	Principal components		
	Total	Variance %	Cumulative %		1	2	3
1	8.904	46.861	46.861	Be	0.158	**0.316**	
2	5.711	30.060	76.921	Mg	0.071	**0.397**	
3	2.370	12.473	89.394	Ca	**0.307**	0.028	0.063
4	0.780	4.105	93.498	Ti	**0.305**	0.133	
5	0.631	3.319	96.818	V	0.143	0.296	**0.434**
6	0.312	1.640	98.457	Cr	**0.307**		
7	0.214	1.127	99.585	Mn	0.077	0.363	
8	0.068	0.357	99.942	Fe	0.241	0.244	
9	0.011	0.058	100.000	Co	0.100	0.340	
				Ni	0.211	**0.249**	0.194
				Cu		0.127	**0.603**
				As	**0.312**		0.023
				Se		**0.324**	0.280
				Mo	**0.299**		0.115
				Ag	**0.263**		0.220
				Cd	**0.174**		
				Sn	**0.280**		0.235
				Sb	**0.290**		0.086
				Pb	**0.307**		

3.2. Geochemical tracers for resuspension processes

The seasonal relative vertical distribution (RVD) of trace elements is shown in Fig. 3. Mostly negative RVD values occur at pre-monsoon and post-monsoon seasons, with relative negative values during winter. Fig. 3 also shows that pedestrian TSPM has a similar enrichment on crustal- and vehicular traffic-related elements such as Pb, Mo, As, V, Ca, K, Al, Na, and Cd. Additionally Sb, V, and Fe have been previously considered as traffic-related metals that enriched the atmospheric particulate matter in Argentina (Gomez et al., 2005; Smichowski et al., 2008), Germany (Weckwerth, 2001), Chile (Quiroz et al., 2013), and Sweden (Sternbeck et al., 2002). The results of enrichment factor (Ef) calculations are shown in Fig. 4, which separates crustal-derived and non-crustal (anthropogenic) derived elements at pedestrian and roof levels. The Ef data agree

with the RVD values since all anthropogenic elements show negative RVD, revealing the presence of an important source of pollution at pedestrian levels. Corroborating these findings, high enrichment factors have been reported for Cr, Ni, Cu, Zn, and Pb in particulate matter collected inside semi-confined bus stops (Godoi et al., 2013). Thus, road dust is an important transport media for traffic-derived pollutants, enhancing local particle emissions in urban sites.

The descriptive statistics of element contents in collected filters is summarized in Table 1. Mean values for all studied metals were higher at pedestrian level when compared to roof samples. However, significant differences on mean values for pedestrian level were detected for crustal derived elements (Al, Na, K, and Sr), as well as traffic related trace elements (Pb, Ce, Ba, Sb, Pb, Cr, and Cu). In order to test similarities between measured proxies, a Pearson
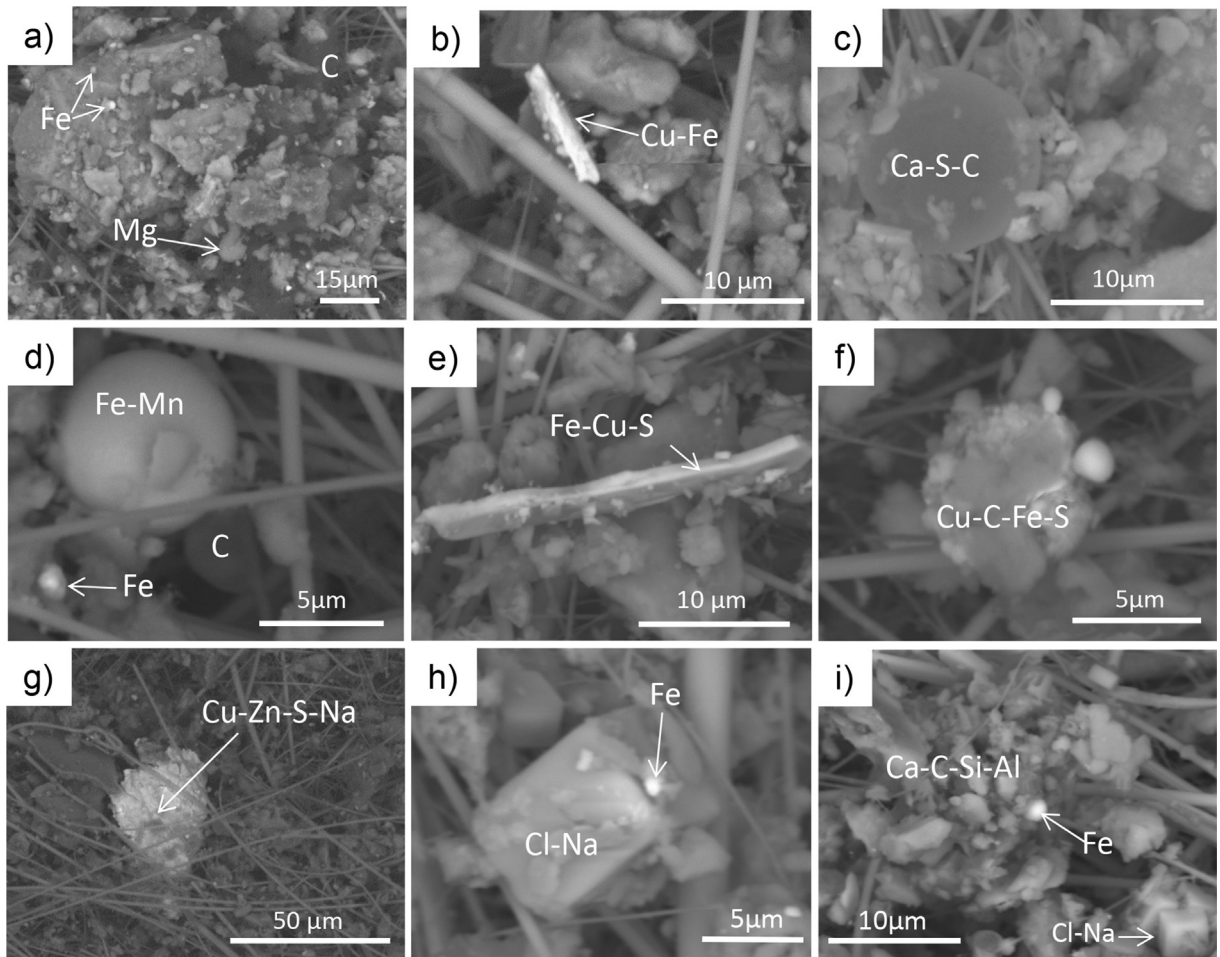
Fig. 6. SEM images and composition of airborne dust particles (TSPM) at pedestrian level.

correlation matrix was performed for trace elements in the TSPM (Table 2). Pedestrian TSPM values show strong correlations for Mn, Fe, Co with Be and Mg; Ca is correlated with Ti, Cr, Mo, Sb, and Pb; Ti is correlated with Pb; and Cr is correlated with As, Mo, Sb, and Pb. TSPM of roof level show that Pb is correlated with Ti, V, As, Mo, Ag, Sn, and Sb; As is strongly correlated to Cr. All correlations are mostly related to traffic sources.

Elements such as Cu, Ce, Mo, platinum group elements (PGE), Ba, Sb, Pb, and Zn are useful markers of anthropogenic contamination in urban areas (Moreno et al., 2007). Traffic emissions produce high concentrations of metals from the exhaust pipe such as PGE, Ce, Mo, and Zn, mechanical abrasion of tires contributes with Zn, and brakes with Ba, Cu, Sb (Gietl et al., 2010). In this study, traffic counting indicated that vehicles with catalytic converters were the major contributors to traffic volume (near 70%, including LDV, cars, vans and motorbikes). It was not possible to identify a maximum traffic hour since the flux of vehicles was rather constant. For the duration of the survey, traffic volume was only significantly decreased during summer holidays.

Principal component analysis allowed establishing different geochemical signatures for pedestrian when compared to roof levels (Fig. 5 and Table 3). The three components are statistically significant, accounting for 89.4% of the total elemental variance. The first component (46.9% of total variance) was dominated by a signature related to traffic source, characterized by the elements: Ca, Ti, Cr, As, Mo, Ag, Cd, Sn, Sb, and Pb. The second component (30% of total variance) is related to a mixture of geogenic and fossil fuel

combustion signature. Also, Fig. 5 shows a geogenic source at pedestrian level, which is important because mineral dust seems to be the main vehicle of transport for traffic derived pollutants. Particularly, trace elements such as Ce, Pb, Ba, Sb, Sn, Cd, Mo, As, Zn, Cu, Cr, Ti, Ca, K, Al, and Be are significantly enriched at pedestrian levels, mainly during post-monsoon and winter seasons. Molybdenum trioxide, calcium carbonate, and barium sulphate are common inorganic space fillers in brake pads (Chan and Stachowiak, 2004). Additionally, cerium oxide has been used as a typical stabilizer in vehicle exhaust catalysts (Lyubomirova et al., 2011). From the above, surface runoff processes could explain the higher concentration of these trace elements at pedestrian levels after monsoon season. The city is characterized by the lack of rain drainage, which promotes erosion of soils and asphalt with the subsequent transport of pollutants among fine sediments into lower topographic areas of the city. Subsequently, dust suspension processes enhance the airborne transport of pollutants (Moreno-Rodríguez et al., 2015).

Rock-derived minerals observed in TSPM collected at both levels are characterized by both, well-formed crystals and irregular aggregates, which contain quartz, feldspar, plagioclase, and calcite, suggesting a typical geogenic composition characterized by Al, Si, K, Na, and Ca (Fig. 6). Mineral aggregates resemble coarse particles with aerodynamic diameter between 5 and 50 μm (Fig. 6a, f–i). However, such aggregates are actually formed by smaller particles (<5 μm) that are a mixture of geogenic and anthropogenic materials, with variable composition including Cu, Ti, Ba, Zn, S, Zr, Pb,
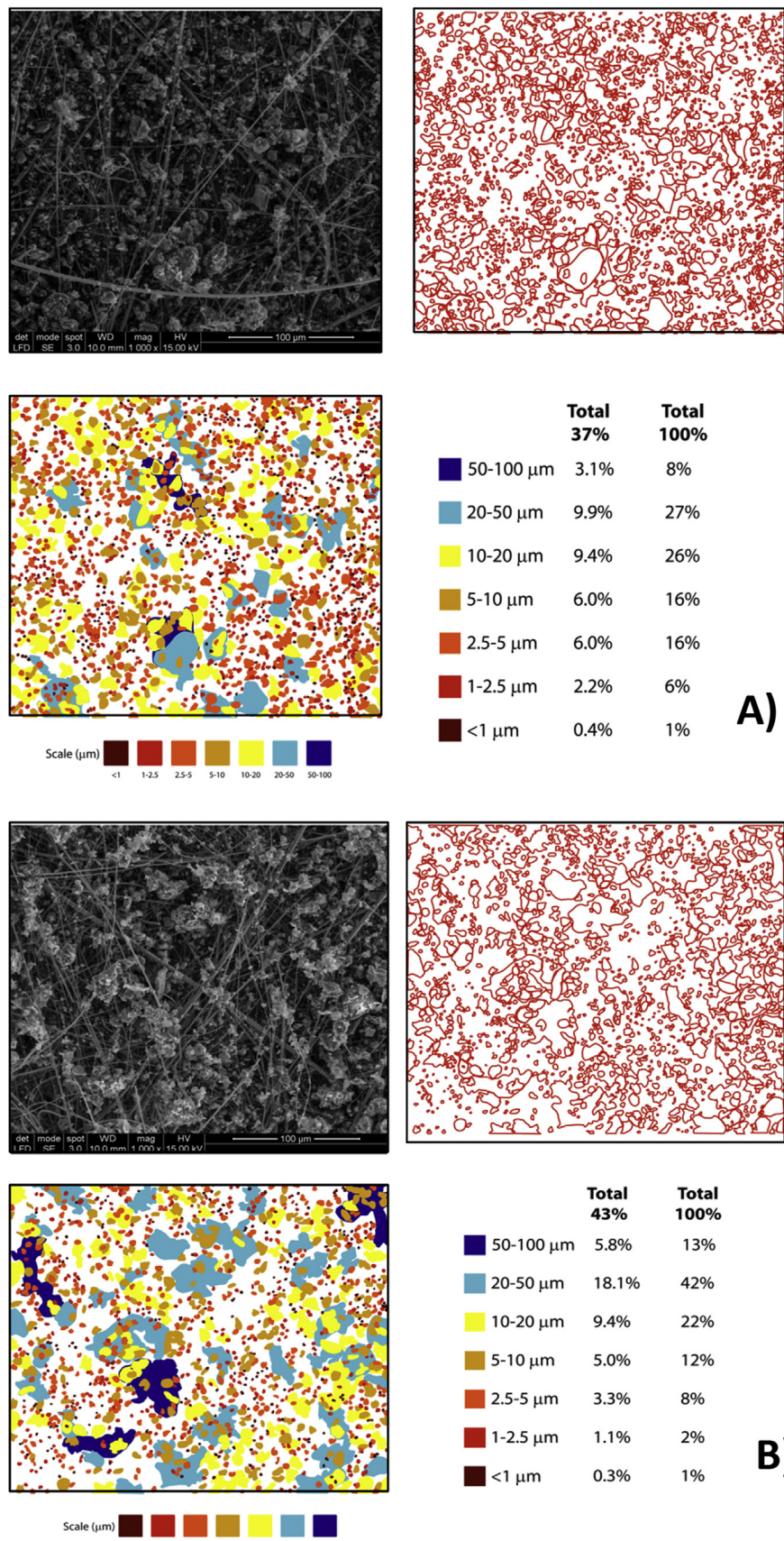
Fig. 7. Particle abundance and size classification of TSPM by means of pixel counting at: A) pedestrian, and B) roof levels.

Mg, and Fe. The cementing material binding the aggregates is mainly salt (NaCl), calcite (Ca), organic material (C), or a mixture of them (Fig. 6g, i). Carbon (organic material) could be originated either from asphalt pavement bitumen or from tire-abrassion (Fig. 6c,d,f and i), explaining the high values of Zn, Fe, Mn, Cu, and Ti found at pedestrian levels. On the other hand, coarse sea-salt crystals or salt cement seem to be the main carrier agent for aggregates at roof levels (Fig. 6h).

Particle abundance and size classification (via pixel counting) show an interesting distribution of fine *vs.* coarse TSPM (Fig. 7). Particles with aerodynamic diameter below 2.5 μm are considered as fine mode, and particles >2.5 μm are considered as coarse mode that are associated with mechanical processes such as aeolian erosion, airborne transport, soil re-suspension and construction operations (Pasha and Alharbi, 2015). Particles smaller than 2.5 μm in pedestrian and roof levels account for 7 and 3%, respectively (Fig. 7A and B). On the other hand, coarse particles (2.5–10 μm) in pedestrian and roof level account for 32 and 20%, respectively. The increase of fine particles and coarse-like particles at pedestrian level is due to the formation of aggregates of fine TSPM binded by either anthropogenic (asphalt) or geogenic (salts), which act also as carriers of traffic pollutants. According to previous work, major elements have been mainly associated with coarse particles and toxic elements such as Cd, Pb, and Zn to finer particles (Hu et al., 2010, 2013). However, the results of this study show the opposite for TSPM collected at pedestrian level. This evidence is therefore novel, and presumably a specific characteristic of semiarid urban sites, providing new insights on the implications of human exposure to traffic-derived metal sources.

4. Conclusions

Temporal variation of TSPM at pedestrian and roof levels were constrained over a year. The TSPM minimum values were reported during Northamerican monsoon and winter seasons. The maximum values are associated with increase and decrease of temperature; humidity percentage is a controlling factor on the TSPM concentrations. In general, the patterns of the TSPM at pedestrian and roof levels are mostly similar throughout the entire year, although higher concentrations were found at pedestrian level during pre-monsoon and post-monsoon seasons, which are in agreement with the input and re-suspension of road dust.

Regarding the geochemical data, pedestrian TSPM is enriched in Pb, Mo, As, V, Ca, K, Al, Na, Cd, Sb, V, and Fe, when compared to roof level. Pb, Sn, Mo, Cu, Zn, Se, and Sb characterize the Ef in the TSPM of pedestrian level, which determines an anthropogenic signature, whereas the Ef in roof level is characterized by As, Pb, Sn, Mo, Cu, Se, Cd, and Sb.

Pixel counting on TSPM filters indicates that particles smaller than 2.5 μm account for 7 and 3% for pedestrian and roof levels, respectively. Coarser particles (2.5–10 μm) account for 32 and 20% for pedestrian and roof levels, respectively. Furthermore, finner particles form agglomerates that resemble coarser particles, which can be erroneously classified as geogenic coarse particles.

The present study can shed new lights on: i) the underestimation of the amount of finner particles in aggregates classified as coarser particles, ii) the importance of using TSPM samplers in semiarid environments, and iii) the implication on human health at pedestrian level.

Conflict of interest statement

We declare that we have no financial and personal relationships with other people or organizations that can inappropriately influence our work. Opinions in the paper do not constitute an endorsement or approval by the funding agencies and only reflect the personal views of the authors.

Appendix A. Supplementary data

Supplementary data related to this article can be found at http://dx.doi.org/10.1016/j.atmosenv.2016.05.005.

References

Barrios, C.C., Domínguez-Sáez, A., Rubio, J.R., Pujadas, M., 2012. Factors influencing the number distribution and size of the particles emitted from modern diesel vehicle in real urban traffic. Atmos. Environ. 56, 16–25.

Berger, J., Denby, B., 2011. A generalised model for traffic induced road dust emissions. Model description and evaluation. Atmos. Environ. 45, 3692–3703.

Chan, D., Stachowiak, G.W., 2004. Review of automotive brake friction materials. P. I. Mech. Eng. D. J. Aut. 218, 953–966.

Chithra, V.S., Nagendra, S., 2013. Chemical and morphological characteristics of indoor and outdoor particulate matter in an urban environment. Atmos. Environ. 77, 579–585.

Coimbra, R., Olóriz, F., 2012. Pixel counting for percentage estimation: applications to sedimentary petrology. Comput. Geosci. 42, 212–216.

Csavina, J., Field, J., Félix, O., Corral-Avitia, A.Y., Sáez, A.E., Betterton, E.A., 2014. Effect of wind speed and relative humidity on atmospheric dust concentrations in semi-arid climates. Sci. Total Environ. 487, 82–90.

Fenger, J., 1999. Urban air quality. Atmos. Environ. 33, 4877–4900.

Fujiwara, F., Jiménez Rebagliati, R., Marrero, J., Gómez, D., Smichowski, P., 2011. Antimony as a traffic-related element in size-fractionated road dust samples collected in Buenos Aires. Microchem. J. 97, 62–67.

Gietl, J.K., Lawrence, R., Alistair, J.T., Harrison, R.M., 2010. Identification of brake wear particles and derivation of a quantitative tracer for brake dust at a major road. Atmos. Environ. 44, 141–146.

Godoi, R.H.M., Godoi, A.F.L., de Quadros, L.C., Polezer, G., Silva, T.O.B., Yamamoto, C.I., van Grieken, R., Potgieter-Vermaak, S., 2013. Risk assessment and spatial chemical variability of PM collected at selected bus stations. Air Qual. Atmos. Health 6, 725–735.

Gomez, D.R., Gine, M.F., Bellato, A.C.S., Smichowski, P., 2005. Antimony: a traffic-related element in the atmosphere of Buenos Aires, Argentina. J. Environ. Monit. 7, 1162–1168.

Gualtieri, M., Ovrevik, J., Holme, J.A., Perrone, M.G., Bolzacchini, E., Schwarze, P.E., Camatini, M., 2010. Differences in cytotoxicity versus pro-inflammatory potency of different PM fractions in human epithelial lung cells. Toxicol. Vitro. 24 (1), 29–39.

Hu, H., Yang, Q., Lu, X., Wang, W.C., Wang, S.S., Fan, M.H., 2010. Air pollution and control in different areas of China. Crit. Rev. Env. Sci. Technol. 40, 452–518.

Hu, X., Ding, Z., Zhang, Y., Sun, Y., Wu, J., Chen, Y., Lian, H., 2013. Size distribution and source apportionment of airborne metallic elements in Nanjing, China. Aerosol Air Qual. Res. 13, 1796–1806.

Jalava, P.I., Salonen, R.O., Pennanen, A.S., Happo, M.S., Penttinen, P., Hälinen, A.I., Sillanpää, M., Hillamo, R., Hirvonen, M.R., 2008. Effects of solubility of urban air fine and coarse particles on cytotoxic and inflammatory responses in RAW 264.7 macrophage cell line. Toxicol. Appl. Pharmacol. 229 (2), 146–160.

James, K., Farrell, R.E., Siciliano, S.D., 2012. Comparison of human exposure pathway in an urban brownfield: reduced risk from paving roads. Environ. Toxicol. Chem. 31 (10), 2423–2430.

Janhäll, S., Molnár, P., Hallquist, M., 2003. Vertical distribution of air pollutants at the Gustavii Cathedral in Göteborg. Swed. Atmos. Environ. 37, 209–217.

Laidlaw, M.A.S., Filippelli, G.M., 2008. Resuspension of urban soils as a persistent source of lead poisoning in children: a review and new directions. Appl. Geochem 23, 2021–2039.

Lee, P.K., Jo, J.Y., Kang, M.J., Kim, S.O., 2015. Seasonal variation in trace element concentrations and Pb isotopic composition of airborne particulates during Asian dust and non-Asian dust periods in Daejeon, Korea. Environ. Earth Sci. 74,

3613–3628.

Lippmann, M., Chen, L.C., 2009. Health effects of concentrated ambient air particulate matter (CAPs) and its components. Crit. Rev. Toxicol. 39, 865–913.

Liu, L., Urch, B., Poon, R., Szyszkowicz, M., Speck, M., Gold, D.R., Wheeler, A.J., Scott, J.A., Brook, J.A., Thorne, P.S., Silverman, F.S., 2015. Effects of ambient coarse, fine, and ultrafine particles and their biological constituents on systemic biomarkers: a controlled human exposure study. Environ. Health Perspect. 123 (6), 534–540.

Lyubomirova, V., Djingova, R., van Elteren, J.T., 2011. Fractionation of traffic-emitted Ce, La, and Zr in road dusts. J. Environ. Monit. 13, 1823–1830.

Meister, K., Johansson, C., Forsberg, B., 2012. Estimated short-term effects of coarse particles on daily mortality in Stockholm. Swed. Environ. Health Perspect. 120 (3), 431–436.

Michikawa, T., Ueda, K., Takeuchi, A., Tamura, K., Kinoshita, M., Takamichi, I., Nitta, H., 2015. Coarse particulate matter and emergency ambulance dispatches in Fukuoka, Japan: a time-stratified case-crossover study. Environ. Health. Prev. Med. 20, 130–136.

Mirzamostafa, W., Hagen, L.J., Stone, L.R., Skidmore, E.L., 1998. Soil aggregate and texture effects on suspension components from wind-erosion. Soil Sci. Soc. Amer. J. 62 (5), 1351–1361.

Moreno, T., Alastuey, A., Querol, X., Font, O., Gibbons, W., 2007. Identification of metallic pathfinder elements in PM derived from fossil fuels at Puertollano. Int. J. Coal. Geol. 71, 122–128.

Moreno-Rodríguez, V., Del Rio-Salas, R., Adams, D.K., Ochoa-Landin, L., Zepeda, J., Gómez-Alvarez, A., Palafox-Reyes, J., Meza-Figueroa, D., 2015. Historical trends and sources of TSP in a Sonoran desert city: can the North America monsoon enhance dust emissions? Atmos. Environ. 110, 111–121.

Nicholson, K.W., Branson, J.R., 1990. Factors affecting resuspension of particulate material. Atmos. Environ. 27A, 181–188.

Park, E.J., Roh, J., Kim, Y., Park, K., Kim, D.S., Yu, S.D., 2011. $PM_{2.5}$ collected in a residential area induced Th1-type inflammatory responses with oxidative stress in mice. Environ. Res. 111, 348–355.

Pascheke, F., Barlow, J.F., Robins, A., 2008. Wind-tunnel modelling of dispersión from a scalar area source in urban-like roughness. Bound. Layer Meteorol. 126 (1), 103–124.

Pasha, M.J., Alharbi, B.H., 2015. Characterization of size-fractionated PM_{10} and associated heavy metals at two semi-arid holy sites during Hajj in Saudi Arabia. Atmos. Pollut. Res. 6, 162–172.

Peel, M.C., Finlayson, B.L., McMahon, T.A., 2007. Updated world map of the Koppen-Geiger climate classification. Hydrol. Earth Syst. Sci. 11, 1633–1644.

Pirintsos, S.A., Matsi, T., Vokou, D., Gaggi, C., Loppi, S., 2006. Vertical distribution patterns of trace elements in a urban environment as reflected by their accumulation in Lichen transplants. J. Atmos. Chem. 54, 121–131.

Quiroz, W., Cortés, M., Astudillo, F., Bravo, F., Bravo, M., Cereceda, F., Vidal, V., Lobos, M.G., 2013. Antimony speciation in road dust and urban particulate matter in Valparaiso, Chile: analytical and environmental considerations. Microchem. J. 110, 266–272.

Rudnick, R.L., Gao, S., 2003. In: Rudnick, Roberta L., Holland, Heinrich D., Turekian, Karl K. (Eds.), Composition of the Continental Crust. Treatise of Geochemistry, vol. 3. Elsevier, pp. 1–64.

Samoli, E., Stafoggia, M., Rodopoulou, S., Ostro, B., Declerq, C., Le Tertre, A., Pandolfi, P., Randi, G., Scarinzi, C., Zouli-Sajani, S., Katsouyanni, K., Forastiere, F., The MED-PARTICLES Study Group, 2013. Associations between fine and coarse particles and mortality in Mediterranean cities: results from the MED-PARTICLES project. Environ. Health Perspect. 121 (8), 932–938.

Schwarze, P.E., Øurevik, J., Hetland, R.B., Becher, R., Cassee, F.R., Låg, M., Løvik, M., Dybing, E., Refsnes, M., 2007. Importance of size and composition of particles for the effects on cells in vitro. Inhal. Toxicol. 19, 17–22.

Smichowski, P., Gómez, D., Frazzoli, C., Caroli, S., 2008. Traffic-related elements in airborne particulate matter. Appl. Spectrosc. Rev. 43, 23–49.

Sternbeck, J., Sjödin, Å., Andréasson, K., 2002. Metal emissions from road traffic and the influence of resuspension-results from two tunnel studies. Atmos. Environ. 36 (30), 4735–4744.

USEPA (United States Environmental Protection Agency), 1997. National ambient air quality standards for particulate matter-final rule. 40 CFR part 50. Fed. Regist. 62 (138), 38651–38760.

USEPA (United States Environmental Protection Agency), 1999. Compendium method IO-3.1 selection, preparation and extraction of filter material. In: Compendium of Methods for the Determination of Inorganic Compounds in Ambient Air, Center for Environmental Research Information, Office of Research and Development. Cincinnati, OH 45268. Document EPA/625/R-96/010ᵃ.

Watson, J.G., Chow, J.C., 2000. Reconciling Urban Fugitive Dust Emissions Inventory and Ambient Source Contribution Estimates: Summary of Current Knowledge and Needed Research. Desert Research Institute, Reno, Nev. Document No. 6110.4F.

Weckwerth, G., 2001. Verification of traffic emitted aerosol components in the ambient air of Cologne (Germany). Atmos. Environ. 35, 5525–5536.

Wilkinson, K., Lundkvist, J., Seisenbaeva, G., Kessler, V., 2011. New tabletop SEM-EDS-based approach for cost-efficient monitoring of airborne particulate matter. Environ. Pollut. 159 (1), 311–318.

Wu, Y., Hao, J., Fu, L., Wang, Z., Tang, U., 2002. Vertical and horizontal profiles of airborne particulate matter near major roads in Macao, China. Atmos. Environ. 36, 4907–4918.

Zheng, N., Liu, J.S., Wang, Q.C., Liang, Z.Z., 2010. Heavy metals exposure of children from stairway and sidewalk dust in the smelting district, northeast of China. Atmos. Environ 44, 3239–3245.

V.3. **Influencia de la mineralogía del suelo en la bioaccesibilidad oral del plomo: Implicaciones para el uso del suelo y la evaluación de riesgos**. Artículo: González-Grijalva, B., Meza-Figueroa, D., Romero, F. M., Robles-Morúa, A., Meza-Montenegro, M., García-Rico, L., Y Ochoa-Contreras, R. (2019). The role of soil mineralogy on oral bioaccessibility of lead: Implications for land use and risk assessment. Science of The Total Environment, 657, 1468-1479. doi: https://doi.org/10.1016/j.scitotenv.2018.12.148

The role of soil mineralogy on oral bioaccessibility of lead: Implications for land use and risk assessment

Belem González-Grijalva [a], Diana Meza-Figueroa [b,f,*], Francisco M. Romero [c,f], Agustín Robles-Morúa [d,f], Mercedes Meza-Montenegro [d,f], Leticia García-Rico [e], Roberto Ochoa-Contreras [e]

[a] Earth Sciences Graduate Program, Institute of Geology, National University of Mexico, Colosio y Madrid, Hermosillo, Sonora 83240, Mexico
[b] Department of Geology, University of Sonora, Rosales y Encinas, Hermosillo, Sonora 83000, Mexico
[c] Institute of Geology, National University of Mexico, Ciudad Universitaria, Delegación Coyoacán, Ciudad de México 04510, Mexico
[d] Department of Natural Resources, Technological Institute of Sonora, Cd. Obregón, Sonora, Mexico
[e] Center of Research in Food and Development, A.C., Carretera a la Victoria km 0.6, 83304 Hermosillo, Sonora, Mexico
[f] National Laboratory of Geochemistry and Mineralogy - LANGEM, Mexico

HIGHLIGHTS

- Bioaccessibility of lead was analyzed using PBET.
- Natural soils were spiked with lead-based paint.
- Soils mineralogy affect lead bioaccessibility.
- Soil type influences health-risk assessment.
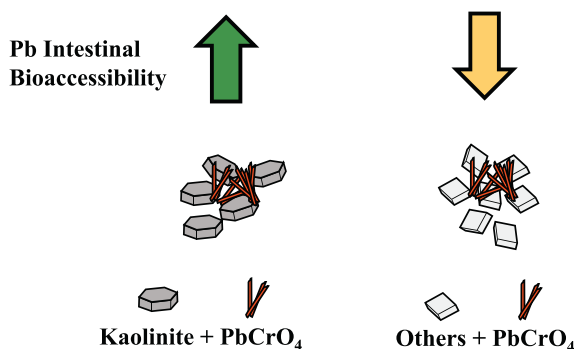
GRAPHICAL ABSTRACT

ABSTRACT

Understanding the oral bioaccessibility of lead (Pb) present in soils in urbanized areas is important for the human exposure risk assessment. In particular, the role of the soil-mineralogy in the oral bioaccessibility has not been extensively studied. To investigate bioaccessibility, five types of periurban soils were collected, samples were spiked with the same amount of lead-chromates from traffic paint, and subjected to the in vitro Physiological Based Extraction Test (PBET). Ten samples of urban topsoils were collected at elementary schools playgrounds, Pb-bioaccessibility was measured, and a prediction equation for bioaccessibility was constructed. Mineralogy, and metal content were identified with a combination of X-ray powder diffraction, scanning electron microscopy, and portable X-ray fluorescence techniques. Traffic paint sample is made of 15% quartz (SiO_2), 13% crocoite ($PbCrO_4$), 55% calcite ($CaCO_3$), and 17% kaolinite ($Al_2Si_2O_5(OH)_4$) and it contains high metal content (Pb, Cr, Zn, and Ca). Studied soils are characterized by variable amounts of acid-neutralizing minerals (carbonates) and low metal content. Spiked soils contained almost equal concentration of Pb, Cr, and Zn, because the contribution of these metals is from the added paint. However, obtained Pb-bioaccessibility at gastric and intestinal conditions are variable (40 to 51% gastric, 24 to 70.5% intestinal). Carbonate content shows significant correlation ($p < 0.05$) with Cr, Ca, calcite, crocoite, and Pb-bioaccessible at gastric conditions. Correlation of Pb-bioaccessible at intestinal conditions is significant ($p < 0.05$) with kaolinite.

* Corresponding author at: Department of Geology, University of Sonora, Rosales y Encinas, Hermosillo, Sonora 83000, Mexico.
E-mail address: dmeza@ciencias.uson.mx (D. Meza-Figueroa).

Variability of Pb-bioaccesibility in urban environments is commonly associated to differences in Pb-sources, however, our results show that the bioaccessibility of the same pollutant behaves different for each soil type. This suggests that soil mineralogy may play a role in Pb-releasing at gastrointestinal conditions. Soil information about mineralogical characteristics from this study may help to reduce exposure to lead from urban sources if data are incorporated into urban planning.

1. Introduction

One of the most important environmental challenges for current goverments is to find a balance between the demand for land for urbanization and the assurance of a safe environment for its inhabitants. Urban soils are the main reservoirs for metals released from anthropogenic sources (Wang et al., 2016; Hiller et al., 2017; Meza-Figueroa et al., 2018). Some metals like lead (Pb) have long residence time in soils, so its concentration increases over time and are commonly found in the oldest urbanized areas (Filippelli et al., 2005; Del Rio-Salas et al., 2012). Pb presence in soils is particularly important because even at low environmental concentrations the exposure may cause adverse public health effects. In particular, Pb has been found to affect children's behavior, memory, and a decrease of intelligence quotient (Lin et al., 2013; Schnur and John, 2014; USEPA, 2014; Freire et al., 2018; Joo et al., 2018). The main forms of Pb species in urban soils relate to the historic use of leaded gasoline and Pb-based paint (Taylor et al., 2014; Yang and Cattle, 2015). Metals in polluted soils can enter the human body through different exposure pathways including ingestion, dermal contact or inhalation of fine particles (Pan et al., 2016). Children exposure to metals in urban soils has been well documented (Mielke et al., 1999, 2005) and several publications show that anthropogenic Pb may be transported and further incorporated into soils with complex mixtures of minerals, representing exposure paths to Pb through ingestion (Chen et al., 2005; Habil et al., 2013; Lu et al., 2014; Reis et al., 2014; Meza-Figueroa et al., 2007, 2016).

Published studies show that only a fraction of the total metal content in soil is bioaccessible in such a way that it is adsorbed by the stomach or intestine (Oomen et al., 2002). Bioaccessibility relates to the fraction of a metal that is soluble in the human stomach when compared to its total content in a soil (Oomen et al., 2002). Therefore, health risk assessment for children exposed to Pb through soil ingestion should include the bioaccessible fraction to avoid an overestimation of the risk (Yan et al., 2017). Laboratory processes measure the bioaccessibility using tests which mimic the biochemical conditions in the human gastrointestinal tract; among the published methods, the most commonly used batch extraction technique is the physiologically based extraction test or PBET, developed by Ruby et al. (1993). The chemical composition of gastric fluids varies depending on the presence or absence of food in the stomach. Electrolyte composition is made of a hydrogen sodium-chloride solution with calcium, potassium, and magnesium, with gastric fluids pH around 1.5. The human gastrointestinal tract consists of compartments where ingested food or soil undergo a series of reactions in which fluid composition, pH, and reaction time vary. The physicochemical characteristics of soils influence the lead bioaccessibility (Hiller et al., 2017; Mendoza et al., 2017; Sun et al., 2017), and most published studies test the role of pH, grain size, clay content, soil texture, organic matter, organic carbon, conductivity or metal content (Hiller et al., 2017; Mendoza et al., 2017; Padoan et al., 2017). Few publications address the mineralogy as an important component that influences bioaccessibility for metals (Casteel et al., 2006; Demetriades et al., 2010; Meunier et al., 2010; Vasiluk et al., 2011; Molina et al., 2013; Yan et al., 2017). In gastric conditions, minerals can function as antacids through two mechanisms: (i) neutralization of gastric acid, and (b) adsorption of H^+ ions to surface sites, leading to mineral decomposition. Clay minerals such as palygorskite, sepiolite, montmorillonite,

and saponite behave as antacids through this mechanism (Carretero and Pozo, 2010). Soils naturally contain neutralizing minerals, primarily calcium or magnesium compounds ($CaCO_3$, $MgCO_3$) but also aluminum and silicate compounds. Carbonates have a high neutralization capacity, and can elevate pH levels within seconds. Feldspar group minerals have much slower reaction rates. Aluminum and silicate minerals solubility at gastric conditions depends on the pH which may be modified by the interaction with calcite, aragonite, dolomite, magnesite, and brucite due to their highest reactivity level (Sverdrup, 1990). However, because soils have a complex matrix with mixtures of minerals with variable solubilities, it is unknown how the bioaccessibility of an specific pollutant behaves.

Free acidity in the stomach disappears when the pH increases by 3–4 units. Depending on ingested mineralogy, the acid neutralization process may increase the gastric pH from 1.5 to 7 (Carretero and Pozo, 2010). When pH of the gastric fluid exceeds 7, the parietal glands restore normal stomach acidity causing acid rebound. This process may cause further dissolution of minerals. The pharmaceutical industry uses carbonates (calcite and magnesite), oxides (periclase), and hydroxides (brucite, gibbsite, hydrotalcite) as antacids; among these minerals, calcite tends to cause acid rebound. Kaolinite, however, has a low capacity for neutralizing acids and does not undergo partial degradation in the acidic medium of the stomach (Carretero and Pozo, 2010). Because both kaolinite and calcite are common minerals in soils, it is important to understand the role of these minerals in the in vitro measurement of bioaccessibility of metals such as Pb.

Previous studies on acid rock drainage show that common neutralizing minerals include: (1) calcium and magnesium-bearing carbonates; (2) oxides and hydroxides of calcium, magnesium, and aluminum; (3) soluble, non-resistant silicate minerals; (4) phosphates (Sherlock et al., 1995). The term Total Neutralizing Minerals (TNM) is used here to refer to the group of calcium and magnesium-bearing carbonates, because they can cause an acid rebound at gastric conditions, and they could cause further dissolution of contaminants in the stomach.

Meza-Figueroa et al. (2018) report the presence of lead-chromates as crocoite mineral derived from the road erosion of traffic yellow paint (TP) in the city of Hermosillo in northwest Mexico. This material may contain nearly 20,000 mg.kg^{-1} of Pb, before its emission to the atmosphere. Eventhough lead-chromates from yellow paint is currently acknowledged as an important source of Pb in urban environments in United States, Asia and the United Kingdom (White et al., 2014; Turner et al., 2016; Lee et al., 2016), there is a lack of legislation in many developing countries (Meza-Figueroa et al., 2018). TP thus represents an area source for lead in the urban environment in these countries. Lead isotopic studies in Hermosillo show that Pb-chromates and tetraethyl Pb from pre-catalytic gasoline from polluted soils are the main sources of Pb in atmospheric dust (Meza-Figueroa et al., 2018).

For this work we evaluate the bioaccessibility of Pb from traffic paint when it is incorporated to non impacted or periurban soils. Traffic paint is used here because it represents a documented current source of pollution at the study site. This study, therefore, evaluates the possible effects of common soil mineralogy in Pb-bioaccessibility at gastric and intestinal conditions. To accomplish this, the main goals of this study were, (i) to estimate the fraction of Pb derived from traffic paint, that is orally bioaccessible in five different spiked soils (ii) to assess the role of soil mineralogy in the gastric and intestinal bioaccessible

fractions; (iii) to measure the fraction of bioaccessible Pb in urban top-soils collected at elementary schools; (iv) to provide more data enabling us to understand the role of soil mineralogy in Pb bioaccessibility for land use and urban planning.

2. Materials and methods

2.1. Study site, sampling, and sample preparation

The study area is the city of Hermosillo located in northwest Mexico (Fig. 1). The climate in the area is dry with summer temperatures that range from 35 to 49 °C, and from 8 to 5 °C during the winter. The erosive effects of the moonsonal rainfall in this region influences the generation of greater dust emissions after the summer (Moreno-Rodríguez et al., 2015). Surface runoff and erosion, in combination with traffic highly influence suspension processes (Meza-Figueroa et al., 2016). In the last two decades, the city has experienced rapid growth with a population increase rate of ~3%, greater than the rate of increase for the state population (1.4%) causing a rise in the vehicular traffic volume. Because of the strong erosion of paved roads, traffic signals are frequently re-painted during the year, creating an increased area source emitting Pb-based paint (Meza-Figueroa et al., 2018). The urbanized area is located in a semiarid region with soils of Quaternary age, sedimentary tertiary rocks and intrusive rocks of the Cretaceous (Fig. 1).

We collected five samples of periurban, and ten samples of urban topsoil at schools (0–5 cm, Fig. 1). The periurban soils represent matrices that are barely affected by anthropogenic activities, and the latter encompasses all types of non-paved land within the city. Urban topsoils were from elementary school playgrounds where children spend significant time during the school year. We obtained yellow traffic paint (TP) from a can provided by municipal workers after street painting, and we analyzed samples after drying and grinding in an agate mortar.

All samples were oven-dried at 35 °C, and sieved through the #635 mesh. This fraction represents a particle size smaller than 20 μm in aerodynamic diameter and is the most likely particle size that can be resuspended or could easily be adhered to hands (Ruby and Lowney, 2012). Samples of yellow traffic paint were ground to the same grain size as soils. We spiked 3 g of each sample of the five periurban soils with 0.2 g of traffic paint. This allowed testing the role of soil mineralogy in the bioaccessibility of lead derived from lead chromates in paint, because each soil type contained the same amount of contaminant. We also measured bioaccessibility of soils collected at elementary schools without any paint addition.
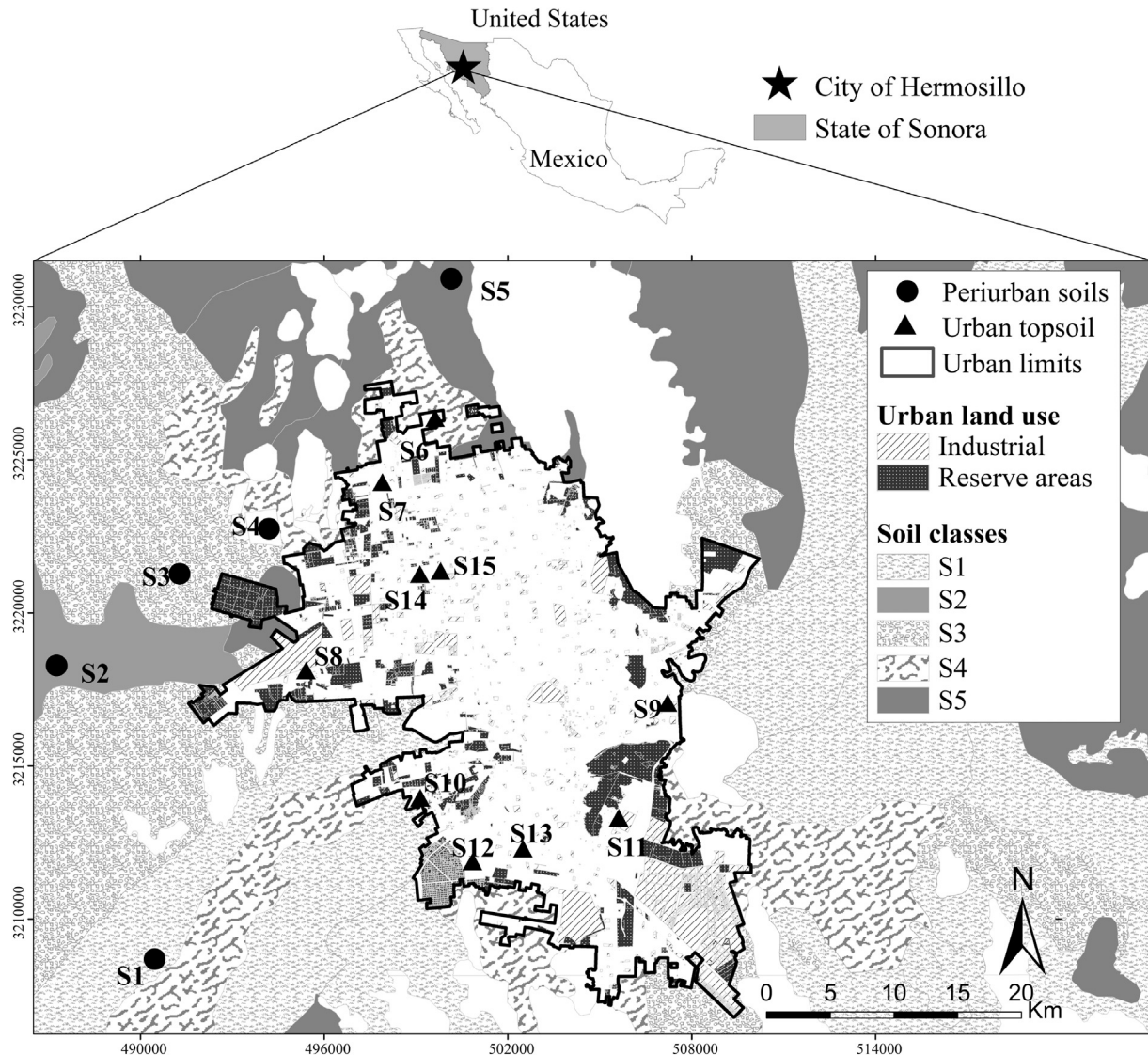

Fig. 1. Map of Hermosillo city showing the location of periurban soils and urban topsoils (collected at elementary schools). White area within the urban area lacks data regarding soil-type ocurrence. Black line is the urbanized area.

2.2. Mineralogy and total Pb concentration

We identified the mineralogy for each sample as well as the traffic paint with a X-ray powder diffraction (XRPD) by a Bruker D8 Advance diffractometer with a Cu-radiation source λ(Kα1) =1.5406 Å. Operating conditions were 40 kV/35 mA at room temperature. The (2theta) scan range was from 6° to 77° with a step size of 0.02° at a time per step of 2 s. Diffrac-plus EVA software was used, supported by the database of the International Centre for Diffraction Data (ICDD) for the scan interpretation phase. XRD provides a semi-quantitative method for obtaining the mineral abundances in weight % (Mandile and Hutton, 1995; Nowak et al., 2018).

Bulk Pb was obtained from concentrations for all studied samples with a Niton XL3t portable XRF analyzer from Thermo Scientific, according to the USEPA Method 6200 (USEPA, 2007). Detection limits for Mo, Sr, Pb, As, Zn, Cu, Fe, Mn, Cr, V, Ti, Sc, Ca, and K are <10 mg.kg^{-1}. Duplicates of silicon dioxide (SiO_2) were used as blanks. Acceptable recovery for all elements was between 90 and 110%, considering seven replicates of three standard reference materials (SRM) from the National Institute of Standards and Technology (NIST) SRM 2709, SRM 2710, and SRM 2711. Samples were analyzed in triplicate, for 60 s. In addition, in order to verify the XRF analysis, we sent 10% of the collected samples to the ALS Laboratory in Toronto, Canada for analysis by plasma-atomic emission spectrometry (ICP-AES), after the EPA Method 3050B and 6010B (USEPA, 1996a, 1996b, and USEPA, 2007). Results agreed within 95% confidence level. The use of portable XRF technique for the analysis of metal concentration in soils has been widely documented (Yang and Cattle, 2015; Bower et al., 2017; Turner and Lewis, 2018).

2.3. Pb bioaccessibility

Physiologically based extraction test (PBET) (Ruby et al., 1993, 1996) were used to assess Pb oral bioaccessibility in (i) soil samples spiked with lead-chromates traffic paint, and (ii) urban topsoils collected at elementary school playgrounds. The PBET is an in vitro test system, which incorporates gastrointestinal tract parameters representative of a human, including stomach and small intestinal pH and chemistry. Synthetic gastric and intestinal fluids were prepared according to the Physiologically Based Extraction Tests-PBET (Ruby et al., 1993, 1996). The gastric fluid was a mixture of one liter of deionized water with pepsin (1.25 g), citric acid (0.50 g), malic acid (0.50 g), lactic acid (0.420 mL), and acetic acid (0.5 ml). The pH was adjusted to 1.3 with 12 N hydrochloric acid (HCl). One hundred fifty millilitres of this gastric fluid were in a 250-mL separator funnel containing 1.5 g of the sample. Before blending, samples were sieved to 20 μm because it is predominantly smaller particles that adhere to children's hands and might be ingested. The bottle was placed in a shaker in a water bath at a controlled temperature of 37 °C for one hour, and argon was injected at 1 L-min^{-1} for the removal of dissolved oxygen. The pH was checked every ten minutes and adjusted with 12 N of HCl as needed. Then, the 10-mL of aliquot was removed from the reaction funnels 1.0 h after initiation of the reactions. The liquid fractions were filtered through a 0.45-
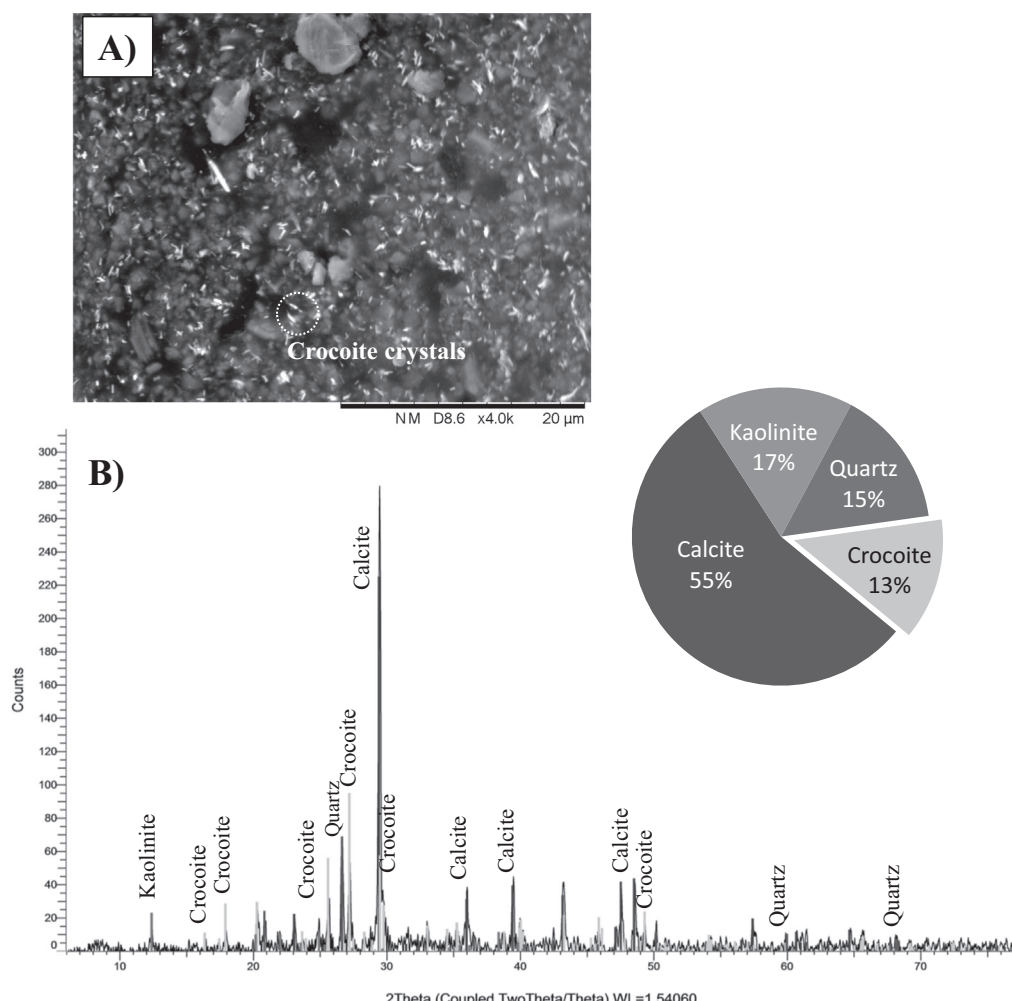

Fig. 2. XRD pattern for traffic paint (TP) with main mineralogical phases of calcite ($CaCO_3$), quartz (SiO_2), kaolinite ($Al_2Si_2O_5(OH)_4$), and crocoite ($PbCrO_4$).

Table 1
Mineralogy of traffic paint, periurban and urban topsoils at 20 μm size. TNM: Total Neutralizing Minerals (the sum of calcite and other carbonates). Mineral abundance is expressed as %. Not reported: n.r. DL: detection limit.

| Mineralogy | Traffic paint | Periurban soils | | | | | Topsoils collected within playgrounds (schools) | | | | | | | | | |
	TP	S1	S2	S3	S4	S5	S6	S7	S8	S9	S10	S11	S12	S13	S14	S15
Quartz	15	44.4	6.3	27.8	12.5	9.8	6.4	29.5	31.1	24.5	26.9	26.1	26	21	25	32
Crocoite	13	n.r.	n.r.	n.r.	n.r.	n.r.	n.r.	n.r.	<DL	n.r.	n.r.	n.r.	n.r.	n.r.	n.r.	n.r.
Calcite	55	4.8	n.r.	n.r.	3.7	42.5	3.1	3.3	4.5	7.7	5.6	15.9	1.8	2.0	8.0	7.0
Kaolinite	17	1.2	1.9	n.r.	n.r.	n.r.	1.1	n.r.	n.r.	n.r.	n.r.	n.r.	n.r.	4.0	n.r.	4.0
Plagioclase	n.r.	32	48.3	21.3	43.5	14.9	46	24	32	30	47	25	45	31	39	35
Feldspars	n.r.	16.2	35.6	23.8	13.7	12.2	23	21	13	20	11	14	17	25	18	n.r.
Micas	n.r.	n.r.	2.1	9.4	7.7	6.1	2.2	9	4.3	3.2	3.4	2.4	1.8	n.r.	5	15
Iron oxides	n.r.	n.r.	2.1	3.3	1.9	4.6	n.r.	n.r.	n.r.	n.r.	n.r.	n.r.	n.r.	n.r.	n.r.	n.r.
Dolomite	n.r.	n.r.	n.r.	n.r.	n.r.	n.r.	n.r.	0.6	2.3	1.9	n.r.	3.1	0.6	n.r.	n.r.	n.r.
Gypsum	n.r.	0.3	n.r.	n.r.	n.r.	n.r.	n.r.	n.r.	n.r.	n.r.	n.r.	n.r.	n.r.	n.r.	n.r.	2
Amphibole	n.r.	n.r.	n.r.	n.r.	12.9	5.7	n.r.	n.r.	n.r.	3.2	n.r	2.7	3.6	3	n.r.	2
Zeolites	n.r.	1.1	n.r.	n.r.	n.r.	2.2	n.r.	n.r.	n.r.	n.r.	n.r.	n.r.	n.r.	n.r.	n.r.	n.r.
Other carbonates	n.r.	n.r.	n.r.	1.5	0.5	n.r.	n.r.	n.r.	n.r.	n.r.	n.r.	n.r.	n.r.	n.r.	n.r.	n.r.
TNM	55	4.8	n.r.	1.5	4.2	42.5	3.1	3.9	6.8	9.6	5.6	19	2.4	2	8	7
Total %	100	100	96	89	96	98	82	88	89	91	94	89.2	96	86	95	97

μm membrane, transferred to polyethylene vials, and stored in the dark at 4 °C until analysis.

The intestinal conditions were simulated by neutralizing the remaining gastric solution to pH 7.0 by adding $NaHCO_3$. After adding the porcine bile salts (70 mg) and porcine pancreatin (20 mg) the bottle was stirred at 37 °C for 3 h with an argon flow of 1 L.min^{-1}. Once again, the 10 mL of aliquot was removed, and we filtered it through a 0.45 μm cellulose membrane. All the solutions were analyzed by an Inductively Coupled Plasma Optical Emission Spectrometer (ICP-OES) Perkin Elmer Optima 8300 DV at the National Laboratory of Geochemistry and Mineralogy, Institute of Geology, National University of Mexico in Mexico city. Detection limit for lead is 0.007 mg.L^{-1}. We analyzed duplicates in 20% of studied samples for quality assurance.

2.4. Statistical analysis

Multivariate techniques such as cluster analysis and principal component analysis (PCA) were used to find underlying controls over a dataset. We analyzed lead total concentration, bioaccessible lead, and mineralogy by principal component and cluster analysis using SPSS Statistics 20 for Windows software package (SPSS Inc., Chicago, IL). PCA with a VARIMAX rotation was applied and factors with eigenvalues greater than unity were retained in the analysis. Cluster analysis to the standarized matrix of samples was applied following Ward's method and the results are shown in dendrograms. The Bartlett sphericity test and the Kaiser-Meyer-Olkin index (KMO) which determine wheter it is possible to efficiently factor the original variables. The Bartlett test should be conducted only if n/k is <5, where n is the sample size and k is the number of variables. In this work, n/k is <5, so the sphericity test of Bartlett was performed in the dataset. The KMO index compares the correlation values between variables and their partial correlations. If KMO has a value close to 1, then the principal component analysis (PCA) can be made. If KMO is close to zero, the PCA is not relevant (Jamhari et al., 2014). The KMO and the Bartlett sphericity test show that the dataset for this study was adequate for PCA analysis.

2.5. IEUBK modeling

The Integrated Exposure Uptake Biokinetic (IEUBK) model for lead in children (USEPA, 2007) was used to predict lead levels in children's blood. Total Pb concentrations were entered into the IEUBK model in order to obtain bioaccessibility values for each studied soil.

Table 2
Total concentrations of metals (mg.kg^{-1}) in periurban and urban soils collected at elementary schools (fraction 20 μm). TP: Traffic paint.

Sample	Mo	Sr	Pb	As	Zn	Cu	Fe	Mn	Cr	V	Ti	Sc	Ca	K
Periurban soils														
S1	<10	448	32	14	93	38	31535	484	71	109	4283	86	25960	18650
S2	<10	245	26	11	90	36	34768	509	80	107	4337	32	7558	19216
S3	<10	265	26	12	85	38	32316	640	91	113	4699	26	7269	18843
S4	<10	277	25	11	63	37	33929	622	87	125	5602	28	6225	20289
S5	<10	519	28	<10	82	44	32040	489	92	99	3448	208	78728	15356
Urban soils														
S6	<10	362	34	<10	122	56	31927	487	72	112	4805	72	25760	18707
S7	<10	323	35	<10	362	52	35990	422	84	128	4833	64	25344	18666
S8	<10	326	43	<10	170	43	28611	399	64	94	3824	74	27206	19254
S9	22	460	90	30	912	3418	45021	565	83	102	3591	123	46762	17272
S10	11	914	42	17	215	50	51747	549	89	148	5802	82	29982	17563
S11	10	499	58	14	907	110	43401	417	102	108	4210	97	33211	18109
S12	<10	437	46	<10	278	42	59104	1325	120	129	4235	86	31717	14899
S13	<10	449	173	<10	235	118	43163	475	103	131	4500	88	32704	19569
S14	<10	360	42	<10	156	52	24306	440	68	101	3061	84	31824	20233
S15	<10	367	36	<10	142	52	36138	561	86	121	4553	84	24829	18124
Traffic yellow paint														
TP	19	134	31958	<10	617	<10	897	<10	4809	58	2786	310	152852	1139

Table 3
Oral bioaccessibility of Pb in spiked soils with traffic paint and soils collected from schools following gastric and gastric/intestinal simulated digestions. NC: Not calculated. Lead levels in blood (PbB) predicted by the IEUBK model for children aged 1 to 7 years old.

Sample	Total Pb mg.kg^{-1}	Bioaccesibility				Risk assessment (IEUBK)			
		Gastric		Intestinal		Predicted % of children (1–7 years old)			
		mg.L^{-1}	%	mg.L^{-1}	%	>5 µg-dL^{-1}	>10 µg-dL^{-1}	>15 µg-dL^{-1}	>20 µg-dL^{-1}
Spiked soils									
S1 + TP	1575	745.83	47.36	123.84	7.86	97.93	71.40	38.30	18.15
S2 + TP	2050	923.12	45.03	206.44	10.07	99.08	81.10	50.75	27.65
S3 + TP	1880	974.6	51.85	41.45	2.21	99.38	84.75	56.48	32.68
S4 + TP	1910	779.18	40.80	129.96	6.80	98.04	72.18	39.19	18.77
S5 + TP	1962	894.95	45.60	72.56	3.70	98.96	79.90	49.02	26.21
Urban Soils (schools)									
S6	34	10.66	31.11	<0.007	NC	4.32	0.071	0.003	0.000
S7	35	11.86	34.37	<0.007	NC	4.53	0.077	0.003	0.000
S8	38	14.19	37.00	<0.007	NC	4.93	0.089	0.003	0.000
S9	90	30.07	33.38	<0.007	NC	7.75	0.188	0.009	0.001
S10	42	29.88	70.45	<0.007	NC	8.50	0.221	0.010	0.001
S11	58	19.58	33.54	<0.007	NC	5.79	0.115	0.005	0.000
S12	46	11.09	23.96	<0.007	NC	4.30	0.071	0.000	0.000
S13	173	97.44	56.20	2.57	1.48	27.01	1.843	0.159	0.018
S14	42	16.84	40.48	<0.007	NC	5.41	0.103	0.004	0.000
S15	36	11.38	31.57	<0.007	NC	4.78	0.084	0.003	0.000

3. Results and discussion

3.1. Mineralogy and Pb content in soils and traffic paint

Lead-chromates based traffic paint contains ground mineral pigments of crocoite ($PbCrO_4$) into an organic matrix of polymers for the characteristic yellow color (Jeffs and Jones, 1999; Walraven et al., 2015). Fig. 2A shows the characteristic crystals of crocoite embedded in the matrix of collected paint for this study; in the image, crocoite minerals appear in white color as subhedral crystals mostly smaller than 1 µm. The diffractogram obtained for the traffic paint is shown in Fig. 2B. Table 1 shows the results of X-ray diffraction analysis (XRD) with the mineralogy of yellow paint, periurban, and topsoils collected from schools. Traffic paint is made of 15% quartz (SiO_2), 13% crocoite ($PbCrO_4$), 55% calcite ($CaCO_3$), and 17% kaolinite ($Al_2Si_2O_5(OH)_4$). Quartz content in periurban soils varies from 6.3 to 44.4%; crocoite was not found in any periurban soil; calcite is absent in S2 and S3, with the highest content in S5 (42.5%); and kaolinite is only detected in S1 and S2. Besides Pb from TP there is "natural" Pb in the samples S1 to S5 but insignificant to influence the PBET. Total Neutralizing Minerals (TNM in Table 1) refer to the carbonate group minerals such as: calcite ($CaCO_3$), dolomite ($CaMg(CO_3)_2$), rhodochrosite ($MnCO_3$),

magnesite ($MgCO_3$) and siderite ($FeCO_3$). The term "Other carbonates" used in this table refers to all carbonate minerals but calcite. The mineral calcite was separated because it appears in most studied topsoils and in the traffic paint. The five soil samples analyzed are characterized by variable percentages of total neutralizing minerals (TNM). Sample S5 (located in the north side of the city) has the highest TNM content associated to calcite content, and sample S2 (located in the southeast) has the lowest. Carbonate minerals give the primary neutralizing capacity because they react rapidly enough to keep up with the rate of acid production when compared to other minerals such as silicates. In soils, it is common that calcite is the dominant neutralizing mineral. In this study, the variation of TNM% is as follows: S5 > S1 > S4 > S3 > S2. According to Fig. 1, the soil map of Hermosillo shows that the surface cover is dominant as follows: S4 > S5 > S1 > S3. The soil type S2 is not present within the urbanized area. The XRD analysis is relevant because it shows that the five chosen periurban soils have a diverse mineralogy.

On the other hand, urban topsoil mineralogy in the 20 µm size is dominated by plagioclase, feldspars, and quartz (Table 1). Calcite ($CaCO_3$) and dolomite ($CaMg(CO_3)_2$) occur in most samples and they constitute the total neutralizing mineralogy (TNM). Calcite was identified in all topsoil samples collected at schools in contents from 2 to 15.9%. Kaolinite was found in samples S13, S14, and S15 in about the
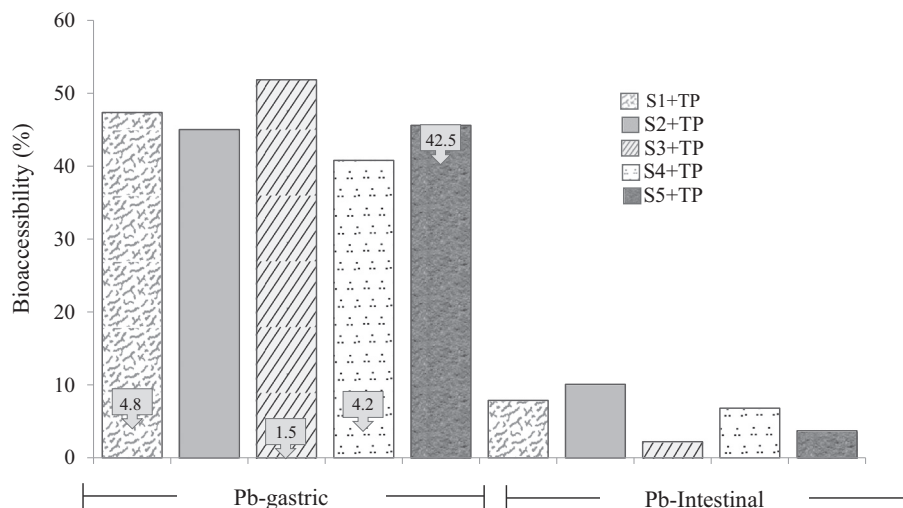

Fig. 3. Lead bioaccessibility in gastric and intestinal phases for periurban soils spiked with traffic paint. In squares the total neutralizing minerals or carbonates (TNM %).

same amount (4%). Crocoite was detected by XRD in sample S8, however, data are semiquantitative and the content of this mineral is very low. Urban topsoil additionally contains mixtures of particles including brake wear, combustion products, and other pollutants related to traffic. They have in common a lack of crystalline structure, so they can not be identified by XRD technique, and they are not described in this work. However, the geochemistry of total metal content in analyzed samples is indicative of most of the identified mineralogy.

Table 2 shows the results of metal content in traffic paint (TP), periurban soils (S1 to S5) and urban topsoils collected at schools (S6 to S15). TP is characterized for its very high metal contents in Pb (nearly 32,000 mg.kg^{-1}) and Cr (4809 mg.kg^{-1}). It also contains important concentrations of Zn (617 mg.kg^{-1}) and Ca (152,852 mg.kg^{-1}). Metals in periurban soils are in low concentrations and their origin is natural (Table 2). In the soil samples to which the traffic paint was added (S1 to S5), the elements expected to have high concentrations are Pb, Cr, Zn, and Ca. These would be contributed in by the traffic paint in concentration equal for each spiked soil. This is important because the differences in the bioaccessibility of lead will be given by the distinct characteristics of the soils.

Urban topsoils have variable Pb-contents, from values close to natural background (32 mg.kg^{-1}) to 176 mg.kg^{-1}. This evidences the variability of Pb in sources emanating from the urban environment. Most samples exceed the background values provided by periurban soils, but samples S9 (92.6 mg.kg^{-1}), and S13 (175.6 mg.kg^{-1}) have the highest Pb content in studied soils. Table 2 shows that for topsoils collected at schools, Zn-Cu-Cr-Sc are in concentrations higher than periurban soils and their origin is most likely associated to urban activities.

3.2. Mineralogy and bioaccessibility

Total and bioaccessible concentrations of lead measured in the samples after digestion in the simulated gastric (PbG) and intestinal fluids (PbInt) are shown in Table 3. The total concentration of Pb in the soil fortified with yellow paint varies from 1575 to 2050 mg.kg^{-1}. Gastric bioaccessibility of Pb varies from 745.8 to 974.6 mg.L^{-1}, with a standard deviation of 87. Gastric bioaccessibility values when compared to the total lead are within a range of 40.8% to 51.9%. The porcentage is the result of the Pb concentration in mg.L^{-1} in bioaccesible aliquot divided by the total Pb content in the sample and multiplied by 100 (Table 3).

Fig. 3 shows the percentage of lead-bioaccessibility in gastric and intestinal phases and the TNM content in each spiked soil. Soil S2 (spiked with TP) has the highest PbInt of 10.1% and also it has the highest kaolinite content (1.9%) but there is no presence of TNM. Fortified soil 3 (S3 + TP) shows the highest gastric bioaccessibility (PbG of 51.85%) but the lowest intestinal bioaccessibility (PbInt of 2.21%). This soil does not contain kaolinite of geogenic source. This sample has 1.5% of other carbonates, mainly magnesite (MgCO$_3$). Sample S4 contains almost the same amount of TNM (4.2%) as sample S1 (4.8%) and the gastric (S1 = 47%, S4 = 41%) and intestinal (S1 = 8%, S4 = 7%) Pb-bioaccessibility is similar. Main mineralogical differences among both samples are as following: S1 has more abundant quartz, kaolinite and zeolites, and sample S4 has more iron oxides, amphiboles and magnesite. Because of similarities in TNM content, it may be interesting to explore the effect of carbonate minerals in Pb-bioaccessibility in further studies. Sample S5 has a very high content of TNM (42.5%), however, Pb-releasing at gastric conditions seems similar to sample S2 with no TNM content. The very high content of TNM in sample S5 may be promoting further dissolution of Pb-minerals by acid rebound at gastric conditions whereas the absence of carbonates in S2 and the presence of kaolinite seem to contribute to the releasing of Pb at intestinal conditions. However, further studies with a higher number of samples is strongly recommended to prove this.

Urban soils collected at elementary schools show more variation in lead bioaccessibilities in the gastric phase, with sample S10 being the

Table 4
Correlation coefficient (Spearman) for metals, bioaccessible Pb at gastric and intestinal conditions, and mineralogy (n = 15).

	Pb	PbG	PbInt	Sr	As	Zn	Cu	Fe	Mn	Cr	V	Ti	Sc	Ca	K	Quartz	Calcite	Kaolinite	Crocoite	TNM
Pb	1.000																			
PbG	0.912**	1.000																		
PbInt	0.867**	0.834**	1.000																	
Sr	−0.059	−0.118	−0.314	1.000																
As	0.376	0.474	0.177	0.254	1.000															
Zn	−0.497	−0.525*	−0.741**	0.411	0.113	1.000														
Cu	0.0508	−0.459	−0.664**	0.535*	−0.065	0.700**	1.000													
Fe	−0.013	−0.132	−0.270	0.425	0.324	0.582*	0.289	1.000												
Mn	0.343	0.232	0.242	−0.086	0.256	−0.289	−0.352	0.414	1.000											
Cr	0.853**	0.729**	0.834**	−0.039	0.208	−0.568*	−0.597*	0.139	0.461	1.000										
V	−0.175	−0.168	−0.068	0.082	0.027	0.171	0.029	0.607*	0.364	0.157	1.000									
Ti	−0.179	−0.029	0.109	−0.246	0.122	−0.182	−0.190	0.254	0.279	0.136	0.771**	1.000								
Sc	0.089	−0.052	−0.181	0.822**	0.103	0.381	0.483	0.191	−0.166	−0.014	−0.263	−0.656**	1.000							
Ca	0.926**	0.835**	0.782**	0.068	0.414	−0.499	−0.425	−0.077	0.366	0.808**	−0.266	−0.288	0.284	1.000						
K	0.068	0.200	0.322	−0.664**	−0.231	−0.364	−0.203	−0.561*	−0.289	−0.121	−0.064	0.186	−0.604	−0.111	1.000					
Quartz	−0.393	−0.293	−0.363	0.139	0.115	0.332	−0.020	0.068	−0.229	−0.300	0.139	0.036	0.148	−0.241	−0.207	1.000				
Calcite	0.637*	0.663**	0.544**	0.066	0.458	−0.477	−0.320	−0.304	−0.016	0.518*	−0.497	−0.273	0.177	0.742**	−0.023	−0.061	1.000			
Kaolinite	0.364	0.367	0.537*	−0.317	−0.244	−0.565*	−0.229	−0.445	0.024	0.289	−0.132	−0.113	−0.079	0.361	0.519*	−0.256	0.256	1.000		
Crocoite	0.819**	0.818**	0.923**	−0.327	0.249	−0.818**	−0.756**	−0.360	0.327	0.818**	−0.196	0.065	−0.197	0.819**	0.164	−0.262	0.688**	0.408	1.000	
TNM	0.06*	0.618*	0.475	0.086	0.485	−0.414	−0.287	−0.275	0.036	0.468	−0.543*	−0.329	0.227	0.745**	−0.107	−0.018	0.979**	0.132	0.655**	1.000

* Correlation is significant at 0.05 level.
** Correlation is significant at 0.01 level.

highest 70.45% and with sample S12 the lowest (23.96%) (Table 3) This could be linked to different anthropogenic urban sources for lead that could be more bioaccessible, for example lead oxides have been previously reported by Meza-Figueroa et al. (2018) at urban dust in the study area. Lead oxides are more soluble than lead chromates. Sample S10 shows the lowest variability in minerals, mostly of natural origin. It contains albite, quartz, microcline, calcite and muscovite when compared to the other samples (Table 2). Most collected samples show PbG higher than 23%, despite low total lead contents in urban soils, this can be due to more soluble Pb-phases in urban environments. In the intestinal phase, only sample S13 has bioaccesible lead. Samples S13, S14, and S15 have similar kaolinite contents, but S13 has high total Pb content (173.38 mg.kg^{-1}). Bioaccessible lead in samples S14 and S15 in the intestinal phase are below detectable levels possibly because of the low total Pb content.

The implications of the variability in the bioaccessibility of lead in all studied samples are shown in Table 3. Lead levels in blood as predicted by the IEUBK model for children aged 1 to 7 years old show important differences when >20 µg.dL^{-1}. Predicted values range from 18 to almost 33% of children for the same concentration of contaminant (lead traffic paint added to soil). The only difference could be related to the soil characteristics, mainly mineralogy. It is commonly assumed that the variability in Pb-bioaccessibility in urban environments is due to different urban sources, however, the results of this work suggest that soil mineralogy, including urban topsoils, may play a role in Pb-releasing at gastrointestinal conditions.

3.3. Correlations and PCA

In order to establish the inter-elemental, minerals and bioaccessibility data relationships, Spearman's correlation coefficients were obtained (Table 4). Lead at gastric conditions (PbG) shows strong correlation (R^2 = 0.99) with total Pb, lead at intestinal conditions (PbInt), total Cr, Ca, calcite and crocoite. The correlation with TNM is also strong (R^2 = 0.95). Pb-releasing at gastric conditions seem to be affected by carbonate content in ingested matrix (TNM) and the pollutant by itself since Cr, Pb, Ca, and crocoite are the main components of the traffic paint.

Correlation of bioaccessible lead at intestinal conditions (PbInt) is strong (R^2 = 0.99) with Pb, Zn, Cu, Cr, Ca, and crocoite. Correlation of PbInt is also strong (R^2 = 0.95) with calcite and kaolinite. Pb, Zn, Cr, Ca, and crocoite are also components of the traffic paint but there is no correlation with TNM at PbInt.

The correlation among minerals and oral bioaccessibility for lead was examined and the results are shown in Table 5. A positive correlation was identified for kaolinite and intestinal lead bioaccessibility, as well as between the content of calcite and total neutralizing minerals for spiked soil samples. A moderate correlation ($r = 0.441$) was obtained for kaolinite and intestinal lead bioaccessibility, and a strong ($r = 0.984$) correlation was identified for total neutralizing minerals and calcite. This supports findings from the PBET test, mineralogy descriptions, and Spearman correlation matrix. The non significant correlations of PbG demonstrate a variability of mineral solubility at gastric acid conditions, as well as the differences among the sources of natural origin represented by the five soil-types from this study mixed with lead from anthropogenic sources. For example, the value of bioaccessibility of lead of 70% in urban topsoil indicates a strong transformation to bioavailable forms of lead, possibly as oxides or carbonates. Meza-Figueroa et al. (2018) reported the presence of highly soluble lead oxides (scrutnyite) in urban dust in the city of Hermosillo. It has been documented that the dissolution of Pb-minerals is controlled by the gastric phase, and the absorption occurs in the intestinal phase, and that the pH in the intestine, strongly influences Pb behavior (Smith et al., 2011). Dissolution of minerals occurs in the stomach, whereas absorption occurs in the intestinal tract (Sipes and Badger, 2001). Not all the materials that are dissolved in the stomach conditions are absorbed in the

Table 5
Correlation coefficient, and Varimax rotated principal components analysis (PCA) for minerals and lead bioaccessibility in spiked soils. PbG: gastric phase; PbInt: intestinal phase; TNM: Total Neutralizing Minerals. Gray area corresponds to urban soil samples.

	Calcite	Kaolinite	TNM	PbInt	PbG	Crocoite
Calcite	1.000	−0.047	**0.984**	−0.327	−0.092	−0.117
Kaolinite	−0.402	1.000	−0.169	0.441	0.136	−0.240
TNM	**0.873**	−0.007	1.000	−0.334	−0.151	0.004
PbInt	−0.400	**0.853**	−0.078	1.000	0.432	−0.111
PbG	−0.125	−0.044	−0.184	−0.530	1.000	−0.056
Crocoite	−0.156	−0.779	−0.515	−0.450	−0.210	1.000

Varimax rotated PCA for periurban soils					*Total explained variance*			
	Component	Component	Component	Component	Total	%variance	%cumulative	
	1	2	3	1	2.540	42.335	42.335	
Calcite	−0.236	**0.958**	−0.014	2	2.104	35.059	77.395	
Kaolinite	**0.979**	−0.183	−0.082	3	1.307	21.777	99.171	
TNM	0.172	**0.974**	−0.067	4	0.050	0.829	100.000	
PbInt	**0.775**	−0.247	−0.578					
PbG	0.015	−0.119	**0.992**					
Crocoite	−0.889	−0.387	−0.245					

Varimax rotated PCA for urban soils (schools)					*Total explained variance*			
	Component	Component	Component	Component	Total	%variance	%cumulative	
	1	2	3	1	2.358	39.293	39.293	
Calcite	**0.992**	−0.085	0.069	2	1.483	24.710	64.003	
Kaolinite	−0.099	0.335	**0.709**	3	0.980	16.332	80.334	
TNM	**0.980**	−0.116	−0.067	4	0.757	12.619	92.954	
PbInt	−0.303	**0.733**	0.323					
PbG	0.013	**0.884**	−0.057					
Crocoite	−0.086	0.098	−0.828					

Bold data indicates the highest correlation coefficient values.

intestinal tract. Diffusion across the intestinal wall into the bloodstream requires the toxin/pollutant to be in the most lipid-soluble/nonionized form, and this depends on its acid/base characteristics (Rozman and Klaasen, 2001). Weak acid is mainly in the lipid soluble form in the stomach, and in the ionized form in the intestine. Bases are ionized in the stomach and nonionized in the intestine. Carbonate minerals that are easily dissolved in the stomach (acidic/oxidized conditions) may adsorb or precipitate as solids in the intestinal media because of less oxygenated and alkaline conditions. This is particularly shown with sample S5 + TP (Fig. 3) having the highest calcite content and a low intestinal lead bioaccessibility. Sample S3 + TP shows the lowest lead bioaccessibility at intestinal conditions. This sample does not contain significant amounts of calcite but it is the only sample with the highly reactive magnesite (Other carbonates in Table 1, content of 1.5%). These results show that future studies that evaluate the role of different minerals with relative highest relative reactivity and intestinal bioaccessibility of lead deserve more detailed attention.

Sample S5 shows the lowest Pb-bioaccesibility at intestinal conditions. This sample has the highest content of calcium carbonate (calcite) in the soil matrix. The dissolution of calcite in gastric conditions may promote the release of lead in the stomach by acid rebound, and the precipitation or adsorption of lead in the intestine, thus decreasing the bioaccesibility at alkaline conditions.

In the PCA, the first two components explained 86.34% of the total variance (Table 5). PC1 shows the control exerted by kaolinite presence on intestinal lead bioaccessibility ($r = 0.8553$, Table 5); PC2 separates total neutralizing minerals-calcite. Cluster analysis was reported as a dendrogram. Three groups are observed for the periurban soils that were spiked with the traffic paint. The first group shows an association of calcite and TNM. Because calcite is the most abundant carbonate in the studied samples, it becomes the dominant mineral in the TNM. The second group contained lead bioaccessible at gastric conditions (PbG) and crocoite (main lead mineral in traffic paint). The third group comprised kaolinite and lead bioaccessible at intestinal conditions (PbInt). These data strongly supports the findings of PCA.

Summarizing, Fig. 4 shows (i) an association between kaolinite content in soils, and intestinal bioaccessibility of lead; (ii) an association of calcite with TNM, and (iii) a dissolution of crocoite in gastric phase, and its further releasing of Pb. Dendrogram of urban topsoils collected at schools shows two groups: (i) TNM-calcite and (ii) kaolinite-PbInt-PbG-Crocoite. Because lead sources at urban topsoils are numerous (traffic, industrial, incinerator ashes, fertilisers, Pb-gasoline residues in
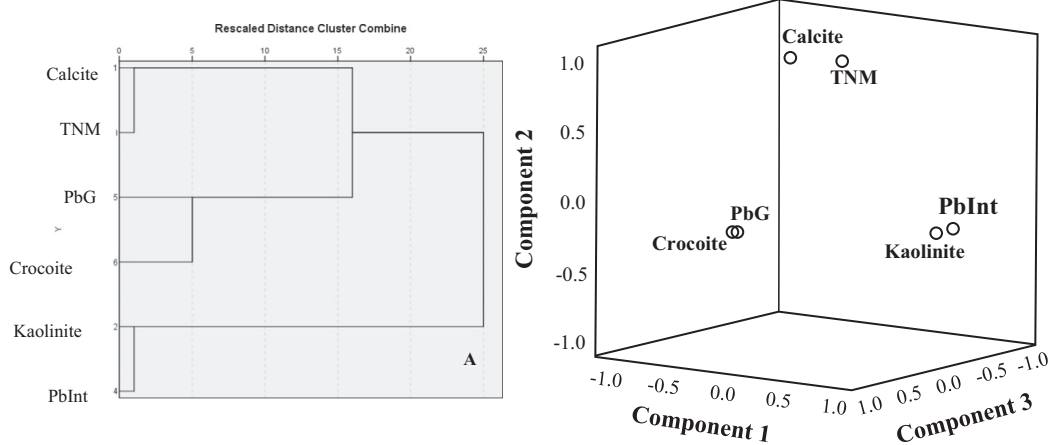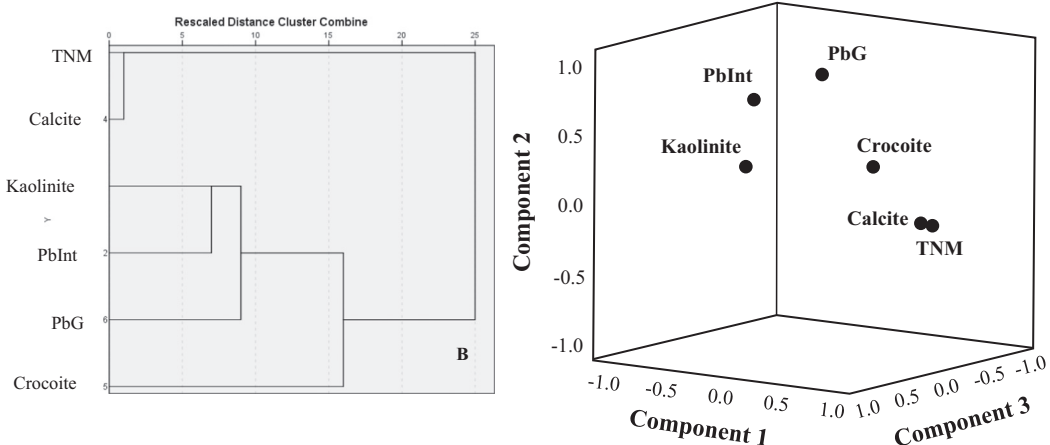

Fig. 4. Dendrogram derived from hierarchical cluster analysis for minerals and values of gastric (PbG), and intestinal (PbInt) lead bioaccessibilities in (i) spiked soils (soil+lead chromates traffic paint); and (ii) urban topsoils collected at schools. Representation of the first three factorial planes of principal component analysis (PCA) for (i) spiked periurban soils, and (ii) urban topsoils in schools, showing interrelationships among minerals and lead bioaccessibility at gastric (PbG) and intestinal (PbInt). Varimax rotation was applied to maximize interpretations.
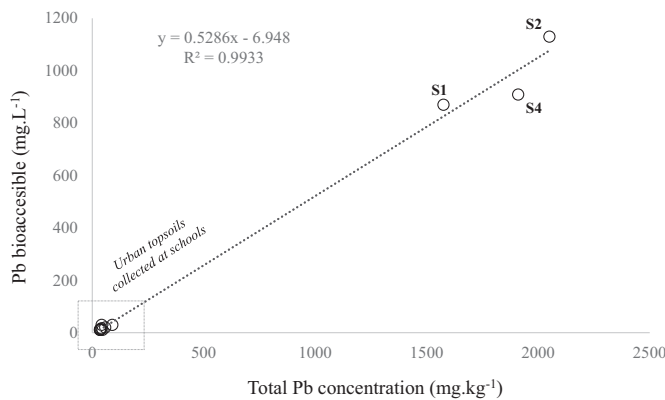
Fig. 5. Bioaccessible vs total Pb in urban soils. Regression formula and *r* value are shown.

soils etc.) further work is required to understand the association of other pollutants with lead bioaccessibility.

3.4. Health risk-assessment and implications for land use

The identification of mineral phases that may enhance lead bioaccessibility at intestinal conditions is important for land use planning in growing cities. The results from this work show that for a same contaminant (traffic paint), soil type influences a different behavior of lead solubility mainly at intestinal conditions where most absorption occurs. In this study, total lead content showed a correlation significant at 0.01 level with lead at gastric (PbG) and intestinal (PbInt) conditions, and the coefficients are 0.912 and 0.867, respectively. Considering this, the total Pb (mg.kg^{-1}) vs bioaccesible Pb (mg.

L^{-1}) were used to construct a linear fit that gives a strong linear correlation ($r = 0.99$) (Fig. 5). The samples used to construct the graph were S1, S2, and S4, as well as topsoil data. The predictability of the equation was tested with the samples: S3, S5, and S13. The regression slope is 0.53, lower than the EPA's estimated bioaccessibility IEUBK parameter of 0.60. This result suggests that the IEUBK modeling could give a higher predicted absorption for children in this study site. The ratio of predicted vs measured bioaccessibility ranged from 0.81 to 0.94, with most values around 0.90. The implications of these results in relation to land use planning are important. We have shown that the same contaminant (lead from traffic paint) behaves differently among the five soil types, but soil S3 has the lowest Pb bioaccessibility in the intestinal conditions where most of the absorption occurs. If we could use the equation to predict which soil represents more vulnerable areas in the case of pollutant addition, this information could be helpful for urban planning. In such case, soil S3 represents a safe choice for metal bioaccessibility because the health risk assesment would be low. On the other hand, the highest Pb bioaccessibility in the intestinal phase corresponds to soil S2 with the highest kaolinite content. S2 does not seem to crop out within the urbanized area, however, an extense area of ocurrence of this soil type is located to the west of the city (Fig. 6). Such area should be avoided for residential use.

Toxicological effects of lead in children can occur at very low concentrations, and therefore, the USEPA does not provide a reference dose. The Center for Disease Control and Prevention (CDC) recommends that the blood lead (PbB) levels should not exceed 5 μg.dL^{-1} in children from 1 to 4 years old. This work shows that 4 to 27% of exposed children were predicted to have PbB levels exceeding the threshold of 5 μg-dL^{-1}. If a soil contains significant amount of traffic paint, up to 99% of exposed children could be exceeding this value.
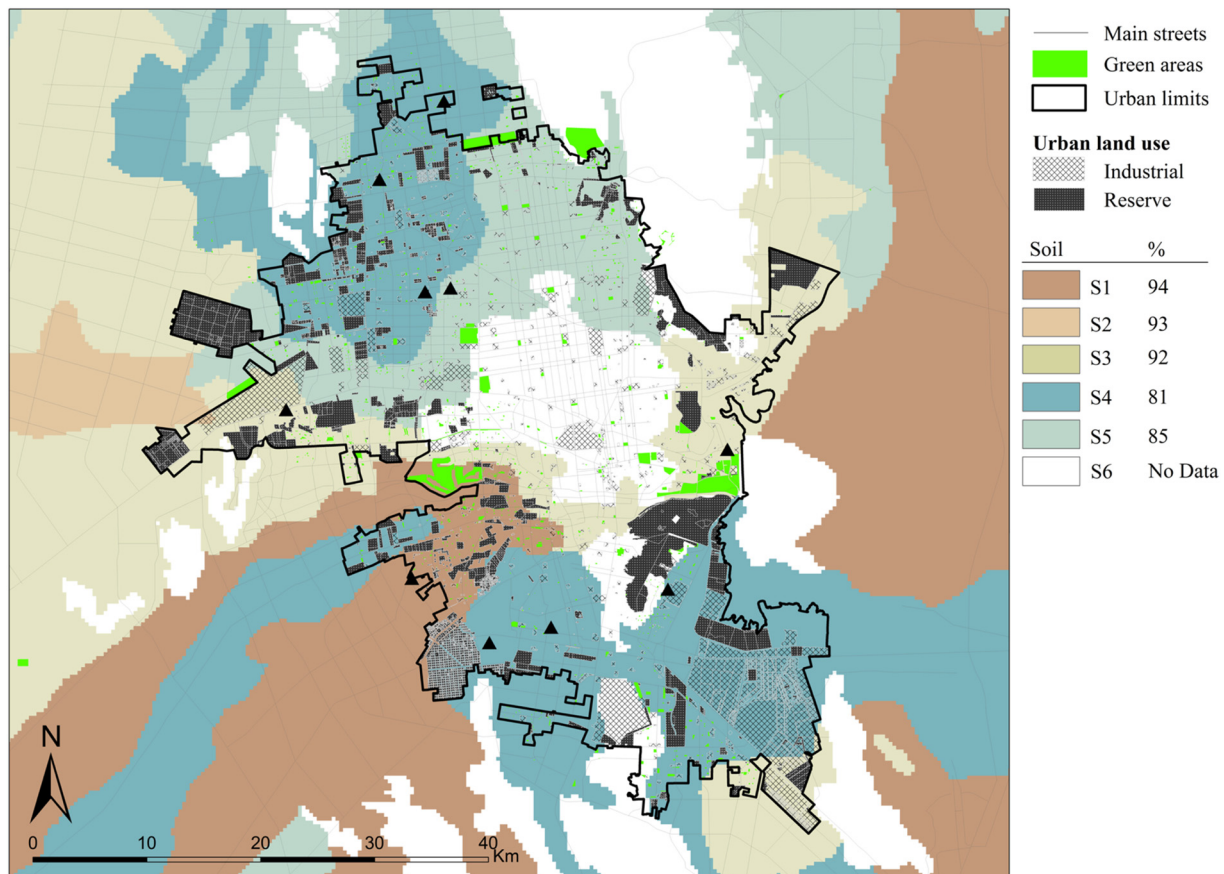

Fig. 6. Spatial distribution of studied soils with % recovery of predicted vs measured bioaccessibility. Reserve are areas considered in the local urban planning for city growth.

The variability of obtained predicted values could also be related to mineralogical diversity in studied soils, so that the risk related to lead exposure in soils could be influenced by the soil type. This work highlights the importance of the bioaccessibility studies and mineralogical characterisation for land use planning in order to reduce lead exposure to children.

4. Conclusions

Previous studies have reported that oral Pb-bioaccessibility of soils polluted with different anthropogenic sources is strongly variable (Walraven et al., 2015). Most studies document that Pb-bioaccessibility depends on: (i) pollutant chemistry, source and solubility; (ii) specific reactive surface of Pb in soils and (iii) the capacity in soils to from secondary Pb-phases (Walraven et al., 2015). This work has explored the possible effect of soil-mineralogy in Pb-bioaccessibility by analyzing the gastric-intestinal bioaccessibility of Pb (PBET) derived from one source (traffic paint) in five types of soil. PBET and statistical analysis indicated that the presence of carbonates as total neutralizing minerals (TNM) in soils may play an important role in gastric bioaccessibility of lead. Additionally, kaolinite, calcite and the contaminant-type may influence the Pb releasing at intestinal conditions. Pb-bioaccessibility in gastric phase, remains within the range of 40.8 to 50.8%, possibly related to acid rebound at stomach conditions and further metal-release. Kaolinite content in soil seems to increase Pb-bioaccessibility in intestinal phase, but further studies are recommended because of the limited number of samples used in this study. The results from this work could help future decisions about urban planning and awareness programs about soil contamination and health effects. Soil information about mineralogical characteristics may help to reduce exposure to lead from urban sources if data are incorporated into urban planning.

Declarations of interest

None.

Acknowledgments

References

Bower, J.A., Lister, S., Hazebrouck, G., Perdrial, N., 2017. Geospatial evaluation of lead bioaccessibility and distribution for site specific prediction of threshold limits. Environ. Pollut. 229, 290–299. https://doi.org/10.1016/J.ENVPOL.2017.05.064.

Carretero, M.I., Pozo, M., 2010. Clay and non-clay minerals in the pharmaceutical and cosmetic industries part II. Active ingredients. Appl. Clay Sci. 47, 171–181. https://doi.org/10.1016/j.clay.2009.10.016.

Casteel, S.W., Weis, C.P., Henningsen, G.M., Brattin, W.J., 2006. Estimation of relative bioavailability of lead in soil and soil-like materials using young swine. Environ. Health Perspect. 114, 1162–1171. https://doi.org/10.1289/ehp.8852.

Chen, T. Bin, Zheng, Y.M., Lei, M., Huang, Z.C., Wu, H.T., Chen, H., Fan, K.K., Yu, K., Wu, X., Tian, Q.Z., 2005. Assessment of heavy metal pollution in surface soils of urban parks in Beijing, China. Chemosphere 60, 542–551. https://doi.org/10.1016/j.chemosphere.2004.12.072.

Del Rio-Salas, R., Ruiz, J., De la O-Villanueva, M., Valencia-Moreno, M., Moreno-Rodríguez, V., Gómez-Alvarez, A., Grijalva, T., Mendivil, H., Paz-Moreno, F., Meza-Figueroa, D., 2012. Tracing geogenic and anthropogenic sources in urban dusts: insights from lead isotopes. Atmos. Environ. 60, 202–210. https://doi.org/10.1016/J.ATMOSENV.2012.06.061.

Demetriades, A., Li, X., Ramsey, M.H., Thornton, I., 2010. Chemical speciation and bioaccessibility of lead in surface soil and house dust, Lavrion urban area, Attiki, Hellas. Environ. Geochem. Health 32, 529–552. https://doi.org/10.1007/s10653-010-9315-9.

Filippelli, G., Laidlaw, M., Latimer, J., Raftis, R., 2005. Urban lead poisoning and medical geology: an unfinished story. GSA Today 15, 4–11.

Freire, C., Amaya, E., Gil, F., Fernández, M.F., Murcia, M., Llop, S., Andiarena, A., Aurrekoetxea, J., Bustamante, M., Guxens, M., Ezama, E., Fernández-Tardón, G., Olea, N., 2018. Prenatal co-exposure to neurotoxic metals and neurodevelopment in preschool children: the environment and childhood (INMA) project. Sci. Total Environ. 621, 340–351. https://doi.org/10.1016/J.SCITOTENV.2017.11.273.

Habil, M., Massey, D.D., Taneja, A., 2013. Exposure of children studying in schools of India to PM levels and metal contamination: sources and their identification. Air Qual. Atmos. Health 6, 575–587. https://doi.org/10.1007/s11869-013-0201-3.

Hiller, E., Mihaljevič, M., Filová, L., Lachká, L., Jurkovič, Ľ., Kulikova, T., Fajčíková, K., Šimurková, M., Tatárková, V., 2017. Occurrence of selected trace metals and their oral bioaccessibility in urban soils of kindergartens and parks in Bratislava (Slovak Republic) as evaluated by simple in vitro digestion procedure. Ecotoxicol. Environ. Saf. 144, 611–621. https://doi.org/10.1016/J.ECOENV.2017.06.040.

Jamhari, A.A., Sahani, M., Latif, M.T., Chan, K.M., Tan, H.S., Khan, M.F., 2014. Concentration and source identification of polycyclic aromatic hydrocarbons (PAHs) in PM$_{10}$ of urban, industrial and semi-urban areas in Malaysia. Atmos. Environ. 86, 16–27. https://doi.org/10.1016/j.atmosenv.2013.12.019.

Jeffs, R.A., Jones, W., 1999. Additives for paint. In: Lambourne, R., Stiven, T.A. (Eds.), Paint and Surface Coatings: Theory and Practice. Woodhead Publishing, Cambridge, England, pp. 185–197.

Joo, H., Choi, J.H., Burm, E., Park, H., Hong, Y.-C., Kim, Y., Ha, E.-H., Kim, Y., Kim, B.-N., Ha, M., 2018. Gender difference in the effects of lead exposure at different time windows on neurobehavioral development in 5-year-old children. Sci. Total Environ. 615, 1086–1092. https://doi.org/10.1016/J.SCITOTENV.2017.10.007.

Lee, P.-K., Yu, S., Chang, H.J., Cho, H.Y., Kang, M.-J., Chae, B.-G., 2016. Lead chromate detected as a source of atmospheric Pb and Cr (VI) pollution. Sci. Rep. 6 (36088). https://doi.org/10.1038/srep36088.

Lin, C.-C., Chen, Y.-C., Su, F.-C., Lin, C.-M., Liao, H.-F., Hwang, Y.-H., Hsieh, W.-S., Jeng, S.-F., Su, Y.-N., Chen, P.-C., 2013. In utero exposure to environmental lead and manganese and neurodevelopment at 2 years of age. Environ. Res. 123, 52–57. https://doi.org/10.1016/J.ENVRES.2013.03.003.

Lu, X., Zhang, X., Li, L.Y., Chen, H., 2014. Assessment of metals pollution and health risk in dust from nursery schools in Xi'an, China. Environ. Res. 128, 27–34. https://doi.org/10.1016/J.ENVRES.2013.11.007.

Mandile, A.J., Hutton, A.C., 1995. Quantitative X-ray diffraction analysis of mineral and organic phases in organic-rich rocks. Int. J. Coal Geol. 28, 51–69. https://doi.org/10.1016/0166-5162(95)00004-W.

Mendoza, C.J., Garrido, R.T., Quilodrán, R.C., Segovia, C.M., Parada, A.J., 2017. Evaluation of the bioaccessible gastric and intestinal fractions of heavy metals in contaminated soils by means of a simple bioaccessibility extraction test. Chemosphere 176, 81–88. https://doi.org/10.1016/J.CHEMOSPHERE.2017.02.066.

Meunier, L., Walker, S.R., Wragg, J., Parsons, M.B., Koch, I., Jamieson, H.E., Reimer, K.J., 2010. Effects of soil composition and mineralogy on the bioaccessibility of arsenic from tailings and soil in gold mine districts of nova scotia. Environ. Sci. Technol. 44, 2667–2674. https://doi.org/10.1021/es9035682.

Meza-Figueroa, D., De la O-Villanueva, M., De la Parra, M.L., 2007. Heavy metal distribution in dust from elementary schools in Hermosillo, Sonora, México. Atmos. Environ. 41, 276–288. https://doi.org/10.1016/j.atmosenv.2006.08.034.

Meza-Figueroa, D., González-Grijalva, B., Del Río-Salas, R., Coimbra, R., Ochoa-Landin, L., Moreno-Rodríguez, V., 2016. Traffic signatures in suspended dust at pedestrian levels in semiarid zones: implications for human exposure. Atmos. Environ. 138, 4–14. https://doi.org/10.1016/J.ATMOSENV.2016.05.005.

Meza-Figueroa, D., González-Grijalva, B., Romero, F., Ruiz, J., Pedroza-Montero, M., Rivero, C.I.-D., Acosta-Elías, M., Ochoa-Landin, L., Navarro-Espinoza, S., 2018. Source apportionment and environmental fate of lead chromates in atmospheric dust in arid environments. Sci. Total Environ. 630, 1596–1607. https://doi.org/10.1016/J.SCITOTENV.2018.02.285.

Mielke, H.W., Gonzales, C.R., Smith, M.K., Mielke, P.W., 1999. The urban environment and children's health: soils as an integrator of lead, zinc, and cadmium in New Orleans, Louisiana, U.S.A. Environ. Res. 81, 117–129. https://doi.org/10.1006/ENRS.1999.3966.

Mielke, H.W., Berry, K.J., Mielke, P.W., Powell, E.T., Gonzales, C.R., 2005. Multiple metal accumulation as a factor in learning achievement within various New Orleans elementary school communities. Environ. Res. 97, 67–75. https://doi.org/10.1016/J.ENVRES.2004.01.011.

Molina, R.M., Schaider, L.A., Donaghey, T.C., Shine, J.P., Brain, J.D., 2013. Mineralogy affects geoavailability, bioaccessibility and bioavailability of zinc. Environ. Pollut. 182, 217–224. https://doi.org/10.1016/J.ENVPOL.2013.07.013.

Moreno-Rodríguez, V., Del Rio-Salas, R., Adams, D.K., Ochoa-Landin, L., Zepeda, J., Gómez-Alvarez, A., Palafox-Reyes, J., Meza-Figueroa, D., 2015. Historical trends and sources of TSP in a Sonoran desert city: can the North America monsoon enhance dust emissions? Atmos. Environ. 110, 111–121. https://doi.org/10.1016/J.ATMOSENV.2015.03.049.

Nowak, S., Lafon, S., Caquineau, S., Journet, E., Laurent, B., 2018. Quantitative study of the mineralogical composition of mineral dust aerosols by X-ray diffraction. Talanta 186, 133–139. https://doi.org/10.1016/J.TALANTA.2018.03.059.

Oomen, A.G., Hack, A., Minekus, M., Zeijdner, E., Cornelis, C., Schoeters, G., Verstraete, W., Van de Wiele, T., Wragg, J., Rompelberg, C.J.M., Sips, A.J.A.M., Van Wijnen, J.H., 2002. Comparison of five in vitro digestion models to study the bioaccessibility of soil contaminants. Environ. Sci. Technol. 36, 3326–3334. https://doi.org/10.1021/es010204v.

Padoan, E., Romè, C., Ajmone-Marsan, F., 2017. Bioaccessibility and size distribution of metals in road dust and roadside soils along a periurban transect. Sci. Total Environ. 601–602, 89–98. https://doi.org/10.1016/J.SCITOTENV.2017.05.180.

Pan, L., Ma, J., Hu, Y., Su, B., Fang, G., Wang, Y., Wang, Z., Wang, L., Xiang, B., 2016. Assessments of levels, potential ecological risk, and human health risk of heavy metals in the soils from a typical county in Shanxi Province, China. Environ. Sci. Pollut. Res. 23, 19330–19340. https://doi.org/10.1007/s11356-016-7044-z.

Reis, A.P., Patinha, C., Wragg, J., Dias, A.C., Cave, M., Sousa, A.J., Batista, M.J., Prazeres, C., Costa, C., Ferreira Da Silva, E., Rocha, F., 2014. Urban geochemistry of lead in gardens, playgrounds and schoolyards of Lisbon, Portugal: assessing exposure and risk to human health. Appl. Geochem. 44, 45–53. https://doi.org/10.1016/J.APGEOCHEM.2013.09.022.

Rozman, K.K., Klaasen, C.D., 2001. Absorption, distribution, and excretion of toxicants. In: Klaasen, C.D. (Ed.), Toxicology: the Basic Science of Poisons, 6th edn McGraw-Hill, New York, pp. 107–132.

Ruby, M.V., Lowney, Y.W., 2012. Selective soil particle adherence to hands: implications for understanding oral exposure to soil contaminants. Environ. Sci. Technol. 46, 12759–12771. https://doi.org/10.1021/es302473q.

Ruby, M.V., Davis, A., Link, T.E., Schoof, R., Chaney, R.L., Freeman, G.B., Bergstrom, P., 1993. Development of an in-vitro screening-test to evaluate the in-vivo bioaccessibility of ingested mine-waste lead. Environ. Sci. Technol. 27, 2870–2877. https://doi.org/10.1021/es00049a030.

Ruby, M.V., Davis, A., Schoof, R., Eberle, S., Sellstone, C.M., 1996. Estimation of lead and arsenic bioavailability using a physiologically based extraction test. Environ. Sci. Technol. 30, 422–430. https://doi.org/10.1021/es950057z.

Schnur, J., John, R.M., 2014. Childhood lead poisoning and the new centers for disease control and prevention guidelines for lead exposure. J. Am. Assoc. Nurse Pract. 26, 238–247. https://doi.org/10.1002/2327-6924.12112.

Sherlock, E.J., Lawrence, R.W., Poulin, R., 1995. On the neutralization of scid rock drainage by carbonate and silicate minerals. Environ. Geol. 25, 43–54.

Sipes, I.G., Badger, D., 2001. Principles of toxicology. In: Sullivan Jr., J.B., Krieger, G. (Eds.), Clinical Environmental Health and Exposures, 2nd edn Lippincott Williams and Wilkins, Philadelphia, pp. 49–67.

Smith, E., Kempson, I.M., Juhasz, A.L., Weber, J., Rofe, A., Gancarz, D., Naidu, R., McLaren, R.G., Gräfe, M., 2011. In vivo–in vitro and XANES spectroscopy assessments of lead bioavailability in contaminated periurban soils. Environ. Sci. Technol. 45, 6145–6152. https://doi.org/10.1021/es200653k.

Sun, F., Polizzotto, M.L., Guan, D., Wu, J., Shen, Q., Ran, W., Wang, B., Yu, G., 2017. Exploring the interactions and binding sites between Cd and functional groups in soil using two-dimensional correlation spectroscopy and synchrotron radiation based spectromicroscopies. J. Hazard. Mater. 326, 18–25. https://doi.org/10.1016/J.JHAZMAT.2016.12.019.

Sverdrup, H.U., 1990. The Kinetics of Base Cation Release due to Chemical Weathering. Lund University Press.

Taylor, M.P., Mould, S.A., Kristensen, L.J., Rouillon, M., 2014. Environmental arsenic, cadmium and lead dust emissions from metal mine operations: implications for environmental management, monitoring and human health. Environ. Res. 135, 296–303. https://doi.org/10.1016/J.ENVRES.2014.08.036.

Turner, A., Lewis, M., 2018. Lead and other heavy metals in soils impacted by exterior legacy paint in residential areas of south west England. Sci. Total Environ. 619–620, 1206–1213. https://doi.org/10.1016/J.SCITOTENV.2017.11.041.

Turner, A., Kearl, E.R., Solman, K.R., 2016. Lead and other toxic metals in playground paints from South West England. Sci. Total Environ. 544, 460–466. https://doi.org/10.1016/J.SCITOTENV.2015.11.078.

USEPA, 1996a. Method 3050B. Acid Digestion of Sediments, Sludges and Soils. United States Environmental Protection Agency.

USEPA, 1996b. Method 6010B. Inductively Coupled Plasma-atomic Emission Spectrometry. SW-846 Compendium. United States Environmental Protection Agency.

USEPA, 2007. Method 6200. Field Portable X-ray Fluorescence Spectrometry for the Determination of Elemental Concentrations in Soil and Sediment. United States Environmental Protection Agency.

USEPA, 2014. Human Health Risk Assessment Research. Available:. https://www.epa.gov/risk/human-health-risk-assessment.

Vasiluk, L., Dutton, M.D., Hale, B., 2011. In vitro estimates of bioaccessible nickel in field-contaminated soils, and comparison with in vivo measurement of bioavailability and identification of mineralogy. Sci. Total Environ. 409, 2700–2706. https://doi.org/10.1016/J.SCITOTENV.2011.03.035.

Walraven, N., Bakker, M., van Os, B.J.H., Klaver, G.T., Middelburg, J.J., Davies, G.R., 2015. Factors controlling the oral bioaccessibility of anthropogenic Pb in polluted soils. Sci. Total Environ. 506–507, 149–163. https://doi.org/10.1016/J.SCITOTENV.2014.10.118.

Wang, J., Li, S., Cui, X., Li, H., Qian, X., Wang, C., Sun, Y., 2016. Bioaccessibility, sources and health risk assessment of trace metals in urban park dust in Nanjing, Southeast China. Ecotoxicol. Environ. Saf. 128, 161–170. https://doi.org/10.1016/J.ECOENV.2016.02.020.

White, K., Detherage, T., Verellen, M., Tully, J., Krekeler, M.P.S., 2014. An investigation of lead chromate (crocoite-PbCrO4) and other inorganic pigments in aged traffic paint samples from Hamilton, Ohio: implications for lead in the environment. Environ. Earth Sci. 71, 3517–3528. https://doi.org/10.1007/s12665-013-2741-0.

Yan, K., Dong, Z., Wijayawardena, M.A.A., Liu, Y., Naidu, R., Semple, K., 2017. Measurement of soil lead bioavailability and influence of soil types and properties: a review. Chemosphere 184, 27–42. https://doi.org/10.1016/J.CHEMOSPHERE.2017.05.143.

Yang, K., Cattle, S.R., 2015. Bioaccessibility of lead in urban soil of Broken Hill, Australia: a study based on in vitro digestion and the IEUBK model. Sci. Total Environ. 538, 922–933. https://doi.org/10.1016/J.SCITOTENV.2015.08.084.

VI. DISCUSIONES

Los resultados de las concentraciones de Cr y Pb en las diferentes matrices estudiadas indican un componente antropogénico en el área de estudio. Decreciendo para ambos elementos de la siguiente manera: pintura amarilla fresca > pintura amarilla degradada > polvo de calle > polvo depositado en techo > polvo atmosférico > suelos locales.

La pintura amarilla de tráfico mediante el análisis de SEM-EDS y RAMAN muestra claramente la composición del pigmento mineral crocoíta ($PbCrO_4$) utilizado para proporcionar el característico color amarillo, mismo que presenta concentraciones elevadas de Pb (42872.8 $mg \cdot kg^{-1}$) y Cr (5839.5 $mg \cdot kg^{-1}$). Los análisis de DRX muestran también la presencia de minerales de calcita ($CaCO_3$), cuarzo (SiO_2) y caolinita ($Al_2Si_2O_5(OH)_4$) en su composición. El mineral de crocoíta en las pinturas amarillas analizadas se presenta en cristales subhedrales de tamaño menor a 1µm y en mayor abundancia en pintura fresca que en pintura degradada presentando esta última cristales de tamaño menor a 0.1 µm. La concentración de Cr y Pb es mayor en pintura amarilla fresca en comparación con la pintura amarilla degradada. Esto sugiere que las nano y microparticulas de crocoita son liberadas al ambiente, al alterarse la matriz de polímero por diferentes mecanismos (erosión, tráfico, altas temperaturas). Estudios previos muestran que la degradación de la pintura se ve favorecida con la presencia del mineral de caolinita y la fotodegradación (White et al., 2014; Wang et al., 2010).

Los polvos de calle presentan valores de Pb (168.5 $mg \cdot kg^{-1}$) y Cr 147.4 $mg \cdot kg^{-1}$), reflejándose mayormente en la zona urbanizada mas antigua, siguiendo el patrón de "ojo de buey" previamente descrito por Filippelli et al. (2005) para Pb. Esta distribución espacial es comúnmente relacionada con la resuspensión de polvos de calle y suelos de carreteras proporcional al volumen de tráfico histórico (Meza-Figueroa et al., 2016, Filipelli et al., 2005). En la ciudad se observan dos principales áreas de concentración de Pb-Cr, considerándose fuentes de emisión debido a la acumulación de polvos y sedimentos que sufren procesos de resuspensión favorecidos por las condiciones climáticas y el bajo porcentaje de humedad en suelos y ambiente. Estas áreas se definen por las calles principales de la ciudad, alto tráfico vehicular, y barreras orográficas como es la formación de granito con orientación NW-SE que evita la dispersión de los vientos dominantes con dirección SW-NE, favoreciendo a la sedimentación de polvos depositados en techo, vía de deposición atmosférica.

La regresión linear de Pb y Cr contenido en polvo atmosférico, polvo de calle, polvo sedimentado en techos y pintura de calle (R^2 0.977) indica como posible fuente en común la crocoita contenida en las pinturas amarillas. Lo anterior se complementa con los resultados de isótopos de Pb donde los cromatos de plomo y el tetraetilo de plomo proveniente de la gasolina utilizada en décadas anteriores son las principales fuentes de contaminación de Pb en polvo atmosférico. Esto es

posteriormente sedimentado en suelos urbanos y periurbanos, contribuyendo a la geoquímica del fondo local.

Los procesos de sedimentación y resuspención se ven directamente influenciados por las temporadas de pre- monson (antes de lluvias) que comprende los meses de octubre a diciembre y prost-monso (después de lluvias) los meses abril-junio.

Los resultados del estudio vertical de la concentración de polvo atmosférico muestran diferencias a nivel techo y nivel peatonal. Durante el periodo de muestreo se presentan valores más elevados a nivel peatonal, teniendo un incremento en la temporada de pre-moonson y post-moonson lo que da lugar a presenciar días "polvosos". El conteo por pixeles revela que las partículas finas, con diámetro aerodinámico menor a 2.5 µm, se incrementan a nivel peatonal al igual que las partículas gruesas con diámetro aerodinámico mayor a 2.5 µm, asociándose a procesos de re-suspensión de suelos, erosión, transporte eólico y construcción (Pasha y Alharbi, 2015). Se encontró que la abundancia de estas partículas a nivel peatonal se debe a la formación de "agregados" de partículas finas que se traduce a partículas gruesas, las cuales a su vez acarrean contaminantes derivados de tráfico. Estudios previos muestran la asociación de los elementos mayores a partículas gruesas, y elementos tóxicos (Cd, Pb y Zn) a partículas finas (Hu et al., 2010, 2013). Sin embargo, los resultados en el presente estudio muestran lo contrario a nivel peatonal. Esta evidencia reciente se puede asociar con características específicas de sitios urbanos semiáridos y provee nuevos paradigmas en la exposición humana a fuentes de tráfico y metales asociados, así como sus implicaciones a la salud.

Ha sido bien documentado que la disolución de Pb es controlada por la fase gástrica y su absorción ocurre en la fase intestinal (Smith et al., 2011). Sin embargo, la influencia de la mineralogía en estas fases ha sido poco estudiado. Por lo anterior, la mineralogía obtenida en la difracción de rayos X (DRX), de los suelos urbanos y periurbanos estudiados, se conjunto para interés del presente, en minerales totales neutralizadores (TNM) a los grupos de carbonatos de calcio y magnesio, debido a que en la industria farmacéutica son utilizados como antiácidos. El ácido clorhidrico (HCl) es una de las sustancias que se encuentran en la secreción de jugos gástricos y es necesaria para la enzima pepsina para la catalización de la digestión de las proteínas que se encuentran en los alimentos que ingerimos. La acidez es un síntoma que resulta con la elevación de producción de ácido en el estómago (Wanamaker y Grimm, 2004). La función principal de los antiácidos es la neutralización del exceso de acidez utilizando compuestos básicos, siendo los carbonatos y bicarbonatos, los grupos de bases comúnmente utilizados en marcas comerciales (ecuación 1 y 2). Al utilizar un antiácido, el pH es elevado en cuestión de segundos, con la posibilidad de causar un "rebote ácido" si el medio gástrico se acerca a pH 7 (Carretero y Pozo, 2010).

Ecuación 1

Carbonato de calcio CaCO3

Reacción química

$CaCO_3$ (s) + 2 HCl (aq) --------> $CaCl_2$ (aq) + H_2O (l) + CO_2 (g)

Ecuación 2

Carbonato de magnesio $MgCO_3$

Reacción química

$MgCO_3$ (s) + HCl (aq) --------> $MgCl_2$ (aq) + H_2O (l) + CO_2 (g)
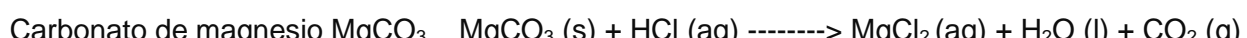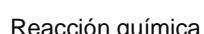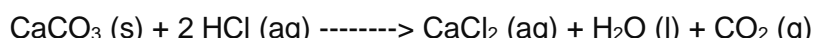
Los TNM presentes en nuestras muestras de suelo son: calcita ($CaCO_3$), dolomita ($CaMg(CO_3)_2$), rodocrosita ($MnCO_3$), magnesita ($MgCO_3$) y siderita ($FeCO_3$). El mineral calcita aparece en la mayoría de los suelos estudiados, así como en la pintura amarilla de tráfico, al igual que el mineral de caolinita ($Al_2Si_2O_5(OH_4)$). A diferencia de los carbonatos, la caolinita no tiene la capacidad de neutralizar el medio gástrico, pero si mejorar las condiciones del medio intestinal (Carretero y Pozo, 2010).

Los resultados del experimento realizado en suelos periurbanos fortificados con crocoíta muestra variación en los porcentajes de bioaccesibilidad de Pb en fase gástrica y fase intestinal y se relaciona con el contenido de TNM. La mayor biaccesibilidad intestinal reportada (10.1%) se da en el suelo con mayor contenido de caolinita (1.9%) sin la presencia de TNM. A nivel gástrico, la mayor bioaccesibilidad (51.85%) se reporta en el suelo con TNM (1.5%) y sin la presencia de caolinita en suelo. Por otro parte, los suelos urbanos ubicados en escuelas primarias muestran variabilidad en el contenido mineral ya que se encuentran expuestos a diferentes fuentes antrópicas. Los niveles de biaccesibilidad de Pb gástrico, son en su mayoría por encima del (30%) y se puede deber a que el plomo se encuentra en diferentes fases (ej. óxidos de Pb) en ambientes urbanos. A nivel intestinal, solo un suelo urbano presento Pb bioaccesible (2.57%) con contenido de caolinita (4.0%). El análisis de componentes principales (PCA) muestra 3 asociaciones importantes: (i) contenido de caolinita con bioaccesibilidad de Pb en fase intestinal; (ii) mineral de calcita y TNM, y (iii) disolución de crocoíta en fase gástrica, teniendo liberación de Pb.

La identificación de las fases minerales de cada tipo de suelo presente en la ciudad, con los datos de bioaccesibilidad de Pb intestinal obtenidas en el presente estudio, nos permite diseñar una ecuación de predicción de bioaccesibilidad (y = 0.5286x - 6.948) siendo "y" la bioaccesibilidad estimada mediante una concentración de Pb total conocida "X"con fuerte correlación lineal (r=0.99). De tal forma que, si tenemos una concentración conocida de Pb total, podemos estimar la fracción bioaccesible de Pb y predecir el tipo de suelo presenta mayor vulnerabilidad en caso de añadírsele contaminantes de este tipo y determinar el nivel riesgo de exposición al Pb en dicha área. Lo anterior, tiene mayor efectos toxicológicos en niños ya que se ha documentado que a concentraciones bajas afecta la memoria, comportamiento y coeficiente intelectual en niños (Lin et al., 2013; Schur y John, 2014; USEPA, 2014; Freire et al., 2018; Joo

et al., 2018). El centro de control de enfermedades y prevención (CDC-U.S) recomienda que los niveles de Pb en sangre de niños no debe exceder 5 $\mu g \cdot dL^{-1}$ para 1 a 4 años de edad. En el presente trabajo se predice que del 4 al 27% de niños expuestos pueden presentar Pb en sangre por encima del nivel establecido por el CDC. En caso de que el suelo contenga alrededor del 6% de presencia de cromatos de Pb, el 99% de los niños expuestos excederían el valor de 5 $\mu g \cdot dL^{-1}$, presentando variaciones asociadas al tipo de suelo (mineralogía).

VII. CONCLUSIONES

En zonas áridas, la variación temporal de la concentración de material particulado se ve influenciada por el aumento y la disminución de la temperatura, así como el porcentaje de humedad. Los procesos naturales como meteorización, erosión, transporte eólico y la deposición de polvo por acción de la gravedad mejoran la movilidad de contaminantes, como los son los cromatos de plomo (crocoíta). Los suelos urbanos y periurbanos son los principales reservorios de contaminantes y el polvo mineral resuspendido podría actuar como transporte de estos, permitiendo que los seres humanos puedan estar expuestos y los contaminantes llegue al interior del organismo por las vías de ingestión o inhalación.

Este trabajo proporciona evidencia de la presencia de minerales de crocoita de tamaño nano a micro en la atmósfera. El destino medioambiental de los pigmentos de crocoita en la pintura amarilla de tráfico en América Latina no se ha abordado previamente, y representa un riesgo de salud desconocido para la población expuesta, principalmente en climas áridos donde la fotodegradación de la pintura es más probable que ocurra.

Los resultados de bioacccesibilidad oral realizados en el presente estudio nos llevan a entender el riesgo real que representa la exposición constante a una fuente de área, en este caso, los cromatos de plomo derivados de las pinturas amarillas de tráfico. Tomando en cuenta un factor poco estudiado, como lo es el papel que juega la mineralogía del suelo en la bioacccesibilidad del Pb en condiciones gástricas e intestinales.

La mayoría de los estudios documentan que la bioaccesibilidad del Pb depende de: (i) la química, la fuente y la solubilidad del contaminante; (ii) específica superficie reactiva de Pb en suelos y (iii) la capacidad en suelos de fases secundarias de Pb (Walraven et al., 2015). Este trabajo ha explorado el posible efecto de la mineralogía del suelo en la bioaccesibilidad del Pb mediante el análisis la bioaccesibilidad gástrico-intestinal de Pb (PBET) derivada de una fuente (pintura de tráfico) en cinco tipos de suelos, indicando que la presencia de carbonatos como minerales neutralizantes totales (TNM) puede jugar un papel importante en la bioaccesibilidad gástrica. Además, la caolinita, la calcita y el tipo de contaminante pueden influir la liberación de Pb en condiciones intestinales. Pb-bioaccesible en fase gástrica permanece dentro del rango de 40,8 a 50,8%, posiblemente relacionado al rebote del ácido en las condiciones del estómago y una mayor liberación de metales.

Los resultados del presente trabajo podrían ayudar a las decisiones futuras sobre planificación urbana y programas de sensibilización sobre la contaminación del suelo y los efectos sobre la salud mientras se tomen en cuenta las características mineralógicas como base para reducir la exposición a un contaminante, en este caso plomo.

VIII. RECOMENDACIONES.

- Continuar con los estudios de bioaccesibilidad oral, con especial énfasis en el estudio de mineral de caolinita contenida en el suelo ya que parece aumentar la bioaccesibilidad de Pb en la fase intestinal.

- Integrar la caracterización mineralogía a los estudios de bioaccesibilidad pulmonar, ya que por el diámetro aerodinámico de los cristales de crocoita identificados, llegan a la parte mas profunda de los pulmones donde se da la mayor disolución.

- Estudiar detalladamente el comportamiento del cromo hexavalente (elemento cancerígeno) que se encuentra en el mineral de crocoita.

- Caracterizar mas fuentes de contaminación de Pb, ya que son diversas en ambientes urbanos, ej., los óxidos de plomo, los cuales son altamente bioaccesibles.

- Considerar el presente trabajo para la implementación de estrategias para reducir emisiones como lo son los cromatos de plomo (crocoita) a través de la pintura amarilla de tráfico.

IX. BIBLIOGRAFÍA

Al-Khashman, O. A. (2004). Heavy metal distribution in dust, street dust and soils from the work place in Karak Industrial Estate, Jordan. Atmospheric Environment, 38(39), 6803-6812. doi:10.1016/j.atmosenv.2004.09.011

Al-Khashman, O. A. (2007). Determination of metal accumulation in deposited street dusts in Amman, Jordan. Environmental Geochemistry and Health, 29(1), 1-10. doi: 10.1007/s10653-006-9067-8

Alatise, O. I., Y Schrauzer, G. N. (2010). Lead Exposure: A Contributing Cause of the Current Breast Cancer Epidemic in Nigerian Women. Biological Trace Element Research, 136(2), 127-139. doi: 10.1007/s12011-010-8608-2

Alimonti, A., Petrucci, F., Krachler, M., Bocca, B., Caroli, S. (2000). Reference values for chromium, nickel and vanadium in urine of youngsters from the urban area of Rome. Journal of Environ Monitoring, 2(4), 351-354. doi: 10.1039/b001616k

Anttila, A., Y Sallmen, M. (1995). Effects of parental occupational exposure to lead and other metals on spontaneous abortion. Journal of Occupment Environvironmental Medicine, 37(8), 915-921. doi: 10.1097/00043764-199508000-00005

ATSDR, U. (2012). Toxicological profile for chromium. In: US Department of Health and Human Services, Public Health Service.

Banerjee, A. D. K. (2003). Heavy metal levels and solid phase speciation in street dusts of Delhi, India. Environmental Pollution, 123(1), 95-105. doi:10.1016/S0269-7491(02)00337-8

Barceloux, D. G. (1999). Chromium. Journal of Toxicology: Clinical Toxicology, 37(2), 173-194. doi: 10.1081/clt-100102418

Carrero, J. A., Arrizabalaga, I., Bustamante, J., Goienaga, N., Arana, G., y Madariaga, J. M. (2013). Diagnosing the traffic impact on roadside soils through a multianalytical data analysis of the concentration profiles of traffic-related elements. Science of The Total Environment, 458-460, 427-434. doi: https://doi.org/10.1016/j.scitotenv.2013.04.047

Carretero, M. I., y Pozo, M. (2010). Clay and non-clay minerals in the pharmaceutical and cosmetic industries Part II. Active ingredients. Applied Clay Science, 47(3), 171-181. doi: https://doi.org/10.1016/j.clay.2009.10.016

Chen, R., Chu, C., Tan, J., Cao, J., Song, W., Xu, X., Jiang, C., Ma, W., Yang, C., Chen, B., Gui, Y., y Kan, H. (2010). Ambient air pollution and hospital admission in Shanghai, China. Journal of Hazardous Matererials, 181(1), 234-240. doi: https://doi.org/10.1016/j.jhazmat.2010.05.002

Cornelis R. (2005). Handbook of elemental speciation II: species in the environment, food, medicine & occupational health. Wiley

Crane, M., Leverett, P., Shaddick, L., Williams, P., Kloprogge, J. T., y Frost, R. (2001). The PbCrO4-PbSO4 system and its mineralogical significance. Neues Jahrbuch Fur Mineralogie-Monatshefte, 505-519.

Creamean, J., Suski, K., Rosenfeld, D., Cazorla, A., DeMott, P., Sullivan, R., White, A., Ralph, F., Minnis, P., Comstock, J., Tomlinson, J., Prather, K. (2013). Dust and Biological Aerosols from the Sahara and Asia Influence Precipitation in the Western U.S. Science (New York, N.Y.), 339. doi: 10.1126/science.1227279

Davies, J. M. (1984). Lung cancer mortality among workers making lead chromate and zinc chromate pigments at three English factories. British Journal of Industrial Medicine, 41(2), 158. doi: 10.1136/oem.41.2.158

Davis, A., Drexler, J. W., Ruby, M. V., y Nicholson, A. (1993). Micromineralogy of mine wastes in relation to lead bioavailability, Butte, Montana. Environmental Science and Technology, 27(7), 1415-1425. doi: 10.1021/es00044a018

Davis, A., Ruby, M. V., y Bergstrom, P. D. (1992). Bioavailability of arsenic and lead in soils from the Butte, Montana, mining district. Environmental Science and Technology, 26(3), 461-468. doi: 10.1021/es00027a002

Davis, A., Ruby, M. V., Bloom, M., Schoof, R., Freeman, G., y Bergstrom, P. D. (1996). Mineralogic Constraints on the Bioavailability of Arsenic in Smelter-Impacted Soils. Environmental Science and Technology, 30(2), 392-399. doi: 10.1021/es9407857

Dieter, M. P., Matthews, H. B., Jeffcoat, R. A., y Moseman, R. F. (1993). Comparison of lead bioavailability in F344 rats fed lead acetate, lead oxide, lead sulfide, or lead ore concentrate from Skagway, Alaska. Journal of Toxicology and Environmental Health, Part A Current Issues, 39(1), 79-93. doi: 10.1080/15287399309531737

Duzgoren-Aydin, N. S., Wong, C. S. C., Song, Z. G., Aydin, A., Li, X. D., y You, M. (2006). Fate of Heavy Metal Contaminants in Road Dusts and Gully Sediments in Guangzhou, SE China: A Chemical and Mineralogical Assessment. Human and Ecological Risk Assessment: An International Journal, 12(2), 374-389. doi: 10.1080/108070305005 38005

Environmental Protection Agency (2009), "Integrated Science Assessment for Particulate Matter". EPA/600/R-08/139F.

Faiz, Y., Tufail, M., Javed, M. T., Chaudhry, M. M.,yNaila, S. (2009). Road dust pollution of Cd, Cu, Ni, Pb and Zn along Islamabad Expressway, Pakistan. Microchemical Journal, 92(2), 186-192. doi: 10.1016/j.microc.2009.03.009

Fergusson, J. E., y Kim,N. D. (1991). Trace elements in street and house dusts: sources and speciation. Science of the Total Environment, 100,125–150. doi:10.1016/0048-9697(91)90376-P

Ferreira-Baptista, L., y De Miguel, E. (2005). Geochemistry and risk assessment of street dust in Luanda, Angola: A tropical urban environment. Atmospheric Environment, 39(25), 4501-4512. doi:10.1016/j.atmosenv.2005.03.026

Filippelli, G. M., Laidlaw, M. A. S., Latimer, J. C., y Raftis, R. (2005). Urban lead poisoning and medical geology: An unfinished story. Geological Society of America Today, 15(1), 4-11. doi: 10.1130/1052-5173(2005)015<4:ULPAMG>2.0.CO;2

Filippelli, G., Adamic J, Nichols D, Shukle J, Frix E. (2018). Mapping the urban lead exposome: a detailed analysis of soil metal concentrations at the household scale using citizen science. International Journal of Environmental Research and Public Health 15(7), 1531

Freire, C., Amaya, E., Gil, F., Fernández, M. F., Murcia, M., Llop, S., Andiarena, A., Aurrekoetxea, J., Bustamante, M., Guxens, M., Ezama, E., Fernandez, G., Olea, N. (2018). Prenatal co-exposure to neurotoxic metals and neurodevelopment in preschool children: The Environment and Childhood (INMA) Project. Science of The Total Environment, 621, 340-351. doi: https://doi.org/10.1016/j.scitotenv.2017.11.273

Frentzel-Beyme, R. (1983). Lung cancer mortality of workers employed in chromate pigment factories. Journal of Cancer Research and Clinical Oncology, 105(2), 183-188. doi: 10.1007/BF00406930

Frost, R. L. (2004). Raman microscopy of selected chromate minerals. Journal of Raman Spectroscopy, 35(2), 153-158. doi: 10.1002/jrs.1121

García-Rico, L., Meza-Figueroa, D., Jay Gandolfi, A., Del Río-Salas, R., Romero, F. M., y Meza-Montenegro, M. M. (2016). Dust–Metal Sources in an Urbanized Arid Zone: Implications for Health-Risk Assessments. Archives of Environmental Contamination and Toxicology, 70(3), 522-533. doi: 10.1007/s00244-015-0229-5

Gottesfeld, P., Pokhrel, D., y Pokhrel, A. K. (2014). Lead in new paints in Nepal. Environmental research, 132, 70-75. doi: 10.1016/j.envres.2014.03.036

Guney, M., Zagury, G. J., Dogan, N., y Onay, T. T. (2010). Exposure assessment and risk characterization from trace elements following soil ingestion by children exposed to playgrounds, parks and picnic areas. Journal of Hazardous Materials, 182(1), 656-664. doi:10.1016/j.jhazmat.2010.06.082

Han, J., Xu, M.H., Yao, H., Furuuchi, M., Sakano, T., Kanchanapiya, P., Kanaoka, C. (2006). Partition of heavy and alkali metals during sewage sludge incineration. Energy Fuel 20 (2), 583–590

Hayes, R. B., Sheffet, A., y Spirtas, R. (1989). Cancer mortality among a cohort of chromium pigment workers. American Journal of Industrial Medicine, 16(2), 127-133. doi: 10.1002/ajim.4700160204

Hooker, P. J., y Nathanail, C. P. (2006). Risk-based characterisation of lead in urban soils. Chemical Geology, 226(3), 340-351. doi:10.1016/j.chemgeo.2005.09.028

Hu, H., Yang, Q., Lu, X., Wang, W., Wang, S., y Fan, M. (2010). Air Pollution and Control in Different Areas of China. Critical Reviews in Environmental Science and Technology, 40(6), 452-518. doi: 10.1080/10643380802451946

Hu, Q., Ewing, R. P., y Dultz, S. (2012). Low pore connectivity in natural rock. Journal of Contaminant Hydrology, 133, 76-83. doi: https://doi.org/10.1016/j.jconhyd.2012.03.006

Hu, X., Ding, Z., Zhang, Y., Sun, Y., Wu, J., Chen, Y., y Lian, H (2013). Size Distribution and Source Apportionment of Airborne Metallic Elements in Nanjing, China. Aerosol and Air Quality Research, 13(6), 1796-1806.

Hurlbut CS, editor. Dana's manual of mineralogy. 18th ed. New York, NY: John Wiley and Sons, Inc.; 1971. pp. 346–347.

International Agency for Research on Cancer. (2012). Arsenic, metals, fibres and dusts. IARC monographs on the evaluation of carcinogenic risks to humans.

Jeffs, R.A., Jones,W., 1999. Additives for paint. In: Lambourne, R., Stiven, T.A. (Eds.), Paint and Surface Coatings: Theory and Practice. Woodhead Publishing, Cambridge, En- gland, pp. 185–197.

Johnson, J., Schewel, L., y Graedel, T. E. (2006). The contemporary anthropogenic chromium cycle. Environmental Science Technology, 40(22), 7060-7069. doi: 10.1021/es060061i

Joo, H., Choi, J. H., Burm, E., Park, H., Hong, Y. C., Kim, Y., Ha, E., Kim, Y., Kim, B., Ha, M. (2018). Gender difference in the effects of lead exposure at different time windows on neurobehavioral development in 5-year-old children. Science of the Total Environment, 615, 1086-1092. doi: 10.1016/j.scitotenv.2017.10.007

Kabata-Pendias, A. (2011). Trace elements in soils and plants (4th ed.,). Boca Raton:The Chemical Rubber Company Press.

Karanasiou, A., Moreno, T., Amato, F., Lumbreras, J., Narros, A., Borge, R., Tobías, A., Boldo, E., Linares, C., Pey, J., Reche, C., Alastuey, A., . . . Querol, X. (2011). Road dust contribution to PM levels – Evaluation of the effectiveness of street washing activities by means of Positive Matrix Factorization. Atmospheric Environment, 45(13), 2193-2201. doi:10.1016/j.atmosenv.2011.01.067

Khairy, M. A., Barakat, A. O., Mostafa, A. R., y Wade, T. L. (2011). Multielement determination by flame atomic absorption of road dust samples in Delta Region, Egypt. Microchemical Journal, 97(2), 234-242. doi:10.1016/j.microc.2010.09.012

Khan, S., Khan, M. A., y Rehman, S. (2011). Lead and Cadmium Contamination of Different Roadside Soils and Plants in Peshawar City, Pakistan. Pedosphere, 21(3), 351-357. doi: 0.1016/S1002-0160(11)60135-5

Kong, S., Ji, Y., Lu, B., Chen, L., Han, B., Li, Z., y Bai, Z. (2011). Characterization of PM_{10} source profiles for fugitive dust in Fushun-a city famous for coal. Atmospheric Environment, 45(30), 5351-5365. doi:10.1016/j.atmosenv.2011.06.050

Laidlaw, M. A. S., y Filippelli, G. M. (2008). Resuspension of urban soils as a persistent source of lead poisoning in children: A review and new directions. Applied Geochemistry, 23(8), 2021-2039. doi:0.1016/j.apgeochem.2008.05.009

Lanphear, B. P., Rauch, S., Auinger, P., Allen, R. W., Y Hornung, R. W. (2018). Low-level lead exposure and mortality in US adults: a population-based cohort study. The Lancet Public Health, 3(4), e177-e184. doi10.1016/S2468-2667(18)30025-2

Lee, P. K., Yu, S., Chang, H. J., Cho, H. Y., Kang, M. J., y Chae, B. G. (2016). Lead chromate detected as a source of atmospheric Pb and Cr (VI) pollution. Scientific reports, 6, 36088.

Leonard, S. S., Roberts, J. R., Antonini, J. M., Castranova, V., y Shi, X. (2004). $PbCrO_4$ mediates cellular responses via reactive oxygen species. Molecular and Cellular Biochemistry, 255(1), 171-179. doi: 10.1023/B:MCBI.0000007273.23747.67

Leonard, S. S., Vallyathan, V., Castranova, V., y Shi, X. (2002). Generation of reactive oxygen species in the enzymatic reduction of $PbCrO_4$ and related DNA damage. Molecular and Cellular Biochemistry, 234(1), 309-315. doi: 10.1023/A:1015917922980

Lin, C.-C., Chen, Y.-C., Su, F.-C., Lin, C.-M., Liao, H.-F., Hwang, Y.-H., Hsieh, W -S., Jeng, S -F., Su, Y -N., Chen, P -C. (2013). In utero exposure to environmental lead and manganese and neurodevelopment at 2 years of age. Environmental Research, 123, 52-57. doi:10.1016/j.envres.2013.03.003

Lu et al. (2009). Contamination assessment of copper, lead, zinc, manganese and nickel in street dust of Baoji, NW China. Journal of Hazardous Materials, 161(2-3), 1058-1062. doi: 10.1016/j.jhazmat.2008.04.052

Lu, X., Wang, L., Lei, K., Huang, J., y Zhai, Y. (2009). Contamination assessment of copper, lead, zinc, manganese and nickel in street dust of Baoji, NW China. Journal of Hazardous Materials, 161(2), 1058-1062. doi:10.1016/j.jhazmat.2008.04. 052

Maas, S., Scheifler, R., Benslama, M., Crini, N., Lucot, E., Brahmia, Z., Benyacoub, S., Giraudoux, P. (2010). Spatial distribution of heavy metal concentrations in urban, suburban and agricultural soils in a Mediterranean city of Algeria. Environmental Pollution, 158(6), 2294-2301. doi:10.1016/j.envpol.2010.02.001

Meza-Figueroa, D., De la O-Villanueva, M., y De la Parra, M. L. (2007). Heavy metal distribution in dust from elementary schools in Hermosillo, Sonora, México. Atmospheric Environment, 41(2), 276-288. doi:10.1016/j.atmosenv.2006.08.034

Meza-Montenegro, M. M., Gandolfi, A. J., Santana-Alcántar, M. E., Klimecki, W. T., Aguilar-Apodaca, M. G., Del Río-Salas, R., De la O-Villanueva, M., Gómez-Alvarez, A., Mendivil-

Quijada, H., Valencia, M., Meza-Figueroa, D. (2012). Metals in residential soils and cumulative risk assessment in Yaqui and Mayo agricultural valleys, northern Mexico. Science of The Total Environment, 433, 472-481. doi:10.1016/j.scitotenv .2012.06.083

Meza-Figueroa, D., González-Grijalva, B., Del Río-Salas, R., Coimbra, R., Ochoa-Landin, L., y Moreno-Rodríguez, V. (2016). Traffic signatures in suspended dust at pedestrian levels in semiarid zones: Implications for human exposure. Atmospheric Environment, 138, 4-14. doi:10.1016/j.atmosenv.2016.05.005

Monico, L., Janssens, K., Cotte, M., Sorace, L., Vanmeert, F., Brunetti, B. G., y Miliani, C. (2016). Chromium speciation methods and infrared spectroscopy for studying the chemical reactivity of lead chromate-based pigments in oil medium. Microchemical Journal, 124, 272-282.doi: 0.1016/j.microc.2015.08.028

Newman, R., Weston, C., y Farrell, E. (1980). Analysis of Watercolor Pigments in a Box Owned by Winslow Homer. Journal of the American Institute for Conservation, 19(2), 103-105. doi: 10.1179/019713680806028867

Nicholson, S. E. (2009). A revised picture of the structure of the "monsoon" and land ITCZ over West Africa. Climate Dynamics, 32(7), 1155-1171. doi: 10.1007/s00382-008-0514-3

Nordstrom, D. K., y Alpers, C. N. (1999). The geochemistry of acid mine waters. The environmental geochemistry of mineral deposits: Part A: Processes, methods and health issues, 133-160.

Occupational Safety and Health Administration. (2006). Occupational Exposure to Hexavalent Chromium. Final Rule. Federal register, 71(39), 10099-10385.

Pan, X., Wang, J., Y Zhang, D. (2009). Biosorption of Co(II) by immobilised Pleurotus ostreatus. International Journal of Environment and Pollution, 37(2-3), 289-298. doi: 10.1504/IJEP.2009.025132

Papp, J. F., y Lipin, B. R. (2001). Chromium and Chromium Alloys. Kirk-Othmer Encyclopedia of Chemical Technology. doi:10.1002/0471238961.0308181523051920.a01.pub2

Pasha, M. J., y Alharbi, B. H. (2015). Characterization of size–fractionated PM10 and associated heavy metals at two semi–arid holy sites during Hajj in Saudi Arabia. Atmospheric Pollution Research, 6(1), 162-172. doi:10.5094/APR.2015. 019

Peña, R., Dumas, S., Villalejo-Fuerte, M., Y Ortíz-Galindo, J. L. (2003). Ontogenetic development of the digestive tract in reared spotted sand bass Paralabrax maculatofasciatus larvae. Aquaculture, 219(1), 633-644. doi: 0.1016 /S0044-8486(02)00352-6

Pirkle, J. L., Kaufmann, R. B., Brody, D. J., Hickman, T., Gunter, E. W., y Paschal, D. C. (1998). Exposure of the U.S. population to lead, 1991-1994. Environmental health perspectives, 106(11), 745-750. doi: 10.1289/ehp.98106745

Plumlee, G. S. (1999). The environmental geology of mineral deposits. The Environmental Geochemistry of Mineral Deposits, Part A. Processes, Techniques, and Health Issues, 6A, 71-116.

Plumlee, G. S., y Ziegler, T. L. (2003). The medical geochemistry of dusts, soils, and other Earth materials: Chapter 7. Treatise on Geochemistry, 9, 263-310. doi: 10.1016/B0-08-043751-6/09050-2

Rasmussen, P. E., Subramanian, K. S., y Jessiman, B. J. (2001). A multi-element profile of house dust in relation to exterior dust and soils in the city of Ottawa, Canada. Science of The Total Environment, 267(1), 125-140. doi:10.1016/S0048-9697(00)00775-0

Romieu, I., Palazuelos, E., Hernandez Avila, M., Rios, C., Munoz, I., Jimenez, C., y Cahero, G. (1994). Sources of lead exposure in Mexico City. Environmental health perspectives, 102(4), 384-389. doi: 10.1289/ehp.94102384

Ruby, M. V., Davis, A., Link, T. E., Schoof, R., Chaney, R. L., Freeman, G. B., y Bergstrom, P. (1993). Development of an in vitro screening test to evaluate the in vivo bioaccessibility of ingested mine-waste lead. Environmental Science and Technology, 27(13), 2870-2877. doi: 10.1021/es00049a030

Ruby, M. V., Davis, A., Schoof, R., Eberle, S., y Sellstone, C. M. (1996). Estimation of Lead and Arsenic Bioavailability Using a Physiologically Based Extraction Test. Environmental Science and Technology, 30(2), 422-430. doi: 10.1021/es950057z

Ruby, M. V., Schoof, R., Brattin, W., Goldade, M., Post, G., Harnois, M., Mosbt, E., Casteel, S., Berti, W., Carpenter, M., Edwards, D., Cragin, D., Chappell, W. (1999). Advances in Evaluating the Oral Bioavailability of Inorganics in Soil for Use in Human Health Risk Assessment. Environmental Science and Technology, 33(21), 3697-3705. doi: 10.1021/es990479z

Schnur, J., y John, R. M. (2014). Childhood lead poisoning and the new Centers for Disease Control and Prevention guidelines for lead exposure. Journal of the American Association of Nurse Practitioners, 26(5), 238-247. doi: 10.1002/2327-6924.12112

Shanker, A. K., Cervantes, C., Loza-Tavera, H., y Avudainayagam, S. (2005). Chromium toxicity in plants. Environment International, 31(5), 739-753. doi: 10.1016/j.envint.2005.02.003

Sipes, I.G., Badger, D., (2001). Principles of toxicology. In: Sullivan Jr., J.B., Krieger, G. (Eds.), Clinical Environmental Health and Exposures, 2nd edn LippincottWilliams andWil- kins, Philadelphia, pp. 49–67.

Shi, G.T., Chen, Z.L., Xu, S.Y., Zhang, J., Wang, L., Bi, C.J., Teng, J.Y. (2008). Potentially toxic metal contamination of urban soils and roadside dust in Shanghai, China. Environmental Pollutution, 156(2), 251–260. doi.org/10.1016/j.envpol.2008.02.027

Smith, E., Kempson, I. M., Juhasz, A. L., Weber, J., Rofe, A., Gancarz, D., Naidu, R., McLaren, R.G., Gräfe, M. (2011). In Vivo–in Vitro and XANES Spectroscopy Assessments of Lead Bioavailability in Contaminated Periurban Soils. Environmental Science and Technology, 45(14), 6145-6152. doi: 10.1021/es200653k

Szolnoki, Z., y Farsang, A. (2013). Evaluation of Metal Mobility and Bioaccessibility in Soils of Urban Vegetable Gardens Using Sequential Extraction. Water, Air, and Soil Pollution, 224(10), 1737. doi: 10.1007/s11270-013-1737-4

Thakur, M., Kanti Deb, M., Imai, S., Suzuki, Y., Ueki, K., y Hasegawa, A. (2004). Load of Heavy Metals in the Airborne Dust Particulates of an Urban City of Central India. Environmental Monitoring and Assessment, 95(1), 257-268. doi: 10.1023/B:EMAS.0000029907.965 62.af

Tiffany-Castiglioni, E. (1993). Cell culture models for lead toxicity in neuronal and glial cells. Neurotoxicology, 14(4), 513-536.

Tong, S., von Schirnding, Y. E., y Prapamontol, T. (2000). Environmental lead exposure: a public health problem of global dimensions. Bulletin of the World Health Organization, 78(9), 1068-1077.

Tong, S. T., y Lam, K. C. (2000). Home sweet home? A case study of household dust contamination in Hong Kong. Science of the Total Environment, 256(2-3), 115-123. doi: 10.1016/s0048-9697(00)00471-x

Turner, A., Kearl, E. R., y Solman, K. R. (2016). Lead and other toxic metals in playground paints from South West England. Science of the total environment, 544, 460-466. doi: 10.1016/j.scitotenv.2015.11.078

Wanamaker, R., y Grimm, I. (2004). Encyclopedia of Gastroenterology. Gastroenterology, 127(4), 1274-1275.

Walraven, N., Bakker, M., Van Os, B. J. H., Klaver, G. T., Middelburg, J. J., y Davies, G. R. (2015). Factors controlling the oral bioaccessibility of anthropogenic Pb in polluted soils. Science of the Total Environment, 506, 149-163. doi: 10.1016/j.scitotenv.2014.10.118

Wang, Y., Xie, Y., Li, W., Wang, Z., y Giammar, D. E. (2010). Formation of Lead(IV) Oxides from Lead(II) Compounds. Environmental Science and Technology, 44(23), 8950-8956. doi: 10.1021/es102318z

White, K., Detherage, T., Verellen, M., Tully, J., y Krekeler, M.P.S. (2014). An investigation of lead chromate (crocoite-PbCrO4) and other inorganic pigments in aged traffic paint samples from Hamilton, Ohio: implications for lead in the environment. Environmental Earth Sciences, 71. doi:10.1007/s12665-013-2741-0.

Wilson, W. E., y Suh, H. H. (1997). Fine Particles and Coarse Particles: Concentration Relationships Relevant to Epidemiologic Studies. Journal of the Air and Waste Management Association, 47(12), 1238-1249. doi: 10.1080/10473289.1997.10464074

Yongming, H., Peixuan, D., Junji, C., y Posmentier, E. S. (2006). Multivariate analysis of heavy metal contamination in urban dusts of Xi'an, Central China. Science of the Total Environment, 355(1), 176-186. doi:10.1016/j.scitotenv.2005.02.026

Zheng, N., Liu, J., Wang, Q., y Liang, Z. (2010). Health risk assessment of heavy metal exposure to street dust in the zinc smelting district, Northeast of China. Science of the Total Environment, 408(4), 726-733. doi:10.1016/j.scitotenv.2009.10.075